Sponsored by the
Department of Science & Technology

This journal is accredited by the South African Department of Education for university subsidy purposes. It is abstracted and indexed in Environment Abstract, Index to South African Periodicals, and the Nexus Database System.

The journal has also been selected into the Science Citation Index Expanded by Thomson Reuters, and coverage begins from Volume 19 No 1.

Administration and subscriptions
Ms Ann Steiner

Annual subscriptions 2012 (four issues)
Individuals (Africa): R160 (single copy R51)
Individuals (beyond Africa): US$109 (single copy US$39)
Corporate (Africa): R321 (single copy R103)
Corporate (beyond Africa): US$218 (single copy US$77)

Cost includes VAT and airmail postage.
Cheques should be made payable to the University of Cape Town and sent to the address given below.

Enquiries may be directed to:
The Editor, Journal of Energy in Southern Africa,
Energy Research Centre, University of Cape Town,
Private Bag, Rondebosch 7701, South Africa
Tel: +27 (021) 650 3894
Fax: +27 (021) 650 2830
E-mail: Richard.Drummond@uct.ac.za

Website: www.erc.uct.ac.za

It is the policy of the Journal to publish papers covering the technical, economic, policy, environmental and social aspects of energy research and development carried out in, or relevant to, South Africa. Only previously unpublished work will be accepted; conference papers delivered but not published elsewhere are also welcomed. Short comments, not exceeding 500 words, on articles appearing in the Journal are invited. Relevant items of general interest, news, statistics, technical notes, reviews and research results will also be included, as will announcements of recent publications, reviews, conferences, seminars and meetings.

Those wishing to submit contributions should refer to the guidelines given on the inside back cover.

The Editorial Committee does not accept responsibility for viewpoints or opinions expressed here, or the correctness of facts and figures.

 ISSN 1021 447X

JOURNAL OF ENERGY IN SOUTHERN AFRICA

Volume 23 Number 3 • August 2012

CONTENTS

A techno-economic study of energy efficiency technologies for supermarkets in South Africa

Simisha Pather-Elias

Stephen Davis

Brett Cohen

Energy Research Centre, University of Cape Town

Abstract

The food retail sector is energy intensive, consuming large amounts of electricity for refrigeration, air-conditioning and cooking. Retailers are aiming to reduce their electricity consumption in supermarkets and thus their carbon footprint using energy efficiency technologies. This paper reports on a techno-economic analysis of energy efficient technologies to recommend to the food retail sector for use in supermarkets. The targets and needs of food retail companies were surveyed and thereafter, the retailers were divided into three categories. Category 1 retailer had the highest targets for electricity and carbon reduction and was willing to take on more risk. Category 2 retailer had intermediate targets and would only use developed technologies, while category 3 retailer would only invest in developed technologies if they were proven to show significant long term saving with short pay back periods. The analysis showed that closed refrigerators had the highest electricity/carbon savings and the highest profit (NPV), followed by heat reclamation from refrigeration. Both these technologies were recommended for category 1 retailers. A combination of heat reclamation, energy efficient lights, fridge curtains, electronic controls for refrigerators and POS power management systems were recommended for category 3 retailers. A combination of the two recommendations was identified for category 2 retailers. Behavioural changes of all staff were identified as important for energy efficiency technologies to work at optimum levels.

Keywords: supermarkets; energy efficiency; lighting; refrigeration; water heating

1. Introduction

Electricity reduction in organizations in South Africa is beginning to emerge as an essential business activity for a multitude of reasons including the electricity price hikes of 25% year on year for the next three years (Nersa, 2009) and the possible adoption of a carbon price (Department of National Treasury, 2010); investor and customer demands due to climate change reasons, and incentives from government. Electricity security is a further concern as shortages are predicted to extend until 2015 when there will be increased capacity from two more power stations (Eskom, 2011). The local food retail sector, although not one of the most electricity intensive sectors in South Africa, is also aiming to reduce its electricity requirements using primarily energy efficiency technologies. By reducing electricity consumption, the three aspects of reduced costs, energy security and climate change can be addressed.

There is, however, a lack of information and demonstration projects which provide guidance in adoption of energy efficiency interventions. With no experience to learn from, retailers are largely looking to their international counterparts, who are more advanced in their implementation. Thus, there is a need for research to determine technologically appropriate measures for South Africa, specifically focusing on the feasibility of electricity reduction in different climatic regions of the country.

In this paper, the opportunities for electricity reduction, and hence, carbon mitigation, in the food retail sector in South Africa are investigated using a techno-economic approach, with a focus on the store level. Several commercially mature and undeveloped technologies are evaluated based on their level of efficiency and their financial rewards. It is envisaged that these results will provide the sector with an analysis that is specific to the South

African context, and that it will be used as a guideline to further explore the reductions within each organization.

2. Method

2.1. Determining motivations of South African food retailers for reducing their carbon footprints

To achieve this aim, several large food retail companies which make up 90% of the market (Weatherspoon, 2003) and consultants were surveyed to determine their views on, and requirements for electricity and carbon reduction in stores. On the basis of the survey outcomes, three types of hypothetical retailer categories were formulated such that different technologies could be recommended to meet the needs of different retailers. Although all the retailers stressed costs as the most important deciding factor, some retailers were able to take on more risk and were interested in meeting consumer demands to capture niche markets. Some companies had also included corporate sustainability reporting. The first category of retailer had the highest targets for electricity and carbon emission reductions and was willing to experiment with technologies to achieve this. The second category of retailer had lower reduction targets and would only use developed technologies. The third category of retailer had no targets for carbon reduction but would invest in proven energy efficient technologies to reduce electricity consumption, if they showed significant long term savings and short payback periods. Table 1 details the requirements for electricity savings and carbon reductions for each category.

2.2 Short-listing applicable energy efficient technologies

A wide variety of technologies was shortlisted to meet these targets. This shortlist was based on technology used in international and local supermarkets, application suitability, potential for electricity reduction, costs, visibility, availability, and technology maturity. The shortlist included:

a) Electronic ballasts,
b) Compact fluorescent lights (CFLs),
c) Power management systems,
d) Automated fridge curtains,
e) Upright fridges with doors (closed refrigerators),
f) Heat reclamation from refrigeration,
g) Electronic controls for refrigeration,
h) Heat pump geysers,
i) Evaporative coolers,
j) CO_2 fridges.

The number of units required for each option, which was required to compare across options, was based on an average store size of 1 500m^2. This information was provided by different retailers. For each option, the current numbers of fridges, lights, geysers, etc. were based on the existing infrastructure and equipment, such that these options would serve as retrofits. The difference in power output between the current equipment and the retrofits was compensated for. Information on costs, installation, maintenance, life span and electricity savings were also provided by suppliers and energy engineers. The average electricity end use used for all calculations was:

- Refrigeration – 45%
- Air conditioning -18%
- Water heating – 12%
- Lights – 8%
- Point of Sales (POS) – 1%
- Heating (ovens) – 16%

2.3 Selecting and calculating criteria for determination of energy efficient technologies

Criteria for the selection of energy efficient technologies included the following, each of which is discussed in more detail:

a) CO_2 reduction,
b) CAPEX,
c) economic profitability,
d) ease of implementation, and
e) awareness and visibility.

Economic profitability was the most important criterion to all retailers surveyed, and the remaining criteria were used as secondary criteria to further

Table 1: Characteristics of the different categories of retailers

	Category 1	*Category 2*	*Category 3*
Carbon reduction targets	30% of current levels by 2013	20% of current level by 2013	No target
Electricity savings	30%	30%	30%
Cost factor, initial costs vs. long term savings (economic profitability)	Important but willing to trial/ demonstrate technologies	Important – use only developed technologies with short pay back periods etc.	Very important – only factor considered, mature technologies only
Staff and customer awareness	Very important	Very important	Neutral

aid in the decision making process. These criteria were chosen according to a combination of retailer needs, data availability and data accessibility for the technology options chosen. Only criteria for which there was a significant difference in performance between technology options were considered.

a. CO_2 savings

The average electricity consumption and end use of a store was calculated using data made available from the large supermarket retail companies, from stores that are located in the Western Cape.

Prior to calculating the CO_2 emissions savings associated with each of the energy efficiency technologies, electricity savings is calculated as follows:

Electricity (kWh) savings per year = average store consumption per month x estimated % use of electricity by the technology1 x estimated energy savings x 12 months. (1)

e.g. total electricity consumed by the store per month = 150 000 kWh; water heating consumes 12% of total electricity; heat pumps save 70% of electricity for lighting;
then electricity savings per year (kWh)
= 150 000 x 12% x 70% x 12 months
= 151 200 kWh

Once the electricity savings has been calculated, the savings in CO_2 emissions is calculated as follows:

CO_2 (tons) savings per year = Electricity (kWh) savings/year x 0.001 ton CO_2eq[2] (2)

It is noted that the standard unit of measurement for energy consumption and efficiency typically used in commercial buildings (kWh/m^2) was not used here as the purpose was not to compare consumption against other buildings, but to meet reduction targets expressed as percentage.

b. CAPEX

Technology costs were obtained from suppliers and included installation (Table 3). These vary depending on supplier/ contractor and the volumes purchased. Initial investment was stressed as an important consideration. The initial investment included CAPEX, and installation costs.

c. Economic profitability

The profitability of technologies was described by all retailers to be very important, although some retailers placed lesser priority on it relative to other criteria and other retailers. To determine the economic profitability of each technology option, the Net Present Value (NPV) was the method of choice due to its advantages of using multiple discount rates and its applicability to long term projects.

The following formula was used for NPV:

$$\sum_{t=1}^{n} \frac{C_t}{(1+R)^t} \quad (3)$$

where:
C_t = discounted cash flow (savings per year)
R = discount rate
savings per year = kWh savings per year x unit cost of electricity
and where the discount rate = interest rate or cost of capital = R
n = no. of periods
t = time

To evaluate all options on a consistent basis, the lifespan for all options was set at 15 years as this time frame was common for most technology options. For those options with shorter life spans, replacements were included in the calculation.

The cash flow was based on electricity savings per year for each technology option, as calculated using equation (1). A unit cost of electricity of 92c/kWh was used for 2011, R1.15 for 2012 and R1.45 for 2013 in line with the NERSA's electricity pricing (NERSA, 2009). Thereafter electricity prices increased by 10% every year (based on historical price increases). The discount rate was pegged to interest rate forecasts provided by Standard Corporate Merchant Bank in South Africa (Darmalingam, 2011). These interest rate forecasts are adjusted for risk premium and inflation and they are commonly used as a discount rate (Darmalingam, 2011).

d. Ease of implementation

The ease of implementation of each technology was noted according to the length of time required for installation, downtime, loss of sales, and if a technician was required to retrofit

e. Awareness and visibility

The visibility of each technology was also noted as to who it would be visible to, i.e. the customer, staff only or technician only.

3. Results

Table 2 shows that the biggest electricity savers are heat reclamation, CFLs, heat pump geysers and evaporative coolers. However, due to the biggest use of electricity being refrigeration (45%), followed by air conditioning (18%), ovens (12%), hot water (12%) and lights (8%), the retrofits that were associated with these end uses produced the highest savings in electricity and thus carbon emissions.

Table 3 shows the CAPEX and economic profitability (NPV) for these energy efficiency technologies.

Table 2: CO_2 savings per year for each technology option

Retrofit Option	*Units*	*Life time (years)*	*Electricity savings (%)*	*Electricity savings / year (kWh)*	*CO_2 saving / year (tons)*
Fridges with doors (closed)	10	15	35	295 000	295
Evaporative cooling A/C	11	15	70	270 000	270
CO_2 fridges	1	25	30	253 000	2533
Heat reclamation from refrigeration	2	15	100	225 000	225
Heat pump geyser (150L)	2	15	70	151 000	151
Electronic controls and monitoring (refrigeration)	1	15	15	126 000	126
Fridge curtains (1.8m)	20	5	20	84 000	84
Electronic ballast & T8 (28W) light	50	7	22	31 000	31
Power management software for POS	10	15	50	9000	9
CFL (28W)	5	3	85	8000	8

The biggest cost savings were through refrigeration, water heating and air conditioning related technologies, as expected due to the ratio of electricity they consume. Fridges with doors saved the most amount of money in the long term and did not have a significant initial investment, compared to energy efficient air conditioning, electronic controls or CO_2 refrigeration. Changing the lighting and installing power management systems, which are frequently regarded as low cost measures, did not show significant savings. However, the results also revealed that there was no relationship between initial investment costs and the long term financial rewards, thus supporting the case for strategic analysis and reviews instead of adopting random technologies.

CO_2 refrigeration is interesting as at first glance the NPV showed a loss which is contradictory to international case studies that show large savings. However, when the project lifetime was increased to 25 years (the expected lifespan), a profit of more than R3.5 million was projected.

The effect of increasing electricity tariffs in the next three years on the financial savings each year is also shown in Table 4. These price hikes have been taken into account for the long term NPV calculations.

Results for the other two criteria – ease of implementation and awareness and visibility as well as the status quo on the usage of these technologies are summarized in Table 5.

4. Discussion

The survey of the food retailers and consultants who participated revealed the various reasons that retailers in South Africa are reducing their electricity consumption and carbon footprints. These reasons are no different to retailers in the rest of the

Table 3: Costs and NPV for technology options considered

Retrofit Option *lifetime*	*Units*	*Capex/unit* *(R)c/osts (R)*	*Total initial* *)otal Mainac (R)*	*Maint. costs* *lifetime (R*	*Total maint.* */year (R)*	*Product* *years) Product l (R)*	*Savings* *(R)*	*NPV (15*
Fridges with doors (closed)	10	10 000	100 000	0	0	15	271 000	4 720 000
Evaporative cooling A/C	11	25 000	275 000	500	5 500	15	248 000	2 520 000
CO_2 fridges	1	5 000 000	5 000 000	8 000	200 000	25	233 000	- 870 000
Heat reclamation from refrigeration	2	20 000	40 000	0	0	15	207 000	3 600 000
Heat pump geyser (150L)	2	9 000	18 0006	500	1 000	15	145 000	2 500 000
Electronic controls and monitoring (refrigeration)	1	60 000	60 000	0	0	15	116 000	2 000 000
Fridge curtains (1.8m)	20	1 500	30 000	0	0	5	78 500	13 000 000
Electronic ballast & T8 (28W) light	50	240	11 200	0	0	7	29 000	495 000
Power management software for POS	10	160	1 600	30	300	15	9 000	140 000
CFL (28 W)	5	35	-257	0	0	3	7 000	126 000

Table 4: The effect of increasing electricity tariffs on savings for each technology

Retrofit option	*Electricity savings /year (kWh)*	*Savings/ year (2010/11) (R)*	*Savings/ year (2011/12) (R)*	*Savings/ year (2012/13) (R)*
Fridges with doors (closed)	295 000	271 000	340 000	423 000
Evaporative cooling A/C	270 000	248 000	310 000	388 000
CO_2 fridges	253 000	233 000	290 000	363 000
Heat reclamation from refrigeration	225 000	207 000	258 000	323 000
Heat pump geyser (150L)	151 000	145 000	180 000	226 000
Electronic controls and monitoring (refrigeration)	126 000	117 000	145 000	182 000
Fridge curtains (1.8m)	84 000	78 000	97 000	121 000
Electronic ballast & T8 (28W) light	31 000	29 000	36 000	45 000
Power management software for POS	9 000	9 000	11 000	13 000
CFL (28W)	8 000	7 000	9 000	11 000

Table 5: Awareness and ease of implementation of each technology

Retrofit option	*Ease of implementation*	*Visibility/awareness*	*Status quo*
Fridges with doors (closed)	New units required and possible change of floor design	Very visible	Few units in most stores
Evaporative cooling A/C	Easy to install, little downtime, but technician required	Hidden	Trialed
CO2 fridges	Complete retrofit, long downtime	Hidden	Trialed
Heat reclamation from refrigeration	Easy to install, no/little downtime, but technician required	Hidden	Trialed
Heat pump geyser (150L)	Easy to install, no/little downtime, but technician required	Hidden	Trialed
Electronic controls and monitoring (refrigeration)	Easy to install, no/little downtime, but technician required	Visible to staff only	Trialed
Electronic ballast & T8 (28W) light	Directly interchangeable with magnetic ballasts	Very visible	Roll out in most stores
Fridge curtains (1.8m)	Units need to be factory fitted	Visible to staff only	Trialed
Power management software for POS	Install programme, no down time	Visible to staff only	Not used
CFL (28W)	Directly interchangeable with incandescent bulbs	Very visible	Roll out in most stores

world (Zipplies, 2010). Although all the retailers recognized the importance of energy saving and climate change, and in particular their part in carbon mitigation, some were leaders while some preferred to delay adopting interventions for reducing their emissions. This delay was ascribed to several reasons including experiential learning, favourable market mechanisms or until it was mandatory. Retailers were also cognizant of the costs associated with these reductions, especially since the food retail sector has small profit margins of between 1 and 2% (Bradshaw, 2011), however, the "leaders" were more willing to accept longer payback timeframes for projects, as long as these projects showed large financial rewards in the future.

Although the carbon reduction targets for each category of retailer were different, the electricity reduction targets were the same for all retailers surveyed (30% by 2013). The biggest reductions in carbon/electricity were from closed refrigerators, evaporative cooling, CO_2 refrigeration and heat reclamation from refrigeration. Using a combination of technologies, the electricity reduction targets can be achieved. The 30% electricity target for all retailers requires a saving of 561 600 kWh/annum (total average annual consumption per store = 1.87 million kWh). Using closed fridges saves 300 000 kWh/ annum (table 2) and heat reclamation from fridges to heat water has a high carbon savings of 225 000 kWh/ annum (Table 2).

Closed refrigerators have also showed the highest profitability, almost R5 million over 25 years. Additional benefits are that they are easy to install and allow the store to maintain a comfortable temperature for customers. Closed refrigerators are also at the front end of the store, and customers interact

with them directly. Therefore, this option is highly recommended. However, it is well known that there is a perception by marketing divisions of retail organizations that closed fridges hamper sales due to their effect on decision making as a result of the inconvenience associated with opening fridges for every item (Smith, 2010). Thus retailers are not keen to install closed fridges throughout the stores. Therefore, closed refrigerators are only recommended for a category 1 retailer.

The heat reclamation system would replace an electrical geyser completely and be more efficient and cost effective than a SWH or heat pump, as it utilizes waste heat. The heat can also be diverted for use in under floor heating and maintaining thermally comfortable temperatures in the stores, thereby reducing the load on the HVAC system. Furthermore, the heat reclamation system does not require any additional servicing as there are no moving parts, and can be maintained as part of the refrigeration units at the back end of the store. A combination of heat reclamation and closed refrigerators meets the electricity targets for the store.

For category 3 retailers, a combination of heat reclamation (225 tons/year CO_2), electronic controls for refrigeration (126 tons/year CO_2), fridge curtains (84 tons/year CO_2), energy efficient lights (40 tons/year CO_2), and POS power management systems (9 tons/year CO_2) are recommended to meet electricity and carbon targets. All of these technologies are low cost adding up to R140 000 for installation per store, which is the same combined cost as installing a heat reclamation system and closed refrigerators that is recommended for category 1 retailer. Additionally, the NPV for the combination of technologies for category 3 retailer amounts to R8 million, slightly less than the technologies recommended for category 1 retailer (R 8.3 million). These technologies are easy to install and require little maintenance. These technologies also complement each other with the heat reclamation system saving the majority of electricity and lights being able to meet visibility requirements for all categories. The added advantage is that all of these technologies are mature technologies and their efficiencies and experiences have been well documented. As mentioned, most stores have already installed CFLs, but magnetic ballasts are not very prominent at present, and their use could be extended.

It is important not to overestimate the potential success of energy efficiency, especially if the high energy consumption is due to low levels of behavioural discipline (Schelly *et al*., 2011) and/or poor insulation. This behavioural discipline stems from poor management and lack of commitment to electricity reduction, and if these attitudes persist when energy efficient technologies are installed, these technologies will lose efficiency over time due to poor maintenance of equipment. Usually simple and regular cleaning methods by staff as well an annual service by qualified technicians is enough to ensure proper operation of most equipment e.g. fridges and air-conditioners (Schlemmer, 2010). Other behavioural changes that will reduce electricity consumption include, amongst others, switching off equipment that is not in use, maintaining appropriate temperatures for cooling and heating equipment for different times of day and year, and not overloading fridges and freezers thereby blocking off air vents. Research shows that the implementation of energy efficient technologies may sometimes have the reverse reaction in behaviour resulting in people consuming more. This is known as the "Rebound Effect". Therefore, energy efficiency technologies go hand in hand with increased staff awareness, training and buy-in, introducing this into key performance areas for employees and including it in sustainability reporting for organizations. Although this study attempted to include criteria such as "Ease of implementation" that assist in the uptake of these selected technologies, this is a technology centric study, and a multi-faceted approach which includes the behaviour of retailers and their staff should also be undertaken.

5. Conclusion

This research forms a preliminary investigation into the techno-economic feasibility of electricity and carbon reduction in supermarkets in South Africa. Closed refrigerators showed the highest electricity/carbon savings and the highest profit (NPV), followed by heat reclamation. Both these technologies were recommended for category 1 retailers who have the largest targets for both electricity and carbon reduction and are willing to trial technologies. A combination of heat reclamation, energy efficiency lights, fridge curtains, electronic controls for refrigerators, and power management systems for point of sales (POS) systems were recommended for category 3 retailers. Category 2 retailers have intermediate targets and can adopt a combination of the two recommendations to meet targets. Further research is needed to determine the feasibility of technologies within specific organizations and specific locations. Behavioural changes are also imperative if energy efficient technologies are required to work at optimal levels to reduce the targeted electricity and carbon reductions.

Notes

1. The number of units per end use was included in calculations
2. The emissions factor varies between years. This factor includes losses in transmission (5.58%) and distribution (1.74%) specific for the Western Cape (Eskom,

2010; Letete et al., 2010)

3. Emissions from leakages not included
4. Includes Eskom rebate for lights at 34c/kWh saved (Eskom, 2010b)
5. Includes Eskom rebate for lights at 34c/kWh saved (Eskom, 2010b)
6. Includes rebate of R3600 per heat pump

References

Bradshaw, J. Forecasts for the food retail sector. Pick n Pay. 12 January 2011.

Darmaligngam, S. South Africa's interest rate forecasts. Standard Coroporate Merchant Bank. 18 Febraury 2011.

Department of National Treasury. (2010). Discus-sion Paper. Reducing Greenhouse Gas Emissions: The Carbon Tax Option.

Eskom. (2010a). *Eskom Annual Report*.

Eskom. (2010b). *Eskom EEDSM Standard Offer Pilot Program Commercial and Industrial energy consumers*. [online]. Available from website: www.eskomidm.co.za/home/eedsm-standard-offer-pilot-program.

Letete, T.; Mungwe, N.; Guma, M. and Marquard, A. (2008). University of Cape Town carbon footprint. Available from website: www.erc.uct.ac.za/Research/publications/10Thapeleetal-UCT_ footprint.pdf.

NERSA. (2009). Multi Year Price Determination 2 (MYPD2).

Schelly, C.; Cross, J.; Franzen, W.; Halle, P. and Reeve, S. (2011). Reducing Energy Consump-tion and Creating a Conservation Culture in Organizations: A Case Study of One Public School District. *Environment and Behaviour*. 43 (3): 316-343.

Schlemmer, K. Energy efficient refrigeration technologies in South Africa. 15 October 2010.

Smith, J. Carbon reduction efforts at Woolworths. 23 August 2010.

Weatherspoon, L. and Reardon, T. (2003). The rise of supermarkets in Africa: implications for agri-food systems and the rural poor. *Development Policy Review*., 21(3): 333-355.

Zipplies, R. Challenges and opportunities for the South African food retail companies. 18 March 2010.

Received 3 October 2011

Efficiency and cost analysis of a designed in-line water heating system compared to a conventional water heating system in South Africa

Rupert Gouws

Estie le Roux

School of Electrical, Electronic and Computer Engineering, North-West University, Potchefstroom, South Africa

Abstract

In this paper, the authors compares the efficiency and cost of a designed in-line water heating system with a conventional water heating system (geyser) in South Africa. The paper provides an overview on water heating systems and heating elements and provides the typical water consumption required by an average household in South Africa. A summary on the design of the in-line water heating system together with a system cost analysis is provided. The designed in-line water heating system takes the energy consumption, temperature and pressure into account during operation. The energy consumption and cost of the designed in-line water heating system is compared to a conventional water geyser. A cost analysis on the designed in-line water heating system, heat pumps and solar water heating systems are also provided. The energy consumption results showed that the conventional water geyser on average consumes 2.5% more energy to heat one litre of water from 15 °C to 60 °C, than the designed in-line water heating system to supply one litre of water at 60°C.

Keywords: efficiency analysis, cost analysis, in-line water heating system, conventional water heating system, design and monitoring

1. Introduction

South Africa currently faces a number of energy related problems; some of these include environmental sustainability, energy reliability and tariff hikes (Sebitosi, 2008; Sebitosi and Pillay, 2008). It is estimated that the electricity utilization of the residential sector in South Africa accounts for almost 35% of the peak demand, with water heating consumption at approximately 40% of this peak demand (EDRC, 2003; DEAT, 2004).

It was therefore decided to investigate the in-line water heating system as an alternative to the conventional water heating system (geyser). It was further decided to design an in-line water heating system which has the following capabilities: 1) energy consumption control, 2) low flow compensation, 3) PID temperature control and 4) automatic switch off during no flow.

Figure 1 shows the experimental setup of the in-line water heating system and the conventional water geyser. The conventional geyser has a cold water inlet at the bottom of the tank and a hot water output at the top. A thermostat (manually set at 60°C) regulates the temperature inside the tank. The conventional geyser supply hot water to the sink on the right hand side and the designed in-line water heating system supply hot water to the sink on the left hand side.The designed in-line water heating system is equipped with a controller with interactive display (set at 60°C) which is installed next to the sink.

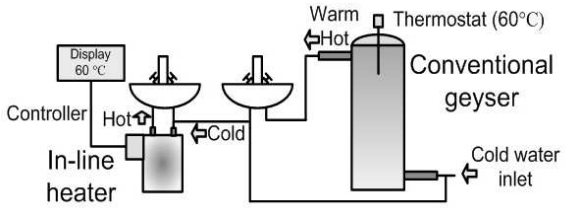

Figure 1: In-line water heating system and conventional water heating system (geyser)

The focus of this paper is on the comparison of the efficiency and cost of the designed in-line water heating system with a conventional geyser. An overview on the design of the in-line water heating

system together with a system cost analysis is provided in section 3. The results on the energy consumption of the designed in-line water heating system and the conventional water heater together with a cost comparison between different water heating systems are provided in section 4. Wilson (1978) provides more detail on the available energy conservation options for residential water heaters.

2. Overview on water heating systems and elements

This section provides an overview on the in-line water heating system, the conventional water heating system, heating elements and the required water consumption per person.

2.1 In-line water heating system

In-line water heating systems are also know as tankless water heaters, on demand water heaters, instant water heaters, instantaneous water heaters and point of use water heaters. The main two types of tank-less water heating systems available are gas fuelled and electric instantaneous water heaters. For this paper, the focus is specifically on the electric instantaneous water heater.

The basic operational principle of an in-line water heating system is the same as the conventional water heating system (geyser). Cold water flows in and warm water flows out (Rollins, 2010).

The main difference between the in-line water heating system and conventional geyser is that the in-line water heating system has no tank and warm water is instantly available and does not take a long period of time to heat up. Water is also not stored in a large tank throughout the day; there are therefore no standing losses. The most basic in-line water heating system has two coils.

The first is the water carry coil, which carries the cold water into the system, heats it up and then warm water is send through the same coil as output to the user. The second coil is known as the heating coil which is twisted around the carrier coil and heats the water as it passes through (Rollins, 2010). The in-line water heating system consists of different types of sensors to ensure correct and efficient working of the system. When the hot water faucet is turned open, the pressure and temperature sensors are activated.

The pressure and temperature of the incoming cold water are measured and the data is send to a microprocessor for calculations. The microprocessor compares the calculated values with the pre-programmed data and adjusts the heating coil accordingly. The sensor constantly sends data to the microprocessor and the data is constantly monitored and regulated throughout the on cycle of the faucet (Etankless, 2010).

When the faucet is turned off the pressure sensor communicates with the microprocessor letting it know to turn off the power and that no more action is required. For the customer's convenience many of these on demand water heating units have a digital display, on which the temperature can be set according to the customer's needs. This functionality can improve the energy consumption of the in-line water heating system, if correctly operated.

2.2 Conventional water heating system

Figure 2 shows an example of a conventional geyser. The conventional water geysers are designed to heat water and store the heated water in an insulated tank. Every water heater consists of a cold water inlet and a hot water outlet. The cold water is routed through a pipe called a dip tube to the bottom of the heater. In some designs, the cold water inlet is found on the bottom of the tank. When warm water is used, the tank automatically fills up with cold water through a one way valve (ACME, 2010; van Amerongen 1972).

All warm water heaters build up pressure and are therefore equipped with a temperature and pressure (T&P) relief valve to ensure safe working condition (Klenck, 1997; van Amerongen, 1972). The heating elements are situated in the middle and the bottom of the tank to efficiently provide heating to the tank. Every heating element also contains a thermostat, which switches the heating element on when the temperature drops below a per-set value and off when it rises above the same per-set value. Changing the per-set value is usually avoided, since the geyser is usually located inside or on the roof.

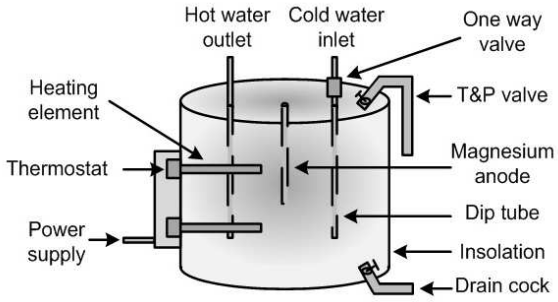

Figure 2: Conventional water heating system (geyser)

The conventional geyser is further equipped with a drain cock, which can be used to empty the tank if required.

Some conventional geysers have two heating elements, which can operate individually. The bottom heating element and thermostat turns on when the temperature drops below the per-set value and the top heating element and thermostat is used as an energy cut off (ECO) device, only switching on when the temperature drops even further (ACME, 2010).

Sowmy and Prado (2008) provide more detail on the assessment of the energy efficiency of electric storage water heaters.

2.3 Heating elements

When designing an in-line water heating system it is important to know what heating elements are available. Heating elements usually range from 150 W to 4 kW and are available in the following materials: copper, steel, stainless steel, cast iron, incoloy, titanium and PFA coated (Omega, 2011).

Immersion heating elements are the most commonly known heating elements, which are normally used in geysers, washing machines, sterilizers and other commercial products. The two basic types of immersion heating elements available are over-the-side and screw-in (or screw plug) (Omega, 2011). Figure 3 shows examples of these two types of heating elements (Swiftheat, 2011).

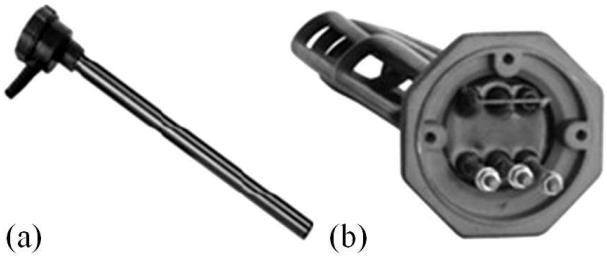

Figure 3: Example of an (a) over-the-side heating element and (b) screw-in heating element

The over-the-side heating elements are designed to hang over the side of a tank and are usually used where the heating element is not able to fit in at the bottom or top of the tank. The sleeve material of the over-the-side heating element is the most important quality to consider when deciding on this product. The sleeve/sheath materials available are: aluminium, brass, copper, fluropolymer, high temperature foil, iron, nickel alloy, polyimide, steel and stainless steel.

Screw plug heating elements consist of tubular elements which can be welded or braced into a screw plug. The element is usually connected to a tank (Tempco, 2011). The sleeve/sheath materials available are: steel, incoloy, copper and 316 stainless steel. The screw plug heating element is usually the most commonly used and affordable.

2.4 Water consumption

Water consumption is usually divided into two parts: 1) the total daily water usage per person and 2) the total daily only warm/hot water usage per person. For an average household, the consumption is usually multiplied by four (Ilsette, 2010). The average hot water consumption for a household of four is approximately 292.8 litres per day in South Africa. This data must be taken in account when a product such as a geyser or an in-line water heating system is bought or designed.

The location of the in-line water heater or geyser also affects the amount of water being used. In-line water heaters are normally installed as close as possible to where hot water is required, whereas conventional water geysers are normally installed at the centre of a household to provide hot water for the whole household. Normally more than one in-line water heater is installed at a household.

3. In-line water heating system design and cost analysis

This section provides a summary on the design and cost analysis of the in-line water heating system. The detailed design and design specifications are provided by Le Roux and Gouws (2011).

For this project, is was decided to build an in-line water heating system with an installed capacity of 12 kW and compare the cost and efficiency of this system with a 150 litres, 47 kg, 600 kPa conventional geyser with an installed capacity of 3 kW. Standard residential in-line water heating systems normally range from 1.2 kW to 4 kW.

3.1 Overview on the design

The components (items) used in the design of the in-line water heating system consists of a PID controller, power inlet at 230 VAC, electromechanical relay, contractor, three 4 kW screw-in type stainless steel elements, three stainless steel cylinders, a PT 100 temperature sensor, a cold water inlet with pressure reducing valve, a warm water outlet faucet with a flow switch mounted inside the outlet pipe and a digital energy meter.

Figure 4 shows the face view of the designed in-line water heating system. The left image shows a detailed drawing with the actual measurements and the right image shows the actual system. In this figure, the temperature controller, earth leakage, contactor, flow switch and temperature probe can be seen.

Figure 5 shows the rear view of the designed in-line water heating system. In this figure, the three 4 kW elements and three stainless steel cylinders can be seen. The use of different types of heating elements will increase the overall efficiency, but will also increase the overall system cost.

For this project it was decided to use 4 kW screw-in type heating elements, since it was the most affordable and was available (in stock) for less than R 120 each.

The heat flow analysis of the stainless steel cylinders was done by using the Cosmosflo tool of Solidworks®. Le Roux and Gouws (2011) provide more detail on the heat flow analysis of the designed in-line water heating system.

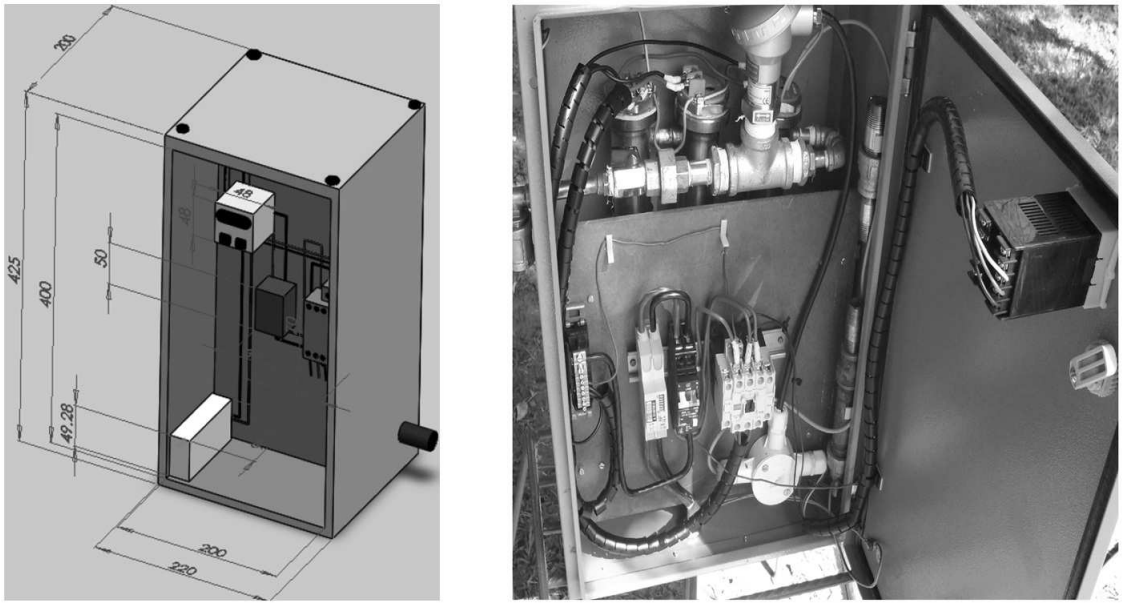

Figure 4: Face view of the designed in-line system (simulated and physical model)

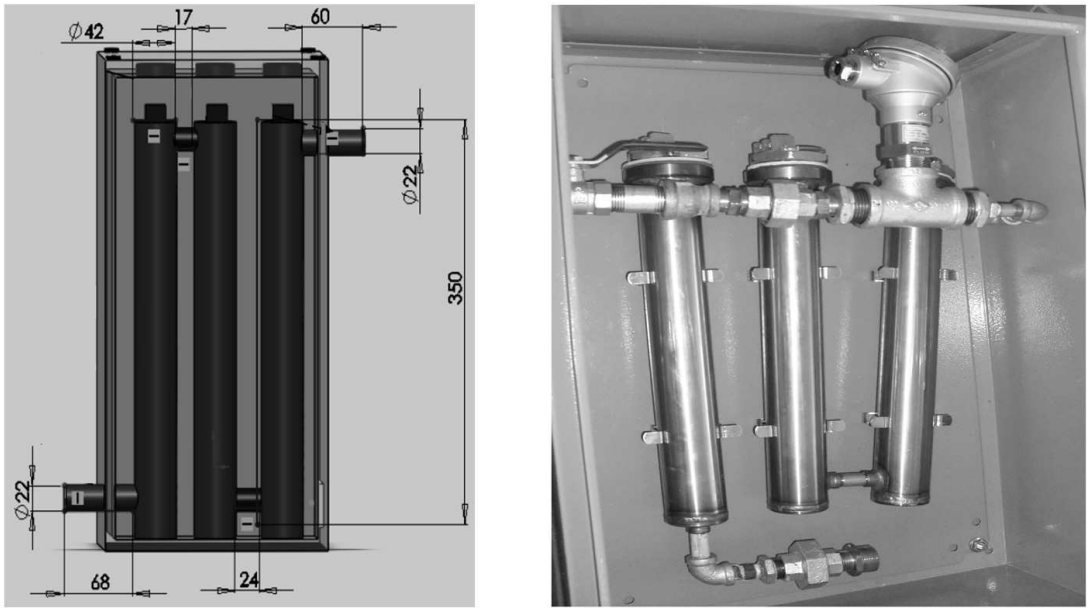

Figure 5: Rear view of the designed in-line system (simulated and physical model)

3.2 Overview on the temperature controller

This section provides an overview on the operating principle of the temperature controller for the designed in-line water heating system.

The temperature controller together with the heating cylinders (or heating elements) is the most important components (items) of the designed in-line water heating system. The temperature controller has a direct influence on the efficiency of the designed in-line water heating system. For this project, the CN-40 temperature controller from TOHO Electronics in Japan was selected, since the temperature controller has build in PID control to improve the speed of the response, suppress disturbances and reduce oscillation.

Figure 6 provides the operating flowchart of the temperature controller. When the in-line water heating system is switched off the heating elements and PID controller is also off.

When the system is switched on, a flow reading is taken. When there is no flow, the heating elements and PID controller is switched off. When a flow is detected, the process value (PV) and set-point value (SV) are measured.

When the PV is not the same as the SV, the PID controller and heating elements is switched on. When the PV and SV are the same, the heating elements and PID controller is switched off. The sys-

tem returns to the initial measurement and reading block after each cycle.

Throughout this cycle the user is always aware of the energy consumption and can choose to switch to a lower temperature setting (lower SV) to save energy.

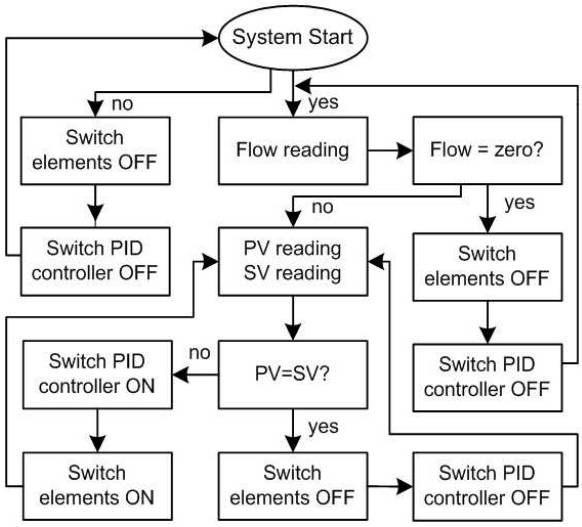

Figure 6: Temperature controller operating flowchart

After the in-line water heating system was successfully build, the system was tested at the maximum flow rate of 8 l/min. The system was able to immediately heat the cold water (at 15°C) to 39°C. The total power required at this rate was 12 kW and the total current drawn was 52.17 A.

3.3 System cost analysis

This section provides the cost analysis of the designed in-line water heating system. Table 1 presents the breakdown of the total integrated cost of the in-line water heating system. Components (items) were chosen according to minimum requirement, safety, availability and available funding.

The total cost of the in-line water heating system resulted to R3 980.26 including tax at 14%. The system could however, be manufactured at an estimated cost of around R3 000 including taxes, if only two heating cylinders were used in the design process and if the components were bought in bulk.

4. Results

In this section, the energy consumption of the designed in-line water heating system is compared to the energy consumption of a conventional geyser. This section also compares the cost of the designed in-line water heating system to other water heating systems.

4.1 Energy consumption comparison

The total average current drawn by the designed in-line water heating system was measured at 44.6 A (during the on cycle at a flow rate of 5.022 l/min),

Table 1: Total cost of the in-line water heating system

Item	Price (R)
Heating elements with pocket (3 x 4 kW)	347.49
Flow switch (flow/pump in-line switch)	520.00
Enclosure (orange stainless steel)	420.31
Stainless steel cylinders (welding & pipe)	1 078.00
Temperature controller (CN-40)	783.00
Temperature sensor (PT100)	
Digital energy meter	195.00
150.00	
Contactor	250.00
Earth leakage (additional)	114.00
Neutral bar and adapter plate	58.58
Galvanized pipe fittings	50.00
Miscellaneous fittings	127.88
Total	3980.26

while the conventional 150 litres geyser only drawn 16.1 A. The in-line water heating system instantly supplied hot water, while the conventional geyser had to heat 150 litres of water before the same temperature of 60°C was reached.

Figure 7 shows the measured profiles of the energy consumption for the designed in-line water heating system and conventional geyser. It can be seen from these profiles that the in-line water heating system follows a linear trend of $y = 1.525x - 1.775$ and the conventional geyser follows a linear trend of $y = 0.6382x - 0.3382$, both with a R^2 value of more than 0.9988.

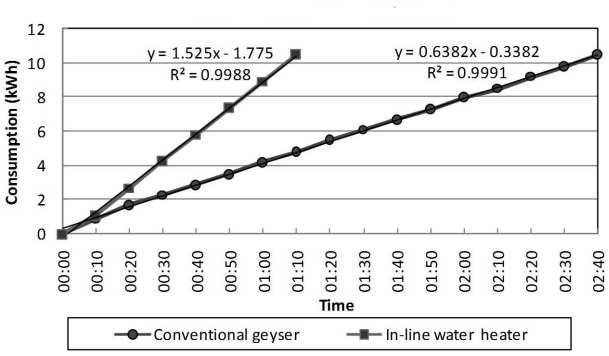

Figure 7: Energy consumption comparison

Table 2 provide a comparison between the measured results of the conventional geyser and the designed in-line water heating system. From this table, it can be seen that the conventional geyser on average consumed 10.5 kWh (over a period of 160 minutes) to heat 150 litres of water from 15°C to 60°C. This means that the conventional geyser on average consumed 26.25 Wh to heat one litre of water from 15°C to 60°C.

The in-line water heating system consumed 10.5 kWh (over a period of 70 minutes) to supply, on

average, 351.54 litres of water at 60°C. The inline water heating system therefore on average consumed 25.60 Wh to heat one litre of water at 60°C.

The conventional geyser therefore on average consumed 0.65 Wh per litre more than the in-line water heating system. The conventional geyser therefore, on average, consumes 2.5% more energy to heat one litre of water from 15°C to 60°C than the designed in-line water heater to supply one litre of water at 60°C.

The measured data was recorded over a period of a few days and the average consumption was then calculated. The standing losses and long pipe losses therefore have an influence on the measured consumption.

Table 2: Energy consumption comparison

	Geyser	*In-line*
Energy consumption	10.5 kWh	10.5 kWh
Recorded time period	160 min	70 min
Water quantity	150 litres	351.54 litres
Water temperature	15°C–60°C	60 °C
Consumption per litre	26.25 Wh/l	25.60 Wh/l
Consumption difference	0.65 Wh/l	
% difference	2.5%	

4.2 Cost comparison between different systems

In this section, the cost of the designed in-line water heating system is compared to the cost of the other water heating systems. Table 3 provide the cost comparison between different water heating systems. From this table, it can be seen that the cost of solar water heating systems ranges between R12 000 and R25 000, and are the most expensive. The cost of conventional geysers ranges between R1 300 and R3 000 and are the most affordable. The cost of heat pumps ranges between R8 000 and R20 000.

The estimated cost of the designed in-line water heating system with two heating cylinders is R3 000 and with three heating cylinders is R4 000. The price on each of the systems in Table 3 depends on the installation size and the variables of the situation. Eskom rebates are however, available on approved solar water heating systems and approved heat pumps, but are not available on conventional geysers and in-line water heating systems.

Table 3: Cost comparison between different water heating systems

Item	*Price (R)*
Conventional geysers	1 300–3 000
Designed in-line heating system	3 000–4 000
Heat pumps	8 000–20 000
Solar water heating systems	12 000–25 000

5. Conclusion

Almost one third of household electricity bills are towards hot water energy consumptions, therefore, improvements and research and in this field will be an ongoing process.

During the control phase of the in-line water heating system, the flow rate instead of the pressure was taken into account. This makes the system more adaptable to areas where a low flow is encountered. The pressure values were only used for safety purposes.

For this project, the energy consumption of the in-line water heating system was measured and compared to a conventional geyser. After performing various tests on both the in-line water heating system and the conventional water heating system, the in-line water heating system showed to be more efficient in terms of watt-hour per litre.

The efficiency analysis results showed that the conventional geyser consumed, on average, 2.5% more energy to heat one litre of water from 15°C to 60°C than the in-line water heating system to supply one litre of water at 60 °C. The data was however, recorded over a period of a few days, therefore, standing losses and long pipe losses have an influence on the result.

The cost analysis results showed that the conventional geyser is more affordable than the in-line water heating system and heat pumps and the solar water heating systems are the most expensive.

It is estimated that a heat pump can potentially provide three times the thermal energy compared to an electrical geyser, which can result in a saving of up to 67% in the water heating cost, depending on the size of the installation and the variables of the situation. Solar water heaters can save up to 70% of your water heating bill, depending on the size of the installation and the variables of your situation.

Apart from the instant and unlimited hot water supply, the in-line water heating system has a number of advantages such as size, adaptability to a variety of locations, and robustness. As with any electrical appliance the consumer can further reduce his or her electricity bill by using the in-line water heating system during off peak periods. Industrial users can preset the unit to deliver a lower temperature during peak periods.

The in-line water heating system can have a lower running cost than the conventional water heating system, if properly managed. The system has no standing losses and no long pipe losses and can save energy and water, if the temperature is correctly chosen. The user can interactively and immediately switch to a lower temperature setting in order to save electricity. It will therefore be possible to only use the correct amount of water (at the correct temperature) with no additional cold water.

The in-line water heating system is a good choice, if hot water is required far from the installed

geyser, heat pump or solar water heating system.

Prud'homme and Gillet (2001) provide more detail on an advanced control strategy for a domestic solar hot water system with a segmented auxiliary heater and LaMeres *et al.* (1999) provide more detail on controlling of the power demand of an average residential electric water heater.

References

ACME, (2010). How does a water heater work. Available at www.acmehowto.com.

DEAT, (2004). A national climate change response strategy for South Africa. Department of environmental affairs and tourism. Available at www.unfccc.int/files/meetings/seminar/application/pdf/sem_ sup3_ south_africa.pdf, Pretoria, September 2004.

EDRC, (2003). Electricity consumption in South African households accounts for approximately 35% of peak demand. Available at www.develop-mentfirst.org/Studies/SouthAfricaCountryStudies.pdf.

Etankless, (2010). Compare electric tankless water heaters. Available at www.etankless.com/compare-tankless-water-heaters.php (Accessed: Dec. 2010).

Ilsette P., (2010). SWH information handbook, [Online] Available at ww.cef.org.za. (Accessed: Dec. 2010]).

Klenck T., (1997). How it works: Water Heater. Available at www.popularmechanics.com (Accessed: Dec. 2010).

LaMeres B.J., Nehrir M.H., Gerez V., (1999). Controlling the average residential electric water heater power demand using fuzzy logic, *Journal on Electric Power Systems Research,* Vol. 52, Issue 3, December 1999, pp. 267-271.

Le Roux E., Gouws R., (2011). Design of an in-line water heating system, North-West University, Project document, Faculty of Engineering, June 2011.

Omega, (2011). Introduction to immersion Heaters. Available at www.omega.com/productinfo/immersion_ heaters.html (Accessed: Jan 2011).

Prud'homme T., Gillet D., (2001). Advanced control strategy of a solar domestic hot water system with a segmented auxiliary heater, *Journal on Energy and Buildings*, Vol. 33, Issue 5, May 2001, pp. 463-475.

Rollins G., (2010). Inline hot water heaters. Available at www.ezinearticles.com. (Accessed: Nov. 2010).

Sebitosi A.B., (2008). Energy efficiency, security of supply and the environment in South Africa: Moving beyond the strategy documents, *Journal on Energy,* Vol. 33, Issue 11, November 2008, pp. 1591-1596.

Sebitosi, A.B., Pillay P., (2008). Renewable energy and the environment in South Africa: A way forward. *Journal on Energy Policy*, Vol. 36, Issue 9, September 2008, pp 3312-3316.

Sowmy D.S., Prado R.T.A., (2008). Assessment of energy efficiency in electric storage water heaters, Elsevier *Journal on Energy and Buildings*, Vol. 40, Issue 12, pp. 2128-2132.

Swiftheat, (2011). Industrial heating elements. Available at www.swiftheat.com (Accessed: June 2011).

Tempco, (2011). Screw plug immersion heaters. Available at www.tempco.com (Accessed: March 2011).

van Amerongen C., (1972). How things work, The Universal Encyclopaedia of Machines, Paladin/Granada Publishing,

Wilson R.P., (1978). Energy conservation options for residential water heaters, *Journal on Energy,* Vol. 3, Issue 2, April 1978, pp. 149-172.

Received 12 August 2011; revised 1 May 2012

Performance of A R22 split-air-conditioner when retrofitted with ozone friendly refrigerants (R410A and R417A)

Bukola Olalekan Bolaji
Department of Mechanical Engineering, Federal University of Agriculture Abeokuta, Nigeria

Abstract
R22 that has been used predominantly in air conditioning and in medium and low-temperature applications contains ozone depleting chlorine atoms and hence will be phased out eventually. This paper presents the experimental performance study of a split-air-conditioner using ozone friendly alternative refrigerants. The existing split-air-conditioner originally designed for R22 as the working fluid was retrofitted with R410A and R417A respectively, and the performance of the system was evaluated and compared with its performance when R22 was used. Experimental results showed that with R417A, the system had 1.9% higher refrigeration capacity and 14.2% lower with R410A when compared to that of R22. The average discharge pressure of the compressor obtained with R417A and R410A were 3.8% lower and 10.3% higher, respectively, than with R22. The lowest compressor power consumption and pressure ratio were obtained with the R417A retrofitted system. The average coefficient of performance (COP) obtained using R417A is 2.9% higher, while that of R410A is 8.4% lower than that of R22. Generally, with R417A the system consistently had the best performance in comparison to both R22 and R410A, indicating that R417A would be a better choice for retrofitting existing split-air-conditioners originally designed to use R22 as working fluid.

Keywords: retrofitting, split-air-conditioners, experimental, performance, R22, R410A, R417A

1. Introduction

The depletion of ozone layer and global warming are still part of the main environment problems that the world is facing today. From the 1930s, chlorofluorocarbon (CFC) substances were widely used as refrigerants, blowing agents, cleaning agents, fire extinguishing agents, spray propellants in refrigeration, air-conditioning, foaming, and the electronics and medicine industries due to their favourable physical and chemical properties. In the 1980s, scientists found that CFC substances not only do great damage to the ozone layer, but also create the greenhouse effect, and badly affect telluric environment and human health (Bolaji, 2005; He *et al.*, 2005).

Hydro-chlorofluorocarbons (HCFCs) cause less harm to the ozone layer. They contain less chlorine atoms in their chemical structure than CFCs. Therefore, they have less ozone depletion potential than CFCs. However, they are considered to be harmful as well. CFCs have been banned in developed countries since 1996, and from January 1st 2010, production and use of CFCs is prohibited completely all over the world. HCFC refrigerants will also be phased out by 2020 and 2030 in developed and developing countries, respectively (Devotta et al., 2005; Bolaji, 2010a; Fatouh et al., 2010).

CFCs and HCFCs are controlled substances by the Montreal Protocol, and greenhouse warming gases are controlled by the Kyoto Protocol. Non-ozone depleting hydrofluorocarbons (HFCs), which have been used as alternative refrigerants for the past two decades, are part of greenhouse warming gases. Consequently, in the long run, refrigerants with low greenhouse warming potential (GWP) and zero ozone depletion potential (ODP) are to be used in refrigeration and air-conditioning applications. At the same time, the performance of refrigeration and air-conditioning equipment has to be improved to reduce the indirect greenhouse warming caused by the use of electricity generated main-

ly by the combustion of fossil fuels (Bolaji, 2010b; Park and Jung, 2009).

R22 has been used predominantly in residential air-conditioners and heat pumps and has the largest sales volume among all refrigerants. R22, however, is an HCFC containing the ozone depleting chlorine atom and hence has to be phased out eventually. The search for alternatives to R22 is a key issue. Many studies have been reported on alternatives to R22 (Fatouh *et al.,* 2010; Park and Jung, 2009; Jabaraj *et al.,* 2006; Chen, 2008; Park *et al*., 2008). At present, alternative refrigerants available for R22 in residential air conditioners and heat pumps can be categorized into three types. First, hydrofluorocarbons (HFCs) represented by R410A, R407C, R417A and R134a. Second, natural substances represented by CO_2 and R717 (Ammonia). However, when working under a supercritical cycle, CO_2 systems have extremely high working pressure, low operation efficiency, and high manufacturing and operation cost. Third, hydrocarbons (HCs) represented by R290 (Propane) and R600a (Isobutene) are also in the group of natural substances. The hydrocarbon has excellent thermal performance and causes a low greenhouse effect, but its safety performance is unacceptable. It is usually flammable or toxic, which limits its use in residential air conditioners and heat pumps (Nicola *et al*., 2005; Bolaji, 2008; Chen, 2008).

Blends of the HFC refrigerants, in the first category of alternative refrigerants, have been considered as the favourite candidates for R22 alternatives (Bitzer, 2007). In middle 1990s, the application of R407C in residential air conditioners and heat pumps received wide acceptance in the European market. R407C is a ternary mixture refrigerant composed of R32/R125/R134a (23/25/52% in weight). The operation pressure and temperature of R407C are equivalent to those of R22, therefore, just small modifications on existing R22 air-conditioners are needed for changing to R407C.

However, Aprea and Greco (2002) compared the performance between R22 and R407C (azeotropic blend) and suggested that R407C is a promising drop-in substitute for R22. Experimental tests were performed in a vapour compression plant with a reciprocating compressor to evaluate the compressor performance using R407C in comparison to R22. The plant overall exergetic performance was also evaluated and revealed that the performance with R22 is consistently better than that when its candidate substitute (R407C) is used. R407C is a non-azeotropic refrigerant mixture, and its temperature glide can reach 4–6°C. The operation efficiency of a R407C air-conditioner is low and it is difficult to repair and maintain the system for its bigger variation of evaporation temperature when R407C is leaked (Han *et al.,* 2007). Therefore, other refrigerants should be considered and studied as alternatives to R22.

Many refrigerants were assessed through the Alternative Refrigerant Evaluation Program (AREP) as potential replacements for R22. Among the promising alternative refrigerants that emerged were R410A a HFC refrigerant mixture and R32 a HFC refrigerant. R410A is a near azeotropic blend composed of R32/R125 (60/40% in weight). The high heat transfer coefficients in the evaporator and condenser provide potential for increased efficiencies. Because of the negligible temperature glide (<0.2 K), the general usability can be seen similar to a pure refrigerant (Bitzer, 2007).

Among all the R22 alternative refrigerants available in the market, is the R417A, which is the ternary mixture refrigerant, composed of R125/R134a/R600 (46.6/50/3.4% in weight). R417A is the mostly recommended for air conditioning equipment and water chillers (Torrella *et al.,* 2010). This refrigerant adds a small percentage of hydrocarbon in order to ensure the return of the lubricant oil to the compressor and the compatibility with traditional mineral oils or new lubricants such as polyol ester oil.

Window air-conditioners are rapidly being replaced by split type air-conditioners due to the latter better performance and lower noise. This paper reports the performances of R410A and R417A investigated experimentally in a split-air-conditioner originally designed to use R22. The air conditioner was retrofitted with the alternative refrigerants and the performance of the system was evaluated and compared with when R22 was used as the working fluid.

2. Materials and methods

2.1 Experimental setup

The split-air-conditioner is composed of the basic components of a vapour compression refrigeration system: a hermetically sealed compressor, a condenser, a capillary tube and an evaporator, and such attachments as accumulator and fans. The schematic diagram representing the experimental air-conditioner is shown in Figure 1. The unit was retrofitted with R410A and R417A, respectively. An oil level indicator was attached to the compressor to check the oil level periodically. To monitor the mass flow rate of the refrigerant in the system, a mass flow meter with ±0.25% accuracy was installed next to the condenser. In order to have a uniform temperature throughout the room, a ceiling fan of 70 W power installed in the centre of the room was used to circulate the air inside the room. To measure the compressor power, a wattmeter with ±0.5% accuracy was used. Room temperature was measured with help of precision thermometer with an accuracy of ±0.1°C. Refrigerant pressures were measured using precision Bourdon's tube pressure gauges with an accuracy of ±5.0 kPa.

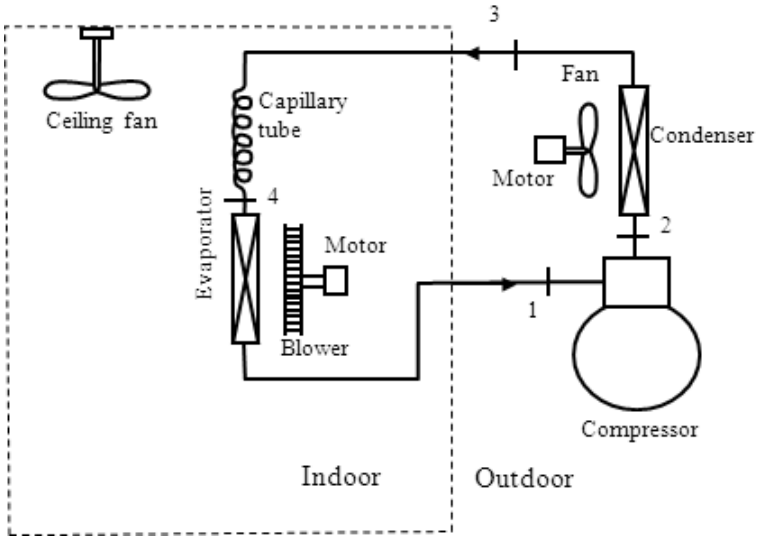

Figure 1: Schematic diagram of the experimental split-air-conditioner

2.2 Retrofitting procedures

The procedure of Devotta *et al.* (2005) was followed. The system was first tested with R22 in order to obtain the baseline data. After the completion of all tests with R22, the air conditioner was retrofitted with R410A and R417A, respectively. Mineral oils and alkyl-benzene lubricants use in R22 systems are immiscible with the alternative refrigerants. R410A and R417A are HFC refrigerants, they have very low solubility and they do not mix well with mineral oil, which could cause poor oil return to the compressor, resulting in possible compressor failure and fouling of expansion device and heat exchanger surfaces, leading to reduced system performance. In order to achieve miscibility of these refrigerants with the lubricant, a polyol ester was used in the retrofitted systems (Bitzer, 2007).

During retrofitting, R22 was first recovered then the compressor was removed from the system and the mineral oil was drained through the suction line of the compressor. The compressor was charged with fresh polyol ester lubricant. The compressor was reinstalled back to the system and the system was recharged with the recovered R22 refrigerant following the standard charging operation. The compressor was operated with the polyol ester lubricant and the R22 refrigerant for 24 hours, after which the polyol ester oil was drained and recharged with fresh polyol ester oil. This was done in order to remove the residual mineral oil from the system. Recharging of the system and running of the compressor were repeated until no significant residual mineral oil was obtained.

R22 was recovered from the system and the capillary tube was replaced with one of greater restriction in order to achieve satisfactory performance. ASHRAE (1998) recommends replacement of the capillary tube with one of the same diameter, but from 70 to 90% longer. Therefore, a 1000 mm long capillary tube used for R22 was changed to 1800 mm long in the retrofitted system. The filter-drier was replaced by a solid core filter-drier compatible with HFC refrigerants. The system was checked for leaks with dry nitrogen. The evacuation of moisture in the system was also carried out through the service ports with the help of a vacuum pump prior to the system being charged with replacement refrigerant. The system was thoroughly checked and commissioned before it was subjected to series of tests at various conditions.

2.3 Performance parameters analysis

The power consumption of the compressor (W_c), the fan in the condensing unit (W_f) and the blower in the evaporating unit (W_b) were measured separately. The total power consumption (W_t) is obtained using Eq. (1):

$$W_t = W_c + W_f + W_b \quad (1)$$

Refrigeration capacity (Q_{evap}) was calculated using the mass flow rate of refrigerant ($\dot{m}$) and enthalpy difference between inlet (h_4) and outlet (h_1) of the evaporator:

$$Q_{evap} = \dot{m}\,(h_1 - h_4) \quad (2)$$

The actual coefficient of performance (COP) for the system is computed at the steady-state when the minimum temperature is achieved in the conditioned room and it is obtained as the ratio between the refrigeration capacity (Q_{evap}) and the total power consumption (W_t). The total power consumption was used in Eq. (3) not just the compressor power in order to obtain the actual overall COP of the system.

$$\text{COP} = \frac{Q_{evap}}{W_t} \quad (3)$$

The compressor pressure ratio is the ratio between the compressor discharge pressure (P_{dis}) and suction pressure (P_{suc}):

$$\text{P}_\text{R} = \frac{P_{dis}}{P_{suc}} \quad (4)$$

3. Results and discussion

R22 and its retrofit refrigerants (R410A and R417A) were used in the split-air-conditioner and the system's performance was evaluated and compared. The result of the refrigeration capacity obtained at different evaporating temperatures is shown in Figure 2. Evaporating temperature was varied between 2°C to 12°C as a result of the variation of the indoor temperatures from 16°C to 27°C using the system temperature control. It was observed that for all the investigated refrigerants, the refrigeration capacity increased with the increase in evaporating temperature. At the same, evaporating temperature, refrigeration capacity obtained with the R417A system is higher than that from the R22 and R410A systems. Average refrigeration capacity of the system containing R417A is higher by 1.9%, while that with R410A is lower by 14.2% than that with R22.

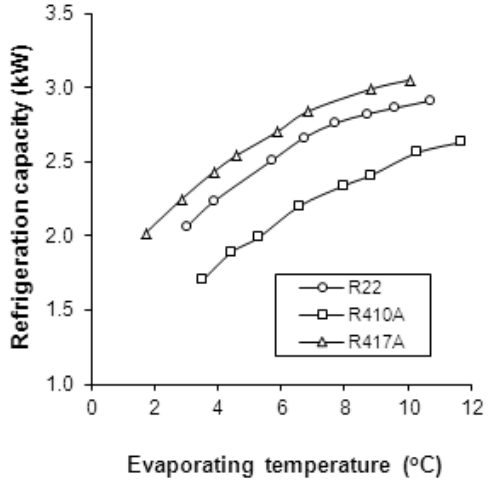

Figure 2: Variation of refrigeration capacity with evaporating temperature

Figure 3 shows the relationship between the compressor power and the evaporating temperature of R22 and the alternative refrigerants. As shown in the figure, the changes of compressor power with evaporating temperature are similar for the three refrigerants; as the evaporating temperature increases, the compressor power also increases. The compressor power with R410A is higher than those with R22 and R417A. Compared with R22, the average compressor power with R410A increased by 11.2%, and that with R417A, reduced by 4.7%.

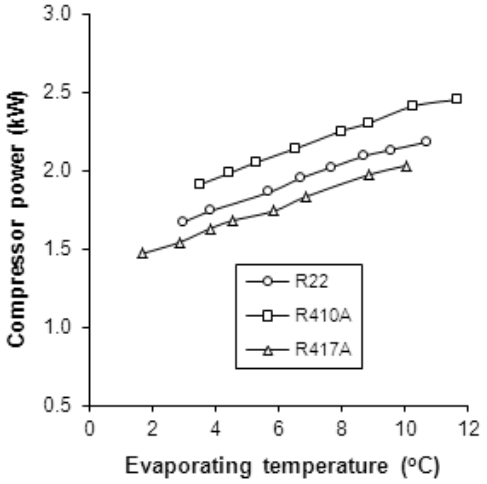

Figure 3: Variation of compressor power capacity with evaporating temperature

The relationship between the coefficient of performance (COP) and evaporating temperature is shown in Figure 4. This figure indicates that when the COP increases the evaporating temperature increases for both R22 and retrofitted refrigerants. The COP with R417A was higher than those with R22 and R410A at all evaporating temperatures. The lowest COP was obtained in the R410A retrofitted system. Compared with R22, the average COP of R417A increased by 2.9%, while that of R410A reduced by 8.4%.

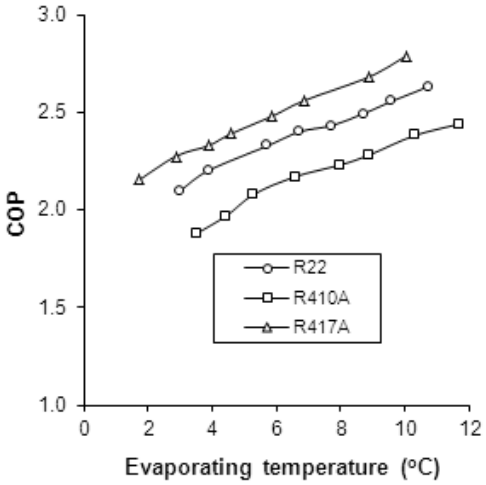

Figure 4: Variation of coefficient of performance with evaporating temperature

The discharge temperature of the compressor is used as a criterion in considering suitability of use. The discharge temperature of the compressor must not be too high since it may impair lubrication and adversely affecting the mechanical parts of the compressor. The relationship between the discharge

temperature of the compressor and evaporating temperature for the investigated refrigerants is shown in Figure 5. It was observed in the figure that when the evaporating temperature changes, the discharge temperature remains almost constant with only a very small change. Increase in the evaporating temperature slightly increases the discharge temperature. The system produced a lowest discharge temperature with R417A than with R22 and R410A refrigerants. The average discharge temperatures of the system with R417A and R410A are 3.8% lower and 10.3% higher, respectively, than with R22 system.

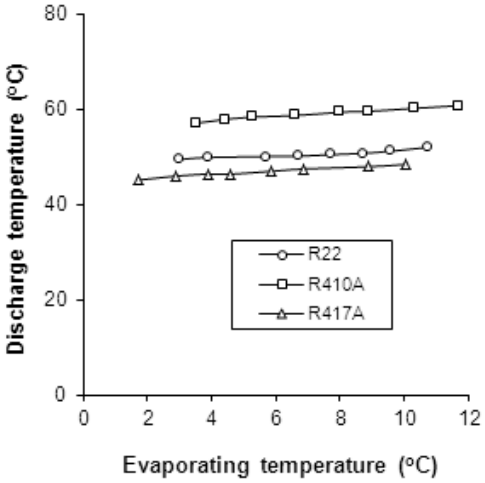

Figure 5: Variation of compressor discharge temperature with evaporating temperature

The performances of investigated refrigerants in the split-air-conditioner were obtained for different ambient air temperatures. The ambient air temperature varied from 26°C in the early hours of the day to 37.5°C in the late afternoon; it increases as the intensity of the solar insolation increases. The refrigeration capacity and COP obtained with R22, R410A and R417A at various ambient temperatures are plotted in Figures 6 and 7, respectively. As shown in these figures, the refrigeration capacity and COP reduce as ambient air temperatures increases. Also, it can be seen from these figures that the performances with R417A system are much better than with R22 and R410A systems.

Figures 8 and 9 compare the variation of compressor power and pressure ratio for the three refrigerants in terms of ambient air temperature. As shown in these figures, compressor power and pressure ratio increase as the ambient temperature increases, but there is considerable difference in the performances with R417A, R22 and R410A. The compressor power and pressure ratio with R410A were found to be the highest among the refrigerants at all ambient air temperatures. Close behaviour was observed when the system was charged with R417A and R22, but with R417A, the system had slightly lower compressor power and pressure ratio, which shows that the split-air-conditioner had better performance with R417A than with R22.

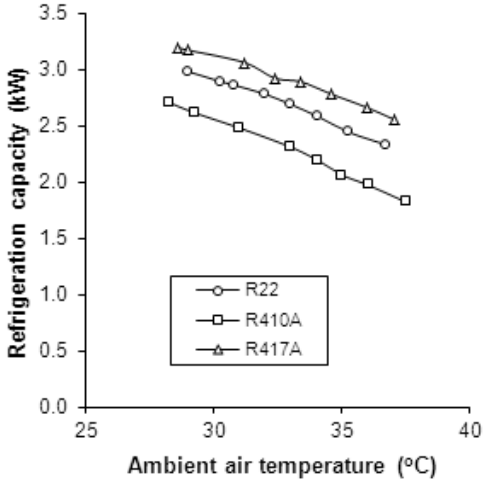

Figure 6: Effect of ambient air temperature on the refrigeration capacity

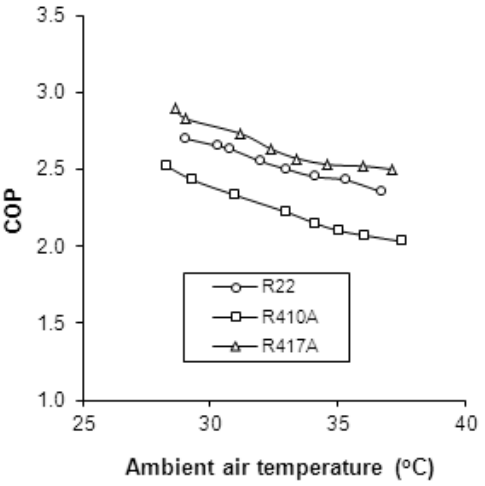

Figure 7: Effect of ambient air temperature on the coefficient of performance (COP)

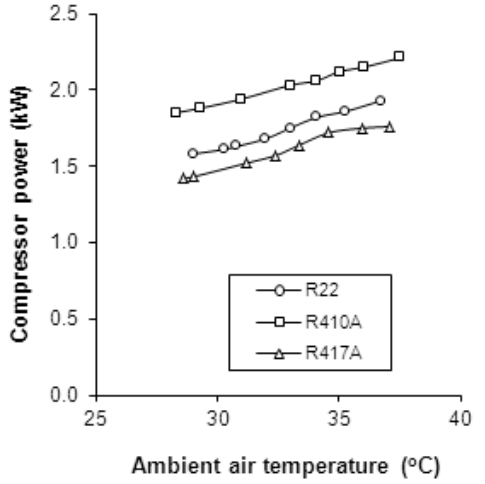

Figure 8: Effect of ambient air temperature on the compressor power

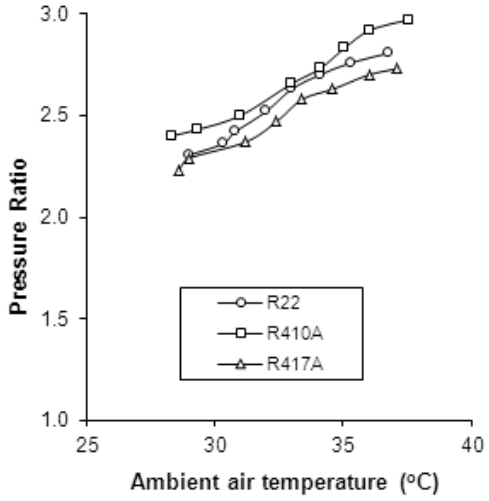

Figure 9: Effect of ambient air temperature on the pressure ratio

4. Conclusion

In this study, experiments were carried out to investigate R22 and its retrofit substitutes (R410A and R417A) in a split-air-conditioner. Based upon the experimental results, the following conclusions were drawn:

(i) For all the investigated refrigerants, the performance parameters increased with the increase in evaporating temperature. Except for compressor discharge, temperature remains almost constant irrespective of evaporating temperature.

(ii) For all the investigated refrigerants, as the ambient air temperature increases, the refrigeration capacity and COP reduce, while the compressor power and pressure ratio increase.

(iii) At the same evaporating temperature, refrigeration capacity obtained with R417A is higher than those obtained with R22 and R410A. The average refrigeration capacity with R417A is higher by 1.9%, while that with R410A is lower by 14.2% than that with R22.

(iv) The lowest power consumption was obtained with R417A retrofitted system. The average compressor power with R417A and R410A was found to be 4.7% lower and 11.2% higher, respectively, than that obtained when using R22.

(v) The average COP with R417A and R410A were found to be 2.9% higher and 8.4% lower, respectively, than that with R22.

(vi) The average discharge pressure of the compressor obtained with R417A and R410A was 3.8% lower and 10.3% higher, respectively, than that with R22.

Finally, the system when charge with R417A consistently had the best performance when compared with when it containing R22 and R410A, therefore, R417A would be a better choice for retrofitting existing split-air-conditioners originally designed to use R22 as the working fluid.

References

Aprea, C., and Greco, A., (2002). An exergetic analysis of R22 substitution. *Applied Thermal Engineering* 22(13): 1455-1469.

ASHRAE, (1998). *Refrigeration Handbook*, American Society of Heating, Refrigerating, and Air-Conditioning Engineers, Chapter 2, Inc. Atlanta (GA), ISBN 1-883413-54-0.

Bitzer, (2012). Refrigerant Report. *Bitzer International*, 15th Edition, 71065 Sindelfingen, Germany, www.bitzer.de Accessed on March 8, 2012.

Bolaji, B.O., (2005). Refrigerants and stratospheric ozone: past, present and future. In: Okoko E, Adekunle, VAJ eds. Environmental Sustainability and Conservation in Nigeria. *Book of Readings of Environment Conservation and Research Team*, Jubee Publisher Akure, Nigeria: 231-239.

Bolaji, B.O., (2008). Investigating the performance of some environment-friendly refrigerants as alternative to R12 in vapour compression refrigeration system. PhD. Thesis in the Department of Mechanical Engineering, Federal University of Technology Akure, Nigeria.

Bolaji, B.O., (2010a). Selection of Environment-Friendly Refrigerants and the Current Alternatives in Vapour Compression Refrigeration Systems. *Proceedings of Multi-Disciplinary International Conference,* Ghana Institute of Management and Public Administration, Ghana: 27-39.

Bolaji, B.O., (2010b). Experimental Analysis of Reciprocating Compressor Performance with Eco-Friendly Refrigerants. *Proc. IMechE, Part A: Journal of Power and Energy* 224: 781-786.

Chen, W., (2008). A comparative study on the performance and environmental characteristics of R410A and R22 residential air conditioners. *Applied Thermal Engineering* 28: 1-7.

Devotta, S., Padalkar, A.S., and Sane, N.K., (2005). Performance assessment of R22 window air conditioner retrofitted with R407C. *Applied Thermal Engineering* 25: 2937-2949.

Fatouh, M., Ibrahim, T.A., and Mostafa, A., (2010). Performance assessment of a direct expansion air conditioner working with R407C as an R22 alternative. *Applied Thermal Engineering* 30: 127–133.

Han, X.H., Wang, Q., Zhu, Z.W., and Chen, G.M., (2007). Cycle performance study on R32/R125/R161 as an alternative refrigerant to R407C. *Applied Thermal Engineering* 27: 2559-2565.

He, M., Li, T., Liu, Z., and Zhang, Y., (2005). Testing of the mixing refrigerants R152a/R125 in domestic refrigerator. *Applied Thermal Engineering* 25: 169-1181.

Jabaraj, D.B., Avinash, P., Lal, D.M., and Renganarayan, S., (2006). Experimental investigation of HFC407C/HC290/HC600a mixture in a window air conditioner. *Energy Conversion and*

Management 47: 2578-2590.

Nicola, G.D., Giuliani, G., Polonara, F., and Stryjek, R., (2005). Blends of carbon dioxide and HFCs as working fluids for the low-temperature circuit in cascade refrigerating systems, *International Journal Refrigeration* 28: 130-140.

Park, K., and Jung, D., (2009). Performance of heat pumps charged with R170/R290 mixture. *Applied Energy* 86: 2598-2603.

Park, K., Shim, Y., and Jung, D., (2008). Performance of R433A for replacing R22 used in residential air-conditioners and heat pumps *Applied Energy* 85: 896-900.

Torrella, E., Cabello, R., Sanchez, D., Larumbe, J.A., and Llopis, R., (2010). On-site study of R22 substitution for HFC non-azeotropic blends (R417A, R422D) on a water chiller of a centralized HVAC system. *Energy and Buildings* 42: 1561-1566.

Received 9 May 2011; revised 19 March 2012

Regression-SARIMA modelling of daily peak electricity demand in South Africa

Delson Chikobvu
Department of Mathematical Statistics and Actuarial Science, University of the Free State, South Africa

Caston Sigauke
Department of Statistics and Operations Research, School of Mathematical and Computer Sciences, University of Limpopo, South Africa

Abstract
In this paper, seasonal autoregressive integrated moving average (SARIMA) and regression with SARIMA errors (regression-SARIMA) models are developed to predict daily peak electricity demand in South Africa using data for the period 1996 to 2009. The performance of the developed models is evaluated by comparing them with Winter's triple exponential smoothing model. Empirical results from the study show that the SARIMA model produces more accurate short-term forecasts. The regression-SARIMA modelling framework captures important drivers of electricity demand. These results are important to decision makers, load forecasters and systems operators in load flow analysis and scheduling of electricity.

Keywords: daily peak demand; SARIMA; regression-SARIMA; short term load forecasting

1. Introduction

Modelling daily peak electricity demand is important as it provides short-term forecasts which will assist system operators in dispatching of electrical energy. Prediction of load demands is very important for decision making processes in the electricity sector. Decision making in this sector involves planning under uncertainty. This involves, for example, finding the optimal day to day operation of a power plant and even strategic planning for capacity expansion. The demand of electricity forms the basis for power system planning, power security and supply reliability (Ismail *et al.*, 2009). It is important therefore, to produce very accurate forecasts as the consequences of underestimation or overestimation can be costly. Underestimation has a serious negative impact on the national electricity supply system of a country. It may result in the national electricity supply system becoming unstable thus leading to supply interruption if left unchecked. This may even lead to further loss of business as restoration of a plant or construction of new plants takes a long time before generation can start. If the entire national electricity supply system were to shut down, it would take days, possibly even weeks to restore. Overestimation results in wastage of resources due to excess production. As noted by Taylor (2008), accurate short-term forecasts are needed by both generators and retailers of electricity particularly, during periods of abnormal peak load demand. Accurate forecasts will enable effective load shifting between transmission substations. In order to improve forecast accuracy it is important to combine statistical forecasting methods together with judgmental techniques. Through experience, the judgmental experts develop intuitive relationships between electrical load and weather parameters, time of day, day of week, season and time lag of response, (Ismail *et al.*, 2009). On the other hand, statistical techniques provide a scientific approach for producing consistent and accurate forecasts.

Load forecasting has been studied extensively for over four decades using classical time series, regression and neural network methods. Amaral *et al.* (2008) developed a smooth transition periodic autoregressive (STPAR) model and this was evaluated against alternative load forecasting models using electricity load series data from Australia. STPAR proved to be a useful tool when forecasting

the electricity load. In their paper, Sumer *et al.* (2009) developed ARIMA, SARIMA (seasonal ARIMA) and regression models with seasonal latent variable in forecasting electricity demand of the data from 'Kayseri and Vicinity Electricity Joint-Stock Company'. Their results show that the regression model with seasonal latent variable is more efficient than ARIMA and SARIMA. Taylor (2008) used minute-by-minute data on British electricity demand to evaluate 10-30 minutes ahead prediction methods. It is argued that such short lead times are important for the real-time scheduling of electricity generation. ARIMA models, an adaptation of the Holt-Winters' exponential smoothing model and an exponential smoothing method that focuses on the evolution of intraday cycle, are used. Out of these methods, the double seasonal adaptation of the Holt-Winters' exponential smoothing model gives the best results and this is consistent with results from previous studies. Soares and Medeiros (2008) consider a two-level method for hourly electricity load. A Two-Level Seasonal Autoregressive (TLSAR) model is developed and compared with a modified version of a SARIMA model called Dummy-Adjusted SARIMA (DASARIMA). A specific class of seasonal ARIMA models (the benchmark model) and the generalized long memory (GLM) model discussed by Soares and Souza (2006) are better than DASARIMA. A possible extension of this methodology to combining forecasts, interval forecasts and forecast density evaluation is suggested.

Use of regression based methods and neural network models are also discussed in the literature. A hybrid neural network model for daily electrical peak load forecasting (PLF) is presented by Amin-Naseri and Soroush (2008). A novel approach for clustering data by using a self-organizing map is proposed, for which a feed forward neural network (FFNN) is developed for each cluster to provide the PLF. It is concluded that the proposed hybrid model produces superior forecasts than those of the linear regression. The modelling and short-term forecast of daily power demand in the state of Victoria, Australia, is discussed in Truong *et al.* (2008). A two-dimensional wavelet based state dependent (SDP) modelling approach is adopted to formulate a compact mathematical model that is used to forecast daily peak power demand from 9 to 24 August 2007. With a MAPE of 1.9%, the model is found to be effective. A non-linear multivariable regression model for mid-term energy forecasting of power systems in annual time base is developed by Tsekouras *et al.* (2007) and applied to the Greek power system using different categories of low voltage customers. The model includes a correlation analysis of the selected input variables and performed an extensive search to select the most appropriate variables. Ismail *et al.* (2009) use a rule-based forecasting approach for forecasting peak load electricity demand. The authors conclude that rule-based forecasting increases the forecast accuracy when compared to the traditional SARIMA model and that improvement depends on the conditions of the data, knowledge development and validation. Ramanathan *et al*. (1997) develop a simple and flexible set of models for hourly load forecasting and probabilistic forecasting. These are multiple regression and exponential smoothing methods. The models developed perform well against a wide range of alternative models.

Some research has been done on South African electric load data. Notable contributions in this area are those of Amusa *et al.* (2009) who apply the bounds testing approach to co integration within an autoregressive distributed lag framework to examine the aggregate demand for electricity in South Africa during the period 1960-2007.

Hahn *et al.* (2009) gave an overview of some of the methods used in demand load forecasting. The methods were classified into regression based, time series, state space and kalman-filtering. Artificial and computational intelligence methods are also suggested. Neural networks and support vector regression methods fall into this class. However, the current trend is to develop hybrid models as they are seen to be more robust. A most recent review forecasting is given in Munoz *et al*., (2010) and Suganthi and Samuel (2011).

The paper discusses the application of the SARIMA and regression with SARIMA errors (regression-SARIMA) to daily peak demand (DPD) forecasting in South Africa. The regression-SARIMA modelling framework captures important drivers of electricity demand. These factors are weather variables, economic and calendar effects and are known to influence electricity demand. An extension of the regression-SARIMA modelling framework is discussed in detail in (Sigauke and Chikobvu, 2011). The rest of the paper is organized as follows. A detailed discussion of the data including fitting a probability distribution is presented in Section 2. SARIMA and regression-SARIMA models are then developed in Section 3. Empirical results from the study are covered in Section 4. A comparative analysis of the two models together with the Winter's triple exponential smoothing model is discussed in section 5. The summary and conclusion of the paper are covered in section 6.

2. Data

It is important that the amount of electricity drawn from the grid and the amount generated balances (Cottet and Smith, 2003; Taylor, 2006) and this amount is called electricity load which is equal to electricity demand in the absence of blackouts and load-shedding. Aggregated DPD data from all sectors of the South African economy for the period January 1996 to December 2009 is used in this

Table 1: Descriptive statistics for DPD

	Mean	*Median*	*Max*	*Min*	*Std Dev*	*Skew*	*Kurtosis*
DPD	27406	27289	37158	16601	3809	0.0703	2.2710

Table 2: Comparison of alternative distributions

Distribution	*Log Likelihood*	*AIC*	*Estimated parameters*
Normal	-49257.4	98518.8	Mean = 27406.05 (53.23) Std dev = 3808.76 (37.69)
Lognormal	-49275.28	98554.55	Meanlog =10.2087 (0.001972) Sdlog = 0.1408 (0.001394)
Weibull	-49368.46	98740.93	Shape = 7.9097 (0.0844) Scale = 29074.87 (54.399)

paper. The data is from Eskom, South Africa's power utility company. DPD is the maximum hourly demand in a 24-hour period. There are 5097 observations. Table 1 gives a summary of the descriptive statistics of DPD.

The time series plot of DPD in Figure 1 shows a positive linear trend and strong seasonality. The null hypothesis of a stochastic trend is accepted under the Augmented-Dickey Fuller unit root test.

A spectral analysis is carried out to investigate the periodicity in the data. The spectral density shows a seven day periodicity. We fit a probability distribution to the sample data. Table 2 shows a comparison of alternative distributions fitted. The normal distribution is the best fitting distribution since it has the largest log likelihood and smallest Akaike information criterion statistics. The estimated parameters of the normal distribution together with the standard errors in parentheses are: mean = 27406.05 (53.23) MW and standard deviation = 3808.76 (37.69) MW. Empirical and theoretical cumulative distribution functions (CDFs) for the Weibull, normal and lognormal distributions given in Figure 2 also show that the normal distribution is the best fitting distribution.

The probability density function of DPD was estimated using kernel density estimation (Silverman, 1986) and is plotted in Figure 3.

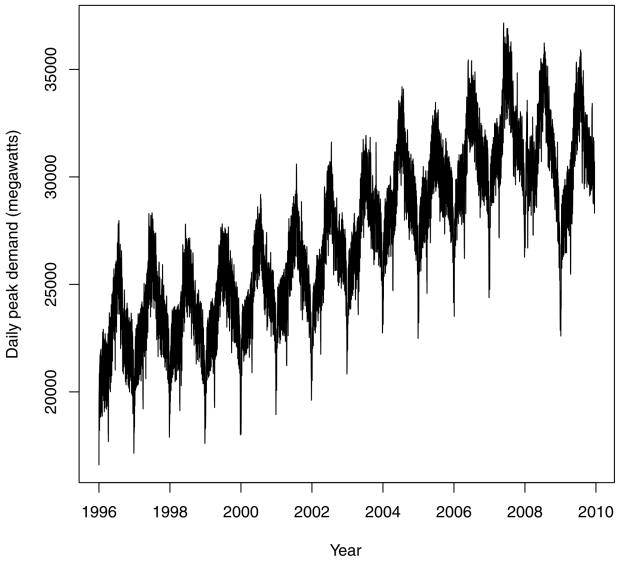

Figure 1: Time series plot of daily peak electricity demand (01-01-1996 to 14-12-2009)

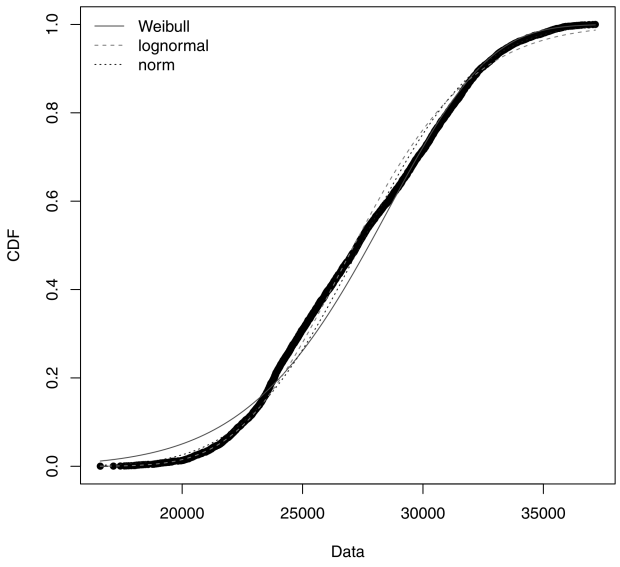

Figure 2: Empirical and theoretical CDFs for the Weibull, normal and lognormal distributions

3. The models

3.1 SARIMA Model

The general SARIMA model can be represented analytically as:

$$\phi(B)\Phi(B^s)\nabla^d\nabla_s^D z_t = \Theta(B)\Theta(B^s)a_t,\ a_t \sim N0,\sigma^2) \quad (1)$$

where z_t represents DPD at time t, $a_t \sim N0,\sigma^2)$ is the error term at time t, s is the seasonal length, B is a backshift operator $(Bz_t = z_{t-1})$. $\phi(B) = \left(1 - \phi_1 B - \cdots - \phi_p B^p\right)$ is the nonseasonal autoregressive (AR) operator, $\Phi(B^s) = (1 - \Phi_1 B^s - \cdots - \Phi_P B^{Ps})$ is the seasonal AR operator, $\Theta(B) =$

$(1 - \Theta_1 B - \cdots - \Theta_q B^q)$ is the nonseasonal moving average (MA) operator, $\Theta(B^s) = (1 - \Theta_1 B^s - \cdots - \Theta_Q B^{Qs})$ is the seasonal MA operator. ∇^d and ∇_s^D are the nonseasonal and seasonal difference operators of order d and D respectively, where $\nabla^d = (1 - B)^d$ and $\nabla_s^D = (1 - B^s)^D$.

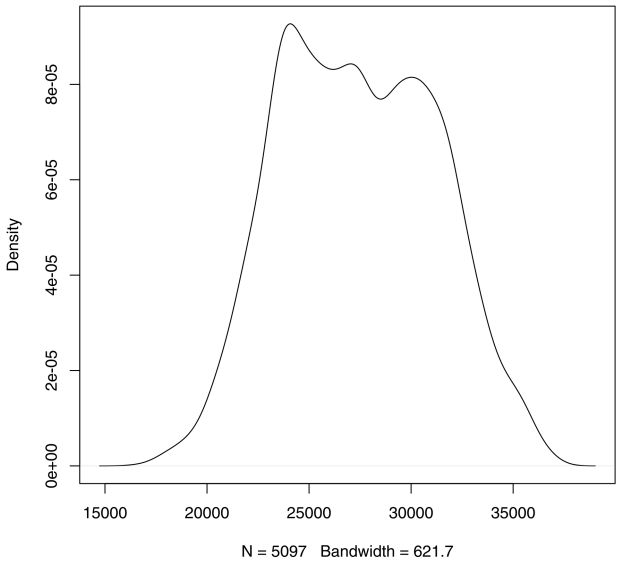

Figure 3: Probability density of DPD. The x-axis represents daily peak electricity demand in megawatts

3.2 Regression-SARIMA Model

Regression-SARIMA models are multivariate linear regression models which work well when the relationship between demand and the predictor variables is linear. Electricity demand is generally divided into short-term, medium-term and long-term forecasting. The regression-SARIMA model is one in which the mean function of the time series is described by a linear combination of regressors. The covariance structure of the series is that of the SARIMA process. The regression-SARIMA model reduces to a SARIMA model if the regressors are not used. The regression-SARIMA model captures important drivers of electricity demand such as calendar, weather and economic factors.

The paper concentrates on short-term forecasting and the inclusion of calendar effects in the modelling framework. Weather variables such as temperature are not included in this study. A detailed discussion of the influence of temperature on electricity demand in South Africa is given in (Sigauke and Chikobvu, 2010). Several papers in literature have adopted the same strategy of not including temperature (Carpinteiro *et al.*, 2004; Taylor *et al.*, 2006; Sores and Souza, 2006; Soares and Medeiros, 2008). The regression-SARIMA model used in this study is given as:

$$\begin{aligned} &\phi(B)\Phi(B^s)\nabla^d\nabla_s^D \\ &\begin{bmatrix} y_t - \sum_{l=1}^{12}\lambda_l m_l - \sum_{r=1}^{7}\tau_r g_r \\ -\gamma \mathrm{H}_{j-1} - \mu \mathrm{H}_j - \rho \mathrm{H}_{j+1} \end{bmatrix} \\ &= \Theta(B)\Theta(B^s)a_t \end{aligned} \quad (2)$$

where $\nabla^d\nabla_s^D = (1 - B)^d(1 - B^s)^D$, y_t is the dependent time series, m_l and g_r are the twelve monthly and seven day regression variables respectively. The monthly seasonal effects are modelled by m_l, while g_r models the day of the week effects. In order to overcome the problem of multicollinearity in the dummy variables m_l and g_r, 11 months in a year are used and January is taken as the base month, while 6 days are used with Monday as a base day. $\mathrm{H}_j, \mathrm{H}_{j-1}$ and H_{j+1} are dummy variables used to model the holiday effect, the day before and after a holiday effects respectively. $\lambda_l, \tau_r, \gamma, \mu$ and ρ are regression parameters and the other variables are as defined in equation (1). A derivation of equation (2) is given in the Appendix.

4. The empirical results

In order to have a better understanding of the daily demand patterns of electricity we calculate the daily seasonal indices. A summary of these daily indices is given in Table 3. Day 7, which is Sunday, had the lowest seasonal index of 93.265% showing that, on average, the consumption of electricity is 6.735% below average consumption. The highest index of 103.078% on day 3, which is Wednesday, indicates that there is an above average consumption of 3.078%. For the rest of the week days the load variations are small (see Figure 4).

Table 3: Daily peak electricity consumption indices

Season	*Index*
Monday	102.343
Tuesday	103.006
Wednesday	103.078
Thursday	102.915
Friday	100.224
Saturday	95.1683
Sunday	93.265

4.1 SARIMA model results

A summary of the estimates of the parameters of the best fitting model together with some important statistics are given in Table 4. The data was transformed using seasonal differencing and also by taking natural logarithms. The transformed data was also found to follow a normal distribution.

Table 4: SARIMA model

Par	ϕ_1	ϕ_2	ϕ_4	ϕ_6	θ_2	θ_3	Θ_1	Θ_2	Θ_6
Coef	0.838	0.385	-0.264	0.029	-0.434	-0.242	-0.807	-0.122	-0.046
	(0.000)	(0.000)	(0.000)	(0.035)	(0.000)	(0.000)	(0.000)	(0.000)	(0.000)

Table 5: Regression-SARIMA

Par	C							
Coef	54.07	1.64	-0.72	0.17	-0.17	0.07	0.69	-0.82
	(0.000)	(0.000)	(0.000)	(0.000)	(0.000)	(0.000)	(0.000)	(0.000)

Par	Θ_1	Θ_2	Θ_{10}	Sunday	Tuesday	Wednesday	Thursday
Coef	-1.44	0.47	-0.02	-29.83	-24.90	-27.82	-24.56
	(0.000)	(0.000)	(0.0515)	(0.000)	(0.000)	(0.000)	(0.000)

Par	Friday	Saturday	October	July	H_j	H_{j-1}
Coef	-25.11	-41.73	159.41	-157.48	-388.09	-116.67
	(0.000)	(0.000)	(0.0027)	(0.0023)	(0.000)	(0.000)

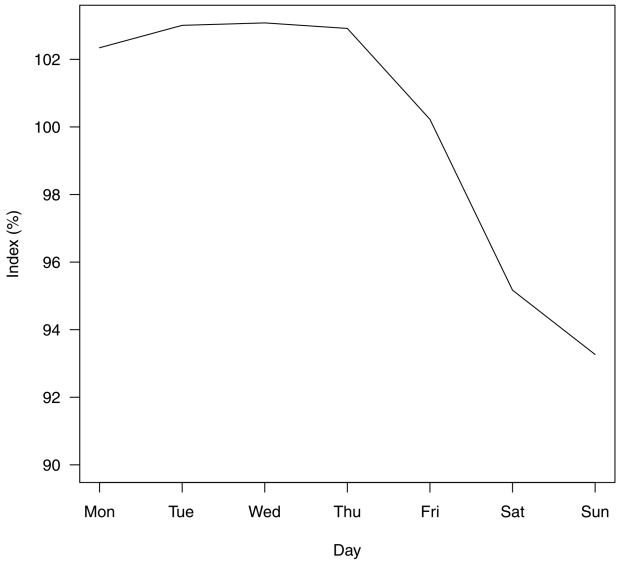

Figure 4: Weekly load profile

The model can be written as:

$$\left(1-\varphi_1 B-\varphi_2 B^2-\varphi_4 B^4-\varphi_6 B^6\right)\left(1-B^7\right)\ln z_t=\left(1-\theta_2 B^2-\theta_3 B^3\right)\left(1-\Theta_1 B^7-\Theta_2 B^{14}-\Theta_6 B^{42}\right)a_t \quad (3)$$

and substituting the values of the parameters we get:

$$\left(1-0.84B-0.39B^2+0.26B^4-0.03B^6\right)\left(1-B^7\right)\ln z_t=\left(1+0.43B^2+0.24B^3\right)\left(1+0.81B^7+0.12B^{14}+0.05B^{42}\right)a_t \quad (4)$$

Several SARIMA models are considered and the best model has a root mean square error (RMSE) of 544.79, mean absolute error (MAE) of 370.81 and a mean absolute percentage error (MAPE) of 1.39%.

4.2 Regression-SARIMA model results

Table 5 shows a summary of the estimates of the variables of the regression-SARIMA model together with the p-values in parentheses. A day before a holiday has a negative coefficient indicating a reduction in electricity consumed. There is a significant reduction in electricity demand during holidays as evidenced by the coefficient of the dummy variable H_j in table 5.

After substituting the values of the parameters into the developed regression-SARIMA model, we get:

$$\begin{aligned}&(1-1.65B+0.73B^2-0.17B^3+0.17B^4-0.07B^5)(1-0.69B^7)(1-B^7)\\&(y_t+157\text{July}-159\text{October}+25\text{Tuesday}+28\text{Wednesday}+25\text{Thursday}+25\text{Friday}+42\text{Saturday}+30\text{Sunday}+388H_j+117H_{j-1})\\&=(1+0.82B)(1+1.45B^7-0.48B^{14}+0.02B^{70})a_t+54\end{aligned} \quad (5)$$

After considering several regression-SARIMA models, the best model has a RMSE of 539.27, MAE of 381.17 and a MAPE of 1.427%.

Table 6: In-sample evaluation of the models

Performance criteria	*Forecasting models*		
	SARIMA model	*Regression-SARIMA model*	*Exponential smoothing*
MAPE	1.392	1.427	1.548
RMSE	544.794	539.274	599.072

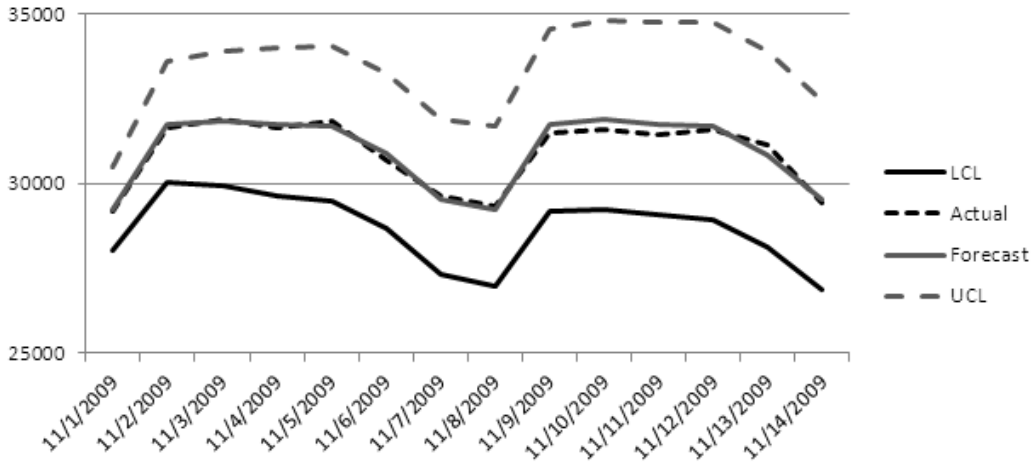

Figure 5: Graphical plot of the forecasts, actual peak demand with residuals and 95% confidence limits. The *x*-axis represents the date and the *y*-axis is demand in megawatts

5. Comparative analysis

The paper concentrated on daily peak demand forecasting, which is important for providing short term forecasts which will assist in optimal dispatching of electrical energy. The mean absolute percentage error (MAPE) and the root mean square error (RMSE) are used for comparing the models in short-term demand forecasting up to seven days ahead. The training period was 1 January 1996 to 30 October 2009. The performance of the developed models is evaluated by comparing them with Winter's triple exponential smoothing model with $\alpha = 0.8$, $\beta = 0.2$, $\gamma = 0.1$. Table 6 shows a comparative analysis of the SARIMA and regression-SARIMA models, together with results from using Winter's triple exponential smoothing model.

The SARIMA model has the least MAPE, showing that it is the best fitting model.

The graphical plot of the out of sample forecasts using the SARIMA model, approximate 95% prediction intervals and actual daily peak for the first 14 days of November 2009, are given in Figure 5. LCL represents the lower 95% confidence interval while UCL represents the 95% upper confidence interval. The actual peak demand falls within the prediction interval for all the 14 days. The SARIMA model seems to be useful for making short-term forecasts of daily peak demand. The probability density of the forecasted values for the first fourteen days of November 2009 is shown in Figure 6. The density shows the full probability distribution of the possible future values of peak demand over the 14 day period. The density is bimodal. This is important for load forecasters and systems operators in load flow analysis and dispatching of electrical energy.

6. Conclusion

In this paper, a time series methodology is presented to forecast DPD for Eskom using SARIMA and

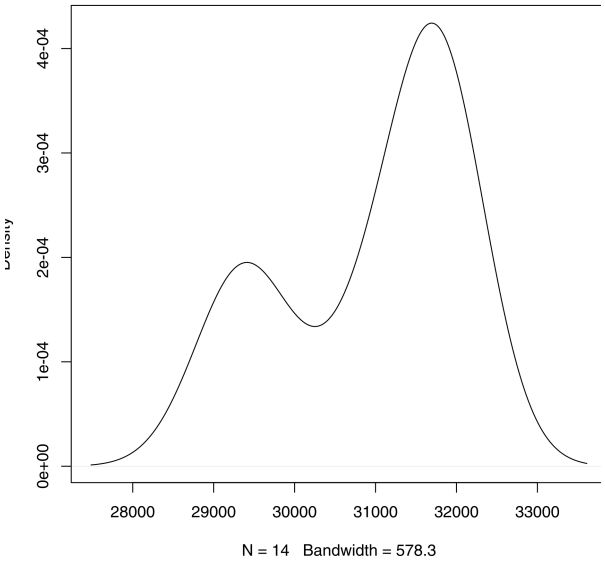

Figure 6. Probability density of the forecasted values for the first 14 days of November 2009. The x-axis represents daily peak electricity demand in megawatts

regression-SARIMA models. The regression-SARIMA model captures important drivers of electricity demand. Empirical results from the study show that the SARIMA model produces more accurate short-term forecasts. The regression-SARIMA model can be improved if weather variables such as temperature are included and also grouping holidays according to their load reduction patterns. The regression-SARIMA model is simple to implement, reliable and provides information about the importance of each predictor variable. The results from using a regression-SARIMA model are relatively robust. Another interesting area for further study would be density forecasting of daily peak electricity demand in which density forecasts provide the estimates of full probability distributions of the possible future values of demand. These areas will be studied elsewhere.

Acknowledgments

The authors are grateful to the power utility company of South Africa, Eskom for providing the data, the University of Limpopo and University of the Free State for using their resources and to the numerous people who assisted in making comments on this paper.

Appendix

A general multiplicative SARIMA model for the DPD time series z_t can be written as:

$$\phi(B)\Phi(B^s)\nabla^d\nabla_s^D z_t = \Theta(B)\Theta(B^s)a_t, \quad a_t \sim N(0,\sigma^2) \tag{6}$$

An extension of the SARIMA model in equation (6) involves the use of a time varying mean function which we model through linear regression effects. A linear regression model which can be used to extend the time varying mean function is given as:

$$y_t = \sum_{f=1}^{k}\beta_f x_{ft} + z_t \tag{7}$$

where y_t is the dependent time series, x_{ft} are the explanatory variables, β_f are the regression parameters and

$$z_t = y_t - \sum_{f=1}^{k}\beta_f x_{ft} \tag{8}$$

We then substitute the expression for z_t in equation (6) to get

$$\phi(B)\Phi(B^s)\nabla^d\nabla_s^D \left[y_t - \sum_{f=1}^{k}\beta_f x_{ft}\right] = \Theta(B)\Theta(B^s)a_t \tag{9}$$

$$\phi(B)\Phi(B^s)\nabla^d\nabla_s^D y_t - \sum_{f=1}^{k}\beta_f\phi(B)\Phi(B^s)\nabla^d\nabla_s^D x_{ft} = \Theta(B)\Theta(B^s)a_t \tag{10}$$

$$\phi(B)\Phi(B^s)\left[\nabla^d\nabla_s^D y_t - \sum_{f=1}^{k}\beta_f\nabla^d\nabla_s^D x_{ft}\right] = \Theta(B)\Theta(B^s)a_t \tag{11}$$

where

$$\nabla^d\nabla_s^D = (1-B)^d(1-B^s)^D \tag{12}$$

In order to capture the day of the week effect dummy variables are introduced and defined as follows:

$$g_r = \begin{cases} 1, r = \text{Mon},\ldots,\text{Sun} \\ 0, \text{ otherwise} \end{cases} \tag{13}$$

The daily peak demand decreases during holidays. Some companies do close earlier on a day before a holiday. There is a reduction in electricity demand a day before and after a holiday (Ismail *et al.*, 2008). To take into account the effects of holidays the following dummy variables, H_j, H_{j-1} and H_{j+1} are introduced

$$\mathrm{H}_j = \begin{cases} 1, j = \text{holiday} \\ 0, \text{ otherwise} \end{cases} \tag{14}$$

$$\mathrm{H}_{j-1} = \begin{cases} 1, j = \text{day before holiday} \\ 0, \text{ otherwise} \end{cases} \tag{15}$$

$$\mathrm{H}_{j+1} = \begin{cases} 1, j = \text{day after holiday} \\ 0, \text{ otherwise} \end{cases} \tag{16}$$

If a holiday falls on a Sunday, the following Monday is declared a public holiday. To take into account the monthly seasonality effect a dummy variable m_l is introduced.

$$m_l = \begin{cases} 1, l = \text{Jan},\ldots,\text{Dec} \\ 0, \text{ otherwise} \end{cases} \tag{17}$$

Our regression-SARIMA model is then written as:

$$\phi(B)\Phi(B^s)\nabla^d\nabla_s^D \left[y_t - \sum_{l=1}^{12}\lambda_l m_l - \sum_{r=1}^{7}\tau_r D_r - \gamma H_{j-1} - \mu H_j - \rho H_{j+1}\right] = \Theta(B)\Theta(B^s)a_t$$

where

$$\nabla^d\nabla_s^D = (1-B)^d(1-B^s)^D$$

References

Amaral, L.F., Souza, R.C. & Stevenson, M. (2008). A smooth transition periodic autoregressive (STPAR) model for short-term load forecasting. *International Journal of Forecasting* 24(4), 603-615.

Amin-Naseri, M.R. & Soroush, A.R. (2008). Combined use of unsupervised and supervised learning for daily peak load forecasting. *Energy Conversion and Management* 49(6), 1302-1308.

Amusa, H., Amusa, K. & Mabugu, R. (2009). Aggregate demand for electricity in South Africa: An analysis using the bounds testing approach to co integration. *Energy Policy* 37(10), 4167- 4175.

Azadeh, A., Ghaderi, S.F., & Sohrabkhani S. (2007). Forecasting electrical consumption by integration on neural network, time series and ANOVA. *Applied Mathematics and Computation* 186(2), 1753-1761.

Carpinteiro, O., Reis, A. & Silva, A. (2004). A hierarchical neural model in short-term load Forecasting. *Applied Soft Computing* 4(4), 405-412.

Feinberg, E. & Genethliou, D. (2005). Load Forecasting. In J. Chow, F. Wu and J. Momoh (Eds.). Applied Mathematics for Restructured Electric Power Systems: *Optimization, Control and Computational Intelligence.* (pp. 269-285). Springer.

Ghosh, S. (2008). Univariate time-series forecasting of monthly peak demand of electricity in northern India. *International Journal of Indian Culture and Business Management* 1, 466-474.

Goia, A., May, C. & Fusai, G. (2010). Functional clustering and linear regression for peak load forecasting. *International Journal of Forecasting* 26(4), 700-711.

Granger, C.W.J. & Jeon, Y. (2007). Long-term forecasting and evaluation. *International Journal of Forecasting* 23(4), 539-551.

Hahn, H., Meyer-Nieberg, S. & Pickl, S. (2009). Electric load forecasting methods: Tools for decision making. *European Journal of Operational Research* 199(3), 902-907.

Harvey, A. & Koopman, S.J. (1993). Forecasting Hourly Electricity Demand using Time-Varying Splines. Journal of the American Statistical Association *88(424), 1228-1236.*

Ismail, Z., Jamaluddin, F. & Jamaluddin, F. (2008). Time series regression model for forecasting Malaysian electricity load demand. *Asian Journal of Mathematics and Statistics*. 1(3), 139-149.

Ismail, Z., Yahya, A. & Mahpol, K.A. (2009). Forecasting peak load electricity demand using statistics and rule based approach. *American Journal of Applied Sciences* 6 (8), 1618-625.

Munoz A, Sanchez-Ubeda EF, Cruz A and Marin J. 2010. Short-term forecasting in power systems: a guided tour. *Energy Systems,* 2, 129-160.

Ramanathan, R., Engle, R., Granger, C.W.J, Vahid-Araghi F. & Brace, C. (1997). Short-run forecasts of electricity loads and peaks. *International Journal of Forecasting* 13(2), 161-174.

Sigauke, C., & Chikobvu, D. (2010). Daily peak electricity load forecasting in South Africa using a multivariate non-parametric regression approach. *ORiON* 26 (2), 97–111.

Sigauke, C., & Chikobvu, D. (2011). Prediction of daily peak electricity demand in South Africa using volatility forecasting models. *Energy Economics* 33, 882–888.

Soares, L. & Souza, L. (2006). Forecasting electricity demand using generalized long memory. *International Journal of Forecasting* 22(1), 17-28.

Soares, L.J. & Medeiros, M.C. (2008). Modelling and forecasting short-term electricity load: A comparison of methods with an application to Brazilian data. *International Journal of Forecasting* 24(4), 630-644.

Suganthi, L. & Samuel A.A. (2012). Energy models for demand forecasting – A review. *Renewable and Sustainable Energy Reviews* 16, 1223– 1240.

Sumer, K.K., Goktas, O. & Hepsag, A. (2009). The application of seasonal latent variable in forecasting electricity demand as an alternative method. *Energy Policy* 37(4), 1317-1322.

Taylor, J., de Menezes, L. & Mcsharry, P. (2006). A comparison of univariate methods for forecasting electricity demand up to a day ahead. *International Journal of Forecasting* 22, 1-16.

Taylor, J.W. (2008) An evaluation of methods for very short-term load forecasting using minute-by-minute British data. *International Journal of Forecasting* 24, 645-658.

Truong, N-V., Wang, L. & Wong, P.K.C. (2008). Modelling and short-term forecasting of daily peak power demand in Victoria using two-dimensional wavelet based SDP models. *International Journal of Electrical Power & Energy Systems* 30(9), 511-518.

Wang, J., Zhu, W. & Sun, D. (2009). A trend fixed on firstly and seasonal adjustment model combined with the – SVR for short-term forecasting of electricity demand. Energy Policy 37(11), 4901-4909.

Received 7 June 2011; revised 14 May 2012

Reliability worth assessment of electricity consumers: a South African case study

Oliver Dzobo

Trevor Gaunt

Ronald Herman

Department of Electrical Engineering, University of Cape Town, South Africa

Abstract

This paper discusses the results obtained from a customer survey conducted in Cape Town, South Africa, using in-person interviews with approximately 275 sample business customers. The survey included customer interruption cost estimation questions based on the direct costing method. The results obtained show that customer interruption cost for business customers varies with duration and time of occurrence of power interruptions. The variation was shown to be dependent on customer segment. Furthermore, it revealed that business customers can be grouped in terms of the investment they make to mitigate the impact of power interruptions on their activities, such as the use of backup power supplies.

Keywords: Energy Bill, customer interruption cost

1. Introduction

South Africa is a developing country with large industrial and commercial consumers. For the overall development of the country, it is important that all resources are used optimally to ensure all sectors of the economy have a sustainable and continuous growth. Availability of reliable power supply at reasonable cost is essential for the economic growth of a country. Power suppliers therefore face particular challenges such as building new supply capacity and distributing energy to manufacturing and service industries to meet growing customer demands as economically as possible.

In recent years, the level of power supply reliability in South Africa has changed. Power supply failure figures have increased and the supply authorities regularly implement curtailment (NERSA, 2008a; NERSA, 2008b). This power supply scenario is common in other parts of Africa where the development of power system facilities has not kept pace with the demand. Significant investment is needed to expand power system facilities and raise the power supply reliability level. It is therefore important that electricity regulators and utilities balance the costs of utility to develop, operate, and maintain the power system against the economic value of supply to customers. This has yet to become a consideration in South Africa where development plans are based on traditional deterministic measures such as the largest single contingency or fixed percentage reserve margin. These criteria cannot be used to measure the economic impacts of changing reliability levels on the utility as well as on the customers and therefore cannot lead to an optimum expansion plan for the power system (Alvehag, 2008). Generally, investment, operating and maintenance costs are obtained using standard engineering cost estimation procedures (Sullivan et al, 1997). The economic value attached by electricity customers to the service provided by the power utility is measured by their customer interruption cost (CIC) (Chowdhury and Koval, 2001; Tiedmann, 2004). Many studies to assess CIC have been conducted internationally (EPRI, 2000). In South Africa, the estimated cost for an interruption, as reported in the Governments IRP2010 policy report (IRP, 2010) was simply R75/kW interrupted. The motivation for this study, therefore, was to develop appropriate methods to determine the CIC models associated with various levels of unreliability in a developing country.

Methods to obtain CIC data can be convenient-

ly grouped into three categories: (i) indirect analytical evaluations, (ii) case studies of actual blackouts, and (iii) customer surveys. Over the past years, the Power System Research Group at the University of Cape Town has developed theoretical structures and conducted various customer surveys to determine the impacts of power interruptions on South African electricity consumers. The group conducted a study of the interruption costs in the residential and commercial sectors in 2008 (Herman and Gaunt, 2008; Jordaan, 2006). The customer survey approach is again utilised as the basic methodology of this study. The basis of the approach is that customers are in the best position to understand and assess how the costs associated with power supply interruptions impact their activities.

This paper presents a general overview of the customer survey methodology utilised in this study, cost data that has been obtained and the analyses which have been performed (Dzobo, 2010). No attempt is made in this paper to present the results from all questions in the survey questionnaire, but solely to give an indication of the general results, especially in the area of cost evaluation.

For the purpose of the present research: interruption means – any outage, planned or unplanned; business customers – industrial and commercial customers combined and all costs are in South African Rand (R). 1 US$ is equivalent to R7 approximately.

2. Methodology

The CICs can be classified as direct and indirect costs (Chowdhury and Koval, 1999). Direct costs are further classified as economic and social. Direct economic costs include cost due to lost production, product spoilage and damage to equipment. The direct social costs include risk of injury or health etc. Indirect costs are associated with the losses incurred subsequently to the power interruption. This includes economic, social and relational effects such as changes in business plans, schedules, looting etc. The magnitude of all these costs is highly dependent on the characteristics of the customer and interruption events (Koskolos *et al,* 1998). Only the direct economic costs were investigated in this research study. This is because direct economic costs are expected to constitute a significant part of the CICs in business customers. The factors contributing to the cost were taken as:

- Wages paid to idle workers
- loss of sales
- overtime costs
- damage to equipment
- spoilage of perishables
- cost of running back-up; and
- cost of any special procedures.

For this research study, business customers of the City of Cape Town constitute the sample for the investigation. The area of Cape Town was chosen because it was the worst affected city during recent power interruptions (Eskom, 2008). Business customers account for about 86% of total energy consumption in Cape Town i.e. about 44% commercial and 42% industrial (City of Cape Town, 2007). The industrial and commercial populations were grouped according to the definition given in SIC (Standard Industrial Code) – StatsSA (1993) (Statistics South Africa, 1993). An industrial customer was defined as a customer engaging in manufacturing of goods and products. A commercial customer was defined as any form of business or commercial activities which are not primarily involved in manufacturing. Mostly small scale industries were considered in the survey. These are normally the majority in Cape Town (City of Cape Town, 2007). The industrial and commercial surveys were conducted concurrently. A business customer with various activities was classified according to the most significant part of that business.

A sample was chosen using a random systematic sampling technique. The actual customers were selected from the list provided in the Cape Peninsula 2008/2009 business directory. Every respondent in the sample was contacted personally. Data for the study was collected through personal contact during the summer months of 2009. Either the owner/partner or manager was asked to answer the questions to ensure the accuracy and reliability of the information. Informed consent was sought from the respondents i.e. permission was obtained from each respondent after the nature of the research study was fully explained. Respondents were informed that their participation was voluntary and the identity of the participants would not be revealed in the reporting and analysis of the results.

2.1 Questionnaire content

Modifications, where necessary, were made to the previously used questionnaire. The questionnaires were designed to progressively lead the respondent in awareness of the effects and costs associated with power supply interruptions and to ask for qualitative and quantitative evaluations at appropriate places. The opening questions seek the respondents opinion and judgment on specific issues. The questionnaire progresses to ask questions about the possible mitigation actions being applied to minimize cost of power interruptions. This set of questions moves the respondent from general thoughts about interruptions to providing valuable information about the things that are used to mitigate interruption costs. A set of specific cost-related questions were then asked and these were the core of the questionnaire. Direct costing questions were used to obtain the customers worst interruption cost estimates for a given set of outage conditions. The

hypothetical scenarios that were provided vary with season, time of day and day of week. The final section contains questions about the demographic characteristics (company size, business activity level and operational characteristics) of the respondent. The questionnaire ends with a blank space for respondents to comment on the improvement they would think their power supplier can implement to reduce impact of power interruptions.

2.2 Modelling approach

The primary purpose of conducting the survey was to identify CIC models that allow reasonably accurate prediction of CICs for various business customer types. The CIC models express CICs as a function of outage duration, season, day of week, time of day and various customer characteristics such as average electricity bill, number of employees, and other variables. Simple linear regression analysis (Navidi, 2008) (standard Ordinary Least Square (OLS)) was used to determine the CIC models. The statistical regression analysis was done using STATA statistical package. Scatter diagrams were used to find the variables that have the highest coefficient of correlation value with CIC. The variable or combination of variables was then used to generate the regression models for specific interruption attributes. The interruption attributes were taken as binary coefficients in the regression models i.e. take the value of 1 if present and zero if not present. Thus, the regression model equations were presented in the form of:

$$\text{CIC}\,[d] = \text{a} + \beta_1\,\beta_2\,\beta_3\,\text{B}\,(\text{X}) \qquad (1)$$

Where d is the duration of power interruption being studied, a is the regression constant, β_1 , β_2 and β_3 are the binary coefficients representing season, day of week and time of day respectively, B is the regression coefficient and X is the predictor variable being investigated.

The accuracy of the regression models prediction R^2 is expressed as:

$$R^2 = \frac{\left[\sum_i \left(y_i - \hat{y}_i\right)\right]^2}{\left[\sum_i \left(y_i - \mu_y\right)\right]^2} \qquad (2)$$

Where y_i is the predicted value from the regression model for observation i, y is the actual value for observation i and μ_y is the mean for all observations.

The coefficient of determination R^2 expresses the strength of the relationship or association between the dependent and independent variables and varies from 0 to 1. When R^2 is 1, there is no prediction error, and the fit of the regression model is exact. When it is zero, the prediction error is very large and the regression model has no predictive power at all. The results of this analysis are reported in terms of their R^2.

3. Results

3.1 Survey response

The respondents were provided with a list of standard company descriptions and asked to select one that best described their company. Table 1 provides details regarding the samples to which the CQ was applied. This information is presented to illustrate the composition and limitation of the survey. From the results, it is evident that it was difficult to obtain interviews in the industrial sector. The main reason for this is that all the major established industrial companies have strict policies that prohibit employees and managers from disclosing any company information without authority from their directors. Interviews were, however, obtained from smaller, newly established industries. In a few unprecedented cases, managers of large industrial firms did provide CIC estimates. Difficulties were experienced when trying to schedule interviews for the warehousing segment customers. These customers are somewhat busy all the time and only four responses were obtained. It was therefore considered important to remove this category from the analysis of CIC.

Table 1: Survey response

Sector	*Business segments*	*No. of respondents*
Industrial	Clothing	22
	Metals	28
	Garages	26
	Warehousing	4
Commercial	Retail	117
	Professional	26
	Office	2
	Hotel	39

In the commercial sector, retail and hotel segment interviews were done with a large variety of businesses. The hotel segment includes family restaurants, fast food establishments, coffee shops, small boutique hotels, and large exclusive hotels. The retail segment constitutes the greater portion of the respondents. Interviews for these segments were easy to schedule and they were more willing to give the information. However, for big establishments similar problems to those experienced in the industrial sector were experienced. Again the office segment was dropped from the analysis of CICs because of the small number of respondents. Interviews for this segment were very difficult to schedule as most of the respondents were not willing to answer the questionnaire because of fear of responsibility. Generally, those establishments where the owner was interviewed were better equipped to estimate possible CICs.

3.2 Power interruption frequency

The questionnaire asks the respondents to indicate the number of power interruptions they had experienced during the past twelve months. Table 2 shows the mean and standard deviation of the number of power interruptions per year experienced by both industrial and commercial samples. Almost 40% of the respondents indicated that they did not have any power interruption for the past 12 months.

Table 2: Number of power interruptions/year for industrial and commercial customers

Type	*Mean*	*Standard deviation*	*Maximum*	*No. of respondents*
Industry	3.93	4.61	19	91
Commercial	3.40	4.61	22	184

This was to be expected since the period when the customer survey was conducted did not coincide with the large scale load shedding implemented by the power suppliers. Figure 1 shows the distribution of the number of power interruptions per customer per year (SAIFI). The results indicate that there was a higher probability of power interruptions per customer per year in the industrial population than in the commercial sample.

3.3 Satisfaction level

Respondents were asked to give their opinions regarding the quality of service provided by their power utility. More than 45% of the respondents were either very dissatisfied or dissatisfied with the service they were receiving, with about 20% being neutral. Only a third of the respondents were satisfied or very satisfied with the power utility service. This means that both samples regard the service provided by their power utility as generally not satisfying their electricity needs. Analysis of the variation of satisfaction level with respect to power interruption frequency was performed after removing all respondents who had indicated zero power interruptions. It was assumed that those respondents with zero power interruptions were all satisfied with the power supply reliability. Any other satisfaction level indicated by these respondents was regarded as a protest answer to other issues concerning the power utility. Figure 2 shows that business customers become neutral in their satisfaction level if they experience less than four power interruptions per year.

3.4 Power supply reliability preferences

Respondents were asked to rate the acceptability of various interruption scenarios for their companies. In each set of scenarios, only one variable was varied at a time, all the other variables were kept constant. Both duration and frequency were found to affect the reliability preference of business customers. The acceptability decreased as duration and frequency increased. There was no difference in the reliability preferences of both industrial and commercial respondents. Figure 3 shows a two

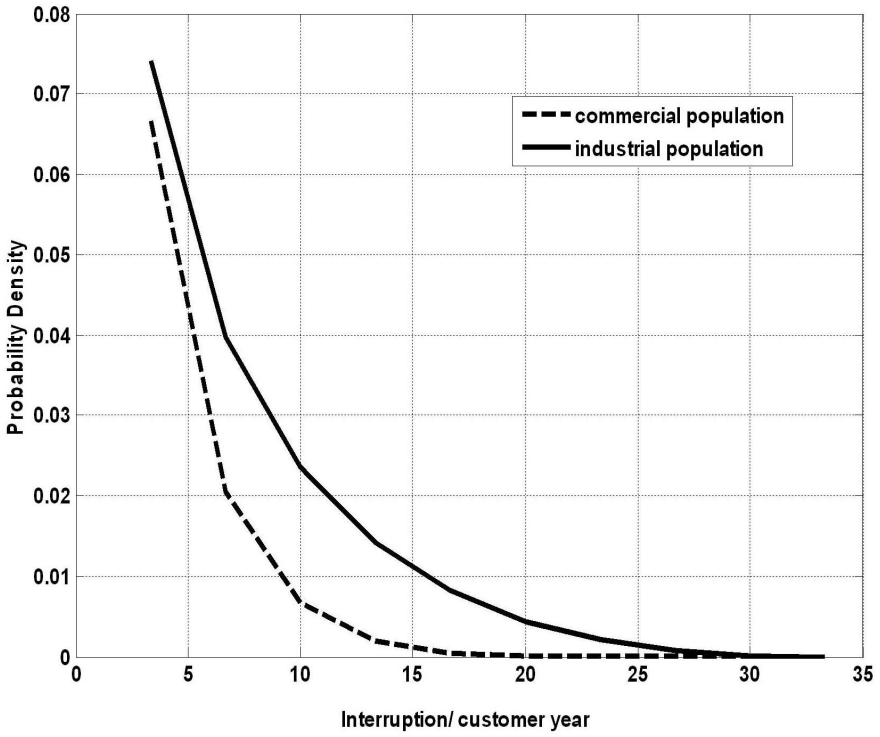

Figure 1: Beta probability function of power interruption/ customer year of both industrial and commercial samples

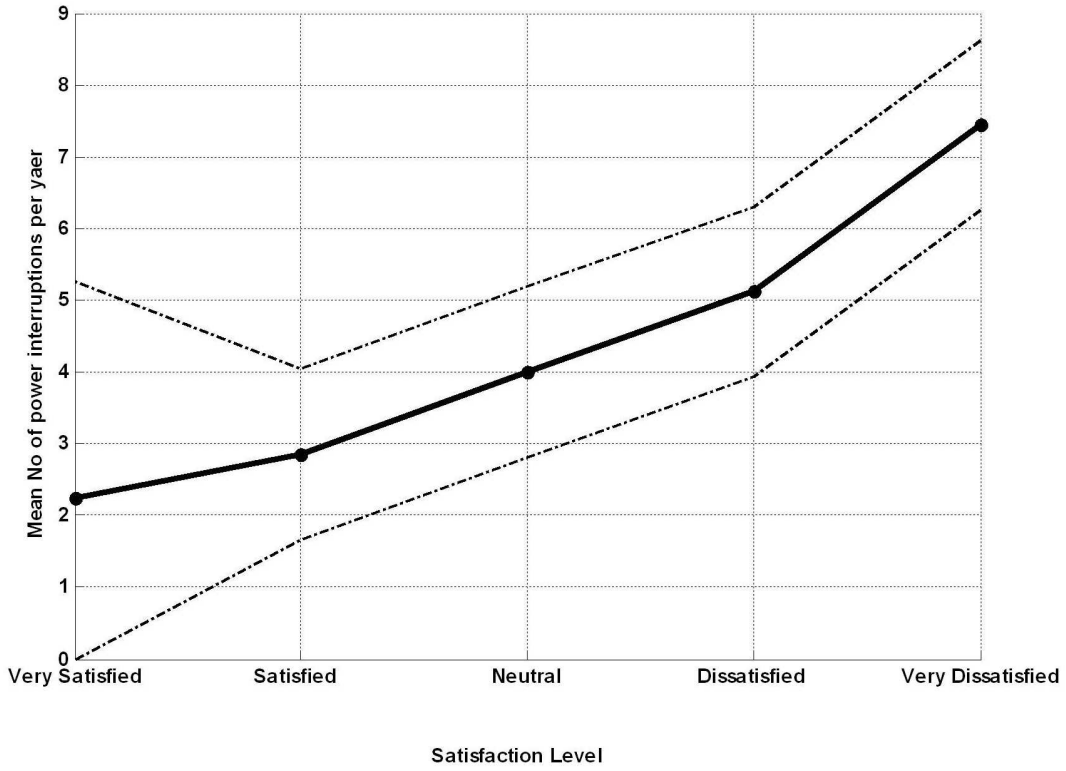

Figure 2: Satisfaction level versus number of power interruptions per year: Mean and 95% confidence interval averaged over all respondents

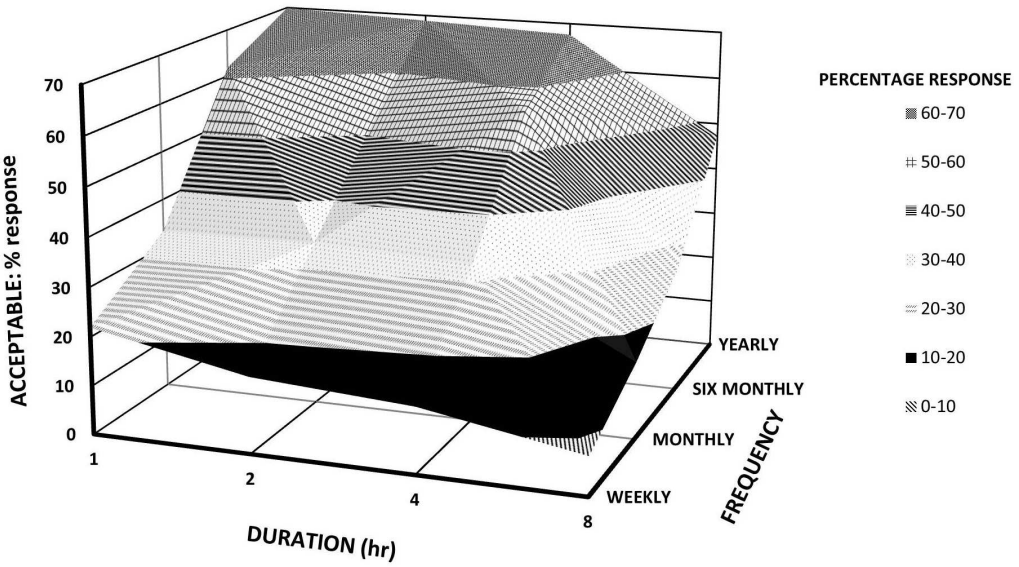

Figure 3: Duration and frequency of power interruptions versus acceptability for all respondents

dimensional distribution of the two factors (duration and frequency) and their effects on reliability preference.

A large majority of the respondents considered weekly failures as undesirable. Over 50% of the respondents considered a 4 to 8 hour failure as unacceptable for all the given duration and frequency scenarios. The majority of respondents stated that a 1 to 2 hour failure is tolerable. Perhaps this is because most business customers are able to make up for their lost production.

3.5 Ability to make up lost production

Category, duration and time of day were found to affect the ability of business customers to make up for their lost production. The ability to make up for lost production in the commercial sector was found to increase as the duration of power interruption decreases. The worst time of occurrence of power interruption to cause major production loss in both

industrial and commercial sectors was found to be in the afternoon.

3.6 Ownership of backup power supply

Respondents were asked to indicate whether they own a backup power supply at their premises. In addition, the respondents were asked to indicate the type of backup power supply equipment, purpose, size, installation cost, running cost, year of installation and the percentage coverage of the plant by the backup power supply. The results showed that only about 25% of the industrial sample indicated the presence of backup power supply. Thirteen percent of the commercial sample indicated that they had backup supply. The purpose of the backup power supply for commercial customers is mainly to maintain essential business activities e.g. for most retail shops, only the emergency lights, security systems, computers, tills and credit card pay point machines are kept running. More than 50% of the generators were installed between 2008 and 2009 (see Figure 4).

This was expected because 2008 was the year that had most of the load shedding schedules. The size of backup power supply equipment varies from 2.5kVA to 200kVA for the industrial sample and only two respondents indicated the use of UPS i.e. 1.1kVA and 690kVA. For the commercial customers, only three respondents managed to give the size of their backup power supplies – generator i.e. 25, 30, 60kVA.

The difference in both size and percentage coverage of backup power supply (see Table 3) is possibly because industrial customers incur higher interruption costs than commercial customers. Only the industrial customers were able to provide the cost structure of their backup power supply (see Table 4).

Table 3: Percentage of coverage of plant by both industrial and commercial samples

Proportion (%) of coverage of plant	*Industry (% respondents)*	*Commercial (% respondents)*
≤ 20	13.04	25.00
20 ≤ 50	17.39	37.50
50 ≤ 80	21.74	4.17
> 80	47.83	33.33

Table 4: Industrial population: Cost structure for backup power supply (generator)

Item	*Mean*	*Standard deviation*	*No. of observations*
Installation cost (R/kVA)	1434.30	444.76	11
Running cost (R/kVA-hr)	7.76	2.14	12

3.7 Customer interruption cost model

The modelling process only uses those predictor variables that contribute significantly (from a statistical point of view) to the prediction of the dependant variable. The variable of interest in the regression analysis is the customer outage cost. Scatter diagrams and correlation values were used to find the predictor variable which contributes significantly to the prediction of the dependent variable. No attempt has been made to presents all the regression models generated from the analysis.

The results showed that there is a high linear correlation between CIC and customer energy bill in both industrial and commercial sectors. The customer energy bill was therefore used to generate

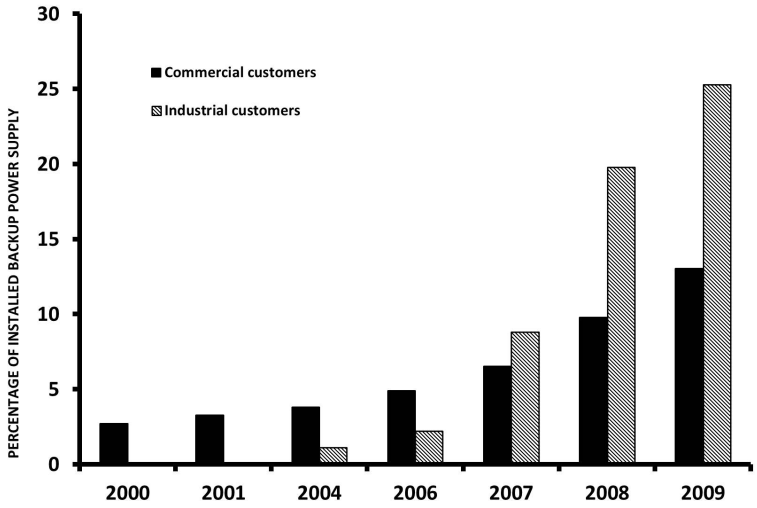

Figure 4: Penetration level of backup power supply installed per year to the total sample surveyed in each group

regression models for business customers presented in this paper. The coefficient of determination (R2) values ranges from 0.599 to 0.998 for all the regression models. This means customer energy bill was able to explain more than 59% variance of CIC that was incurred by business customers. This finding therefore implies that the customer energy bill is a useful variable in predicting the CIC incurred by business customers. The positive correlation means that there is an increase in CIC as the customer energy bill increases. Thus, for the same power interruption, business customers who pay high monthly energy bills tend to incur high CICs than those who pay less.

3.7.1 Duration of interruption

The CIC incurred by business customers increases with the duration of power interruption. This means the longer the power interruption the higher the CIC. The rate of increase of CIC also increases as the duration of the power interruption increases.

3.7.2 Time of occurrence

CIC incurred by business customers was affected by season, day of week and time of day. For example, in Figure, 5 the results showed that summer weekday morning costs are higher than winter weekday morning costs for the garages segment. This may be as a result of that, more travelling is done in the summer and usually service starts at the beginning of the day. For the other power interruption durations the results are similar.

3.7.3 Ownership of backup power supply

Respondents were asked to estimate the worst CIC estimates without including the effect of backup power supply. The results showed that business customers who own backup power supply tend to incur higher CICs than those who do not have them (see Figure 6).

This means that respondents own backup power supply in order to reduce the impact of power interruption on their activities. The research clearly identified that backup supplies are a response to frequency of interruption and expectation of continuing. The finding therefore implies that business customers can be grouped in terms of the investment they make to mitigate the impact of power interruption on their activities.

3.7.4 Customer type

The clothing segment customers have their CIC far outstripping those of any other business activity. They incur more than double those in retail and garages segments for the same power interruption scenario. This finding therefore implies that different customer segments experience different CICs for the same power interruption scenario. Therefore combining different customer segments to form one homogeneous group when estimating CICs, may provide overestimate and/or underestimate to some customer segments. This makes customer segment a very important variable to consider in CIC analysis.

3.7.5 Linearity

Nonlinear regression analysis was used in order to try and force the regression line models to pass through the zero point. The nonlinear regression model agrees with the assumption that for a zero energy bill, a business customer would incur zero CIC.

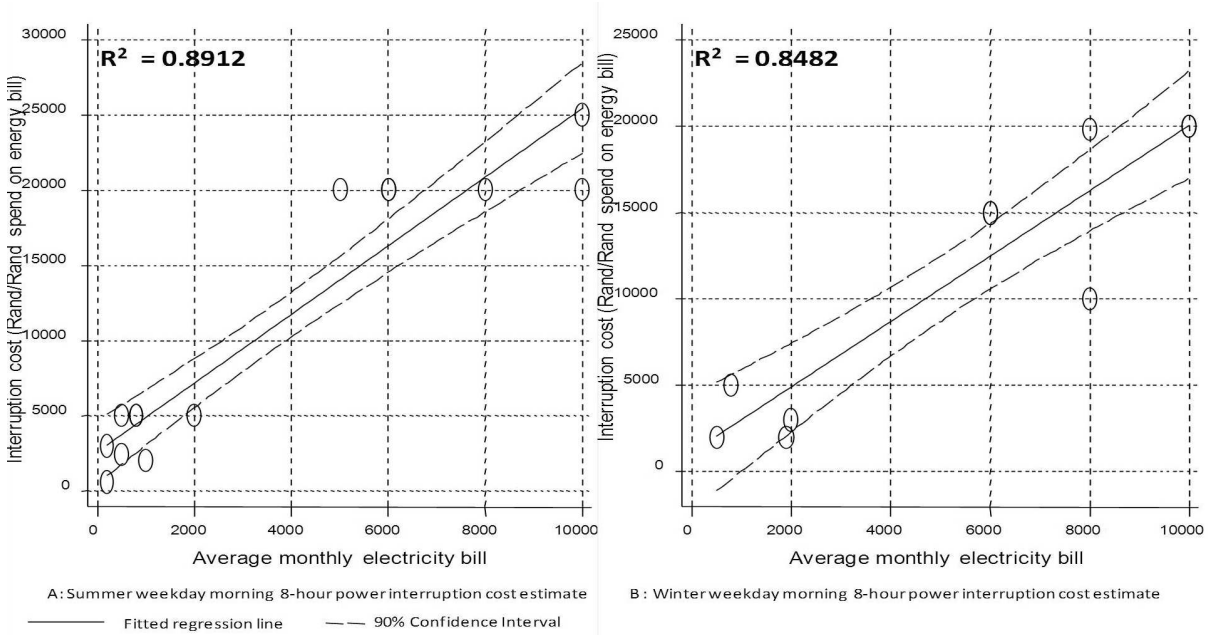

Figure 5: Seasonal variation of interruption cost with average electricity bill of Garage segment

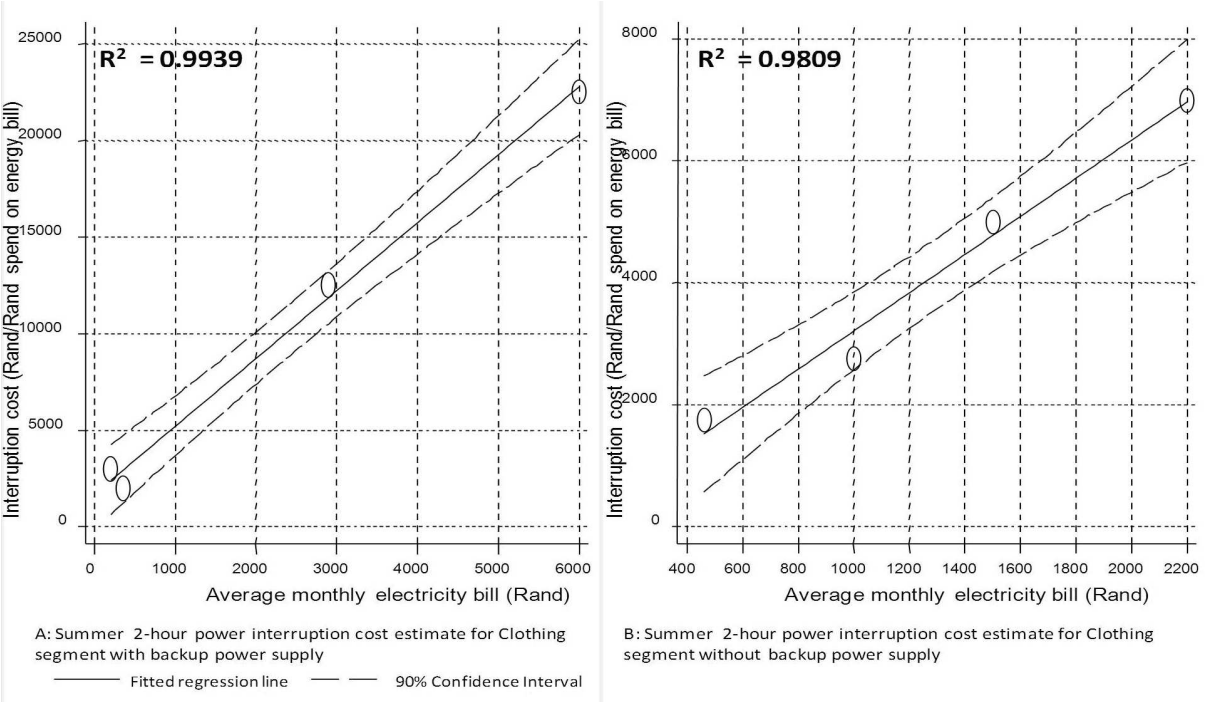

Figure 6: Variation of CIC with average monthly electricity bill for clothing segment with and without backup power supply

Figure 7 shows an example of how the linear regression line model would change for the Garages segment. The graph shows that the nonlinear regression model generates lower predicted values for both lower and high values of energy bill. The gradient is high at the start of the graph and it decreases as the average monthly electricity bill increases. Hence, it overestimates the CIC incurred by business customers in the early hours of a power interruption and also later. However, it should be noted that the accuracy of the nonlinear models (R^2) is lower than that of the linear regression models. Thus, the linear regression model can be regarded as the superior model for business customers who have non-zero energy bill.

The relationship between the number of employees and the worst case cost estimates was examined using scatter grams. Scatter grams were prepared for the individual customer segments and levels of other user characteristics variables without

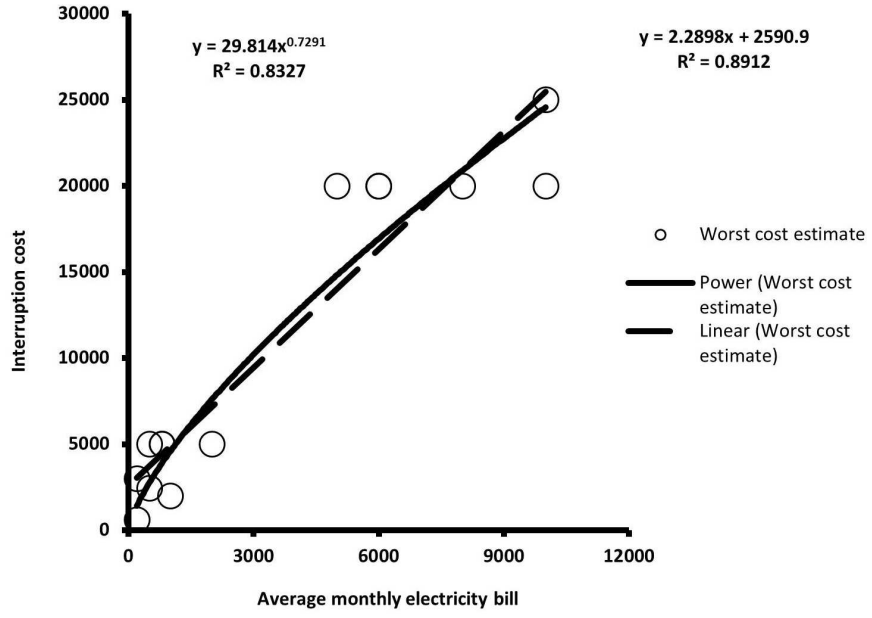

Figure 7: Variation of CIC with average monthly electricity bill for a winter weekday morning power interruption: Garage segment

any success in finding an apparent linear correlation. Therefore, it was concluded that these variables does not have a significant linear relationship with CIC estimates and cannot be used to normalize cost estimates.

4. Conclusions

A probabilistic approach was used to determine the financial impact on customers of a given power interruption allowing for a seasonal variations and time of occurrence. The technique and results obtained from the study demonstrate that CICs can be predicted with a defined level of confidence from the activity category of customer and monthly electricity purchases. Since the time-related CIC values are expressed in a probabilistic manner they can be combined together with probabilistic time-related reliability indices (Edimu, 2009) to give the expected cost impact of power interruptions on customers as probabilistic values associated with different risk levels. Expressing the results in this way will allow non-engineering managers to make meaningful managerial decisions about enhancing power system infrastructure and back-up. It will also assist regulators to determine rewards and penalties necessary to balance cost or tariffs against reliability. Practical applications are being delegated on the basis of the finding of this research project.

It should be noted that the CIC results reported in this paper apply only to the utility under study. Commercial and industrial customers elsewhere, supplied by other utilities, may be affected differently by the same power supply interruption due to difference in tariffs, climate, processes and equipments. Nevertheless, the application of this technique at a single utility demonstrates that CIC are quite predictable and there could be scope to identify more general norms that would be useful for industry regulation. Further survey and modelling efforts will be required to develop realistic probabilistic models for predicting CIC completely for a country or utility.

References

Alvehag, K. (2008). Impact of dependence in risk assessment of power distribution systems, Licentiate Thesis, Royal Institute of Technology, School of Electrical Engineering, Electrical Power Systems, Stockholm, Sweden, 2008.

Chowdhury, A and Koval, D. O. (1999). Value-Based power system reliability planning, IEEE Transactions on Industry Applications ,vol. 35, no. 2, March/April 1999, pp 305 – 311.

Chowdhury, A and Koval, D. O. (2001). Application of customer interruption costs in transmission network reliability planning, IEEE Transactions on Industry Applications, Vol. 37, no. 6, November/December 2001, pp 1590 – 1596

City of Cape Town (2007). State of Energy Report for City of Cape Town 2007, Prepared for the City of Cape Town by Palmer Development Group: www.capetown.gov.za.

Dzobo, O. (2010). Reliability cost and worth assessment of industrial and commercial electricity consumers in Cape Town, M Sc thesis, University of Cape Town, 2010.

Edimu, M. (2009). Evaluation of reliability indices of a composite power system using probability distribution functions, M Sc Thesis, Department of Electrical Engineering, University of Cape Town, South Africa, 2009

EPRI (2000). Customer needs for electric power reliability and power quality, EPRI white paper. Technical Report 2000.1000428, Electrical Power Research Institute, Palo Alto, CA, October 2000.

Eskom (2008). Eskom – Surplus Capacity (visited on 12/08/2008): www.eskom.co.za/live/content.php.

Herman, R and Gaunt, C.T. (2008). Direct and indirect measurement of residential and commercial CIC: Preliminary findings from South Africa Surveys, PMAPS 2008, 2008.

Integrated Resource Plan (IRP) for Electricity (2010). Cost of Unserved Energy (COUE) – IRP 2010 Input Parameter information sheet (Supply input), Department of Energy, South Africa.

Jordaan, G. (2006). Segment specific customer interruption costs in the commercial sector, B Sc (Eng) Project thesis, University of Cape Town, 2006.

Koskolos, N; Megaloconomos, S; Dialynas, E. (1998). Assessment of power interruption costs for the industrial customers in Greece, 8th International Conference on Harmonics and Quality of Power, Anthens, Greece, October 14-16,1998, pp 761-766.

Navidi, W. (2008). Statistics for Engineers and Scientists, Second edition, McGraw- Hill, New York, 2008.

NERSA (2008a). NERSA 2008, Interventions to address electricity shortages, January 2008.

NERSA (2008b). NERSA, Report by the Energy Regulator: Inquiry into the national electricity supply shortage and load shedding, 12 May 2008.

Statistics South Africa (1993). Standard Industrial Classification of all Economic Activities (SIC), 5th edition, Statistics South Africa, January 1993.

Sullivan, M; Vardell, T and Johnson, M. (1997). Power interruption costs to industrial and commercial consumers of electricity, IEEE Transactions on Industry Applications, Vol. 33, No. 6, November/December 1997, pp 1448 – 1458.

Tiedmann, K. (2004). Estimating the value of reliability for business customers, 8th International Conference on Probabilistic Methods Applied to Power Systems, Iowa State University, Ames, Iowa, September 12-16, 2004.

Received 19 May 2011; revised 16 March 2012

Comparing performance of MLP and RBF neural network models for predicting South Africa's energy consumption

Olanrewaju A Oludolapo
Department of Industrial Engineering, Tshwane University of Technology, South Africa

Adisa A Jimoh
Department of Electrical Engineering, Tshwane University of Technology, South Africa

Pule A Kholopane
Department of Industrial Engineering, University of Johannesburg, South Africa

Abstract
In view of the close association between energy and economic growth, South Africa's aspirations for higher growth, more energy is required; formulating a long-term economic development plan and implementing an energy strategy for a country /industry necessitates establishing the correct relationship between energy and the economy. As insufficient energy or a lack thereof is reported to be a major cause of social and economic poverty, it is very important to select a model to forecast the consumption of energy reasonably accurately. This study presents techniques based on the development of multilayer perceptron (MLP) and radial basis function (RBF) of artificial neural network (ANN) models, for calculating the energy consumption of South Africa's industrial sector between 1993 and 2000. The approach examines the energy consumption in relation to the gross domestic product. The results indicate a strong agreement between model predictions and observed values, since the mean absolute percentage error is below 5%. When performance indices are compared, the RBF-based model is a more accurate predictor than the MLP model.

Keywords: multilayer perceptron, radial basis function, energy consumption, gross domestic product

1. Introduction

In 1995, South Africa found itself among the top 50 countries (developed and developing countries) in the world, and first in Africa among countries south of the equator in terms of the per capita commercial energy consumption in 1995 (2 405 kg of oil equivalent per capita in 1995). However, where energy efficiency is measured as the ratio of real GDP to energy use (1 US$ GDP at 1987 values per kg of oil equivalent), South Africa's ranking was very low (among the last 50 out of a possible 150 countries) (World Bank, 1998). Long-term development can only take place when there is access to affordable energy. Insufficient energy or a lack thereof has been reported to be a cause of social and economic poverty, so it is very important to select a model to forecast consumption of energy reasonably accurately.

Accurate forecasting is important to both government and industry who need to provide viable estimates on future revenue, cost, demands (Wedding and Cios, 1996) and energy consumption. A lack or a shortage of energy is perceived to have a detrimental effect on the economy and gross domestic growth (Anonymous, 2003). Energy is the basis for sustainable development and the means to ensure a healthy economy (Wang, 2009). Implementing a long-term economic development plan and an energy strategy for a country/industry requires establishing the optimal relationship between energy supply and the economy.

It is worth noting that economic events and regime changes in the economic environment, in energy policy and fluctuations in energy prices can lead to structural changes in the pattern of energy consumption in a period under study(Chiou-Wei *et al.,* 2008), consequently, the relationship between energy consumption and economic growth (Chiou-Wei *et al.,* 2008; Lee and Chang 2005) should be regarded as non-linear.

A sound forecasting technique is crucial to develop an accurate plan and to formulate an energy strategy. To date, the most popular modelling

technique used to predict energy consumption has been regression analysis. To predict energy consumption based on adequate data analysis, this study has used data from the gross domestic product (GDP) of South Africa's industrial sector, as well as total energy consumption in neural network analysis, to achieve more reliable results.

Using an artificial neural network method rather than a traditional classification method derives from the success in estimating the non-linear function (Mabel and Fernandez 2008). However, apart from estimating the non-linear function in a shorter period of time, the advantage of the artificial neural network (ANN) approach is that energy applications are more viable, making them more attractive to potential users such as energy engineers *(Kaukal et al.,* 2011).

ANNs are computer programs that are designed to recognize both linear and non-linear relationships between the input and the output variables in a given data set (Al-Alawi *et al.*, 2003). ANNs are able to process information and provide models even when the information and data are complex, noise-contaminated, non-linear or incomplete. The goal of an ANN is to map a set of input patterns against a corresponding set of output patterns. The network accomplishes this mapping by learning from a series of examples and defining the input and output sets for a given system (Amir Heydari *et al.*, 2006). The network then applies what it has learnt to a new input pattern to predict the appropriate output (Amir Heydari *et al.,* 2006; Zuptan and Gasteiger 1999).

Many studies on energy demand and consumption forecasting exist in the literature. Among these studies, linear and non-linear statistical models, including ANN programs, have been used by Pao (2006) to determine the influence of four economic factors on the electricity consumption in Taiwan and to develop an economic forecasting model. An ANN model that has four independent variables, namely GDP, population, and import and export costs has been used by Geem and Roper (2009) to estimate the energy demand in South Korea accurately, and Bianco *et al.*, (2009) took into account the influence of several economic and demographic variables related to the annual electricity consumption in Italy, to develop a long-term consumption forecasting model.

The industrial sector is at the core of developing projects because it is the most important end-user in developing countries, to ensure economic growth (Lee and Chang, 2007).This study aims to determine the empirical factors affecting estimation of energy consumption in the industrial sector of South Africa by using the multilayer perceptron (MLP) and radial basis function (RBF) of artificial neural network (ANN) models, and comparing the prediction capabilities of the models.

It was found from the comparison of performance indices, based on the statistical measures namely, mean absolute percentage error (MAPE), coefficient of correlations and visual inspection, that prediction performance of the RBF model was superior to that of the MLP function.

2. Data

In this paper, the industrial sector of South Africa, a developing country was assessed. Annual data from 1993 to 2000 reflected in Table 1 on total energy consumption and real GDP were used. These were obtained from the Integrated Energy Plan for the Republic of South Africa, and the Department of Minerals and Energy (Anonymous 2003). Total energy consumption is measured in Peta Joules (PJ) with renewable and waste excluded and for GDP, 1995 was used as the base year.

3. MLP neural network and RBF neural network

3.1. MLP structure and design

Since their inception in the 1940s, different neural network models have been developed, but the MLP is still the most widely used (Mata, 2011). This network consists of three layers namely, input layer, hidden layer and output layer, with each layer having one or more neurons. In addition, bias neurons are connected to the hidden and output layers as shown in Figure 1.

The computational procedure of the network is described below(Hsu and Chen, 2003):

$$Y_j = f(\Sigma_i w_{ij} X_{ij}) \quad (1)$$

where Y_j is the output of node j, $f(.)$the transfer function, w_{ij} the connection weight between node j and node i in the lower layer and X_i the input signal from the node *i* in the lower layer. The backpropagation is based on the steepest descent technique with a momentum weight (bias function) which calculates the weight change for a given neuron. It is expressed as follows (Hsu and Chen, 2003; Huang *et al.,* 2002): let $\Delta w^p_{ij}(n)$ denote the synaptic weight connecting the output of neuron *i* to the input of neuron *j* in the *p*th layer at iteration *n*.

The adjustment $\Delta w^p_{ij}(n)$ to $w^p_{ij}(n)$ is given by

$$\Delta w^p_{ij}(n) = \eta(n)\frac{\delta E(n)}{\delta^p_{ij}} \quad (2)$$

where $\eta(n)$ is the learning rate parameter. By using the chain rule of differentiation, the weight of the network with the backpropagation learning rule is updated using the following formulae:

$$\Delta w^p_{ij}(n) = \eta(n)\delta^p(n)\, X^{p-1}_i(n) m(n) \Delta w^p_{ij}(n-1) \quad (3)$$

$$\Delta w^p_{ij}(n+1) = w^p_{ij}(n) + \Delta w^p_{ij}(n) \quad (4)$$

Table 1: Industrial sector data

	1993	*1994*	*1995*	*1996*	*1997*	*1998*	*1999*	*2000*
GDP - All industries	472	486	500	521	534	538	549	571
Total final energy consumption (PJ)	1766	1789	2016	1996	2071	2098	2026	2003

All industries are listed at basic prices Rand (R) - billion (constant 1995 prices), Renewable and Waste are excluded.

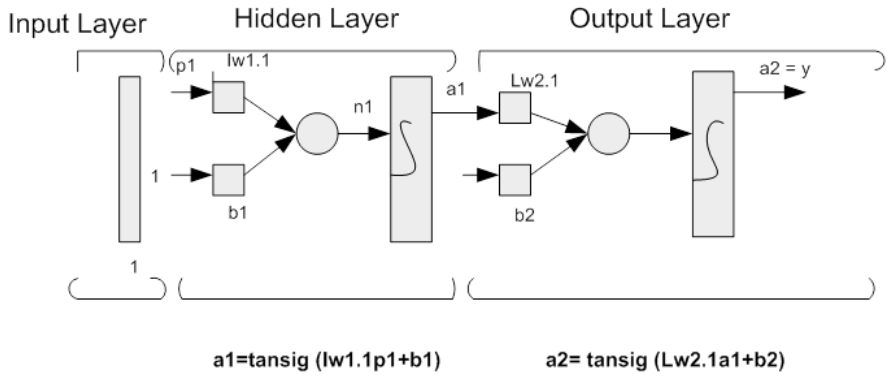

Figure 1: MLP Single hidden layer neural network structure

where $\delta^{p}_{i}(n)$ is the nth error signal at the jth neuron in the pth layer, $X^{p-1}_{i}(n)$ is the output signal of neuron *i* in the hidden layer, and m is the momentum factor.

Newff is a Matlab code which creates a feed-forward backpropagation network. This was used to calculate a precise function of the MLP neural network. The number of hidden neurons was determined by comparing the performance of different cross-validated networks, with 1–15 hidden neurons, and choosing the number that produced the greatest network performance. This resulted in a network with single input neuron (GDP), five hidden neurons and a single output neuron (energy consumption). In the analyses, network parameters of learning rate and momentum were set at 0.05 and 0.7, respectively. A variable learning rate with momentum (trainlm) as the network's training function, and tansig as activation functions for all layers was used. The data used by the network must be scaled for the network to be effectual. In theory, the inputs to the network can be any value. However, scaling values to the same order of magnitude (generally in the range 0 to 1 or -1 to 1) enables the network to learn relationships more quickly (Hart, 1992). In this paper, the data was scaled to the range -1 to 1 to ensure a consistent scaling regime for input and output. The Matlab code for the design is as follows:

```
p=[472 486 500 521 534 538 549 571];
t=[1766 1789 2016 1996 2071 2098 2026
2003];
[pn,minp,maxp,tn,mint,maxt] = premnmx(p,t);
iitst = 2:4:Q;
iival = 4:4:Q;
iitr = [1:4:Q 3:4:Q];
val.P = pn(:,iival); val.T = tn(:,iival);
test.P = pn(:,iitst); test.T = tn(:,iitst);
ptr =pn(:,iitr); ttr = tn(:,iitr);
net = newff(minmax(ptr),[5 1],{'tansig' 'tan-
sig'},'trainlm');
net.trainParam.show=50;
net.trainParam.lr=0.05;
net.trainParam.mc=0.7;
[net,tr]=train(net,ptr,ttr,[],[],val,test);
an=sim(net,pn);
a = postmnmx(an,mint,maxt);
error=(t-a)
```

3.2. RBF structure and design

Due to their better approximation capabilities, simpler network structures and faster learning algorithms, RBF networks have been widely used in many science and engineering applications (Benghanem and Mellit, 2010; Mellit and Kalogirou, 2008).

The RBF neural network is a kind of feed-forward neural network (Tong *et al.*, 2009). The RBF neural network (Bishop, 1991; Wedding and Cios, 1996) comprises three layers: input layer, hidden layer and output layer. Between the input and output layers is a layer of processing units known as hidden units. Each of these implements a radial basis function (Tong *et al.*, 2009). The distance between hidden-layer neurons is connected with the input of the weight and the vector a_p, multiplied by the threshold as their own input, as shown in Figure 2.

A hidden layer of *i* input:

$$t_i^q = \sqrt{\sum_j (w1_{ji} - a_j^p)^2} \times d1_i \quad (5)$$

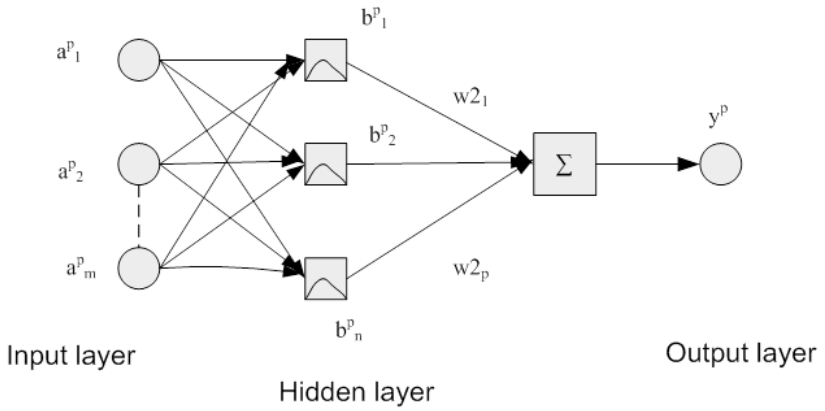

Figure 2: RBF Neural network structure

The output:

$$b_i^p = \exp\left[-t_i^{q\,2}\right] = \exp(\sqrt{\sum_j (w1_{ji}} - a_j^p)^2 \text{X } d1_i)$$
$$= \exp\{\left(\left|\left|w1_i - a_p\right|\right| \text{X } d1_i\right)^2\} \quad (6)$$

Although RBF threshold d1 can adjust the sensitivity function, in this work, another parameter C (expansion constant) was used. To determine the neural network, the relationship between C and d1 in the Matlab Toolbox is:

$$d1_i = 0.8326/C_i \quad (7)$$

The output of the hidden-layer neurons at this point can be represented by the following equation:

$$S_j^p = \exp\{\frac{0.8326\ X\sqrt{\sum_j (w1_{ji}} - a_j^p)^2}{c_i}\} \quad (8)$$
$$= exp(0.8326^2 \text{X}\left\{\frac{\{\left|\left|w1_i - a_p\right|\right|\}^2}{c_i}\right\})$$

The weighted sum of the hidden layer neurons output serves as input data for the output:

$$y^p = S^n_{i=1} b_i \text{ X } w2_i \quad (9)$$

Training the RBF network entails two steps: the first step is to learn without been taught, determining weight w1 between input layer and hidden layer; the second step is to identify weight w2 between the hidden layer and output layer (Caiqing et al., 2008).

Newrbe is a Matlab code which designs a radial basis network with zero error in the design vectors. The code was used to create a precise function for the RBF neural network, which automatically chooses the number of the hidden layer, making predictions more accurate (Caiqing et al., 2008). In the analysis, the network parameter SPREAD which is the distribution density of RBF was set to 2.3 for the network. The Matlab code for the design is as follows:

```
p=[472 486 500 521 534 538 549 571];
t=[1766 1789 2016 1996 2071 2098 2026
2003];
p=mapminmax(p,0,1);
[t,ts]=mapminmax(t,0,1);
spread=2.3;
net=newrbe(p,t,spread);
yn=sim(net,p)
```

4. Prediction performance comparisons

Two different statistical measures were employed to evaluate the energy consumption prediction capability of each of the ANN models.

4.1. Coefficient of correlation R2 and mean absolute percentage error (MAPE)

Table 2 reflects the R^2 and MAPE for the energy consumption for each model. The total sum of squared deviations in Y (energy consumption) can be decomposed into two qualities, the first, SSR, measures the quality of x (GDP) as a predictor of Y, and the second, SSE, measures the error in the prediction. Thus, the square of the correlation coefficient between the response variable Y and the predictor x is:

$$R^2 = 1 - \frac{SSE}{SST} = \frac{SSR}{SST} \quad (10)$$

where SST = SSR + SSE (11)

SST = Total sum of squares, *SSR* = Sum of squares due to regression and *SSE* = Sum of squares due to error.

It should be noted that $0 \leq R^2 \leq 1$ because SSE ≤ SST. If R^2 is near 1, then x (GDP) accounts for a large part of the variation in Y (energy consumption) (Chatterjee and Hadi, 2006).

The mean absolute percentage error (MAPE) which is a measure of accuracy in a fitted series value in statistics, is expressed in per cent

$$\text{MAPE} = \frac{1}{N}\sum_{i=1}^{N}\left|\frac{Ai-Pi}{Ai}\right| \text{ x } 100 \quad (12)$$

where A_i is the actual value, P_i is the predicted value and N is the number of data. A MAPE below 5% is the measure of a highly accurate prediction.

5. Results and discussion

Computer codes for MLP and RBF-models were developed in Matlab Software (version 2010a). The models were trained until the best performance was obtained. The optimal parameters (weights and bias) of the networks were saved and used for testing and validating operation of the models.

In order to test and validate the different models, two statistical tests (the correlation coefficient and the mean absolute percentage error 'MAPE') between the measured and the estimated annual energy consumption data using the MLP and RBF network were carried out. The results obtained are summarised in Table 2. From the simulations carried out, it was found that better performance was delivered by the RBF-model according to the correlation coefficient between both sets of data (measured and estimated).The obtained is 0.9998, is higher than the corresponding one in the MLP-model, while the MAPE is lower than that of the MLP-model. In order to demonstrate the efficiency of the proposed RBF-model, a comparison was done between the developed RBF, and MLP models in Figures 3 to 6. Figure 7 illustrates the deviation from actual data of the two models. The RBF model easily learnt to capture the industrial sectors' energy consumption (with the least forecasting errors).

Table 2: Performance indices for models

Model	MAPE	R^2
MLP	3.3×10^{-2}	0.9959
RBF	2.07×10^{-2}	0.9998

MAPE = mean absolute percentage error, R^2 = correlation coefficient

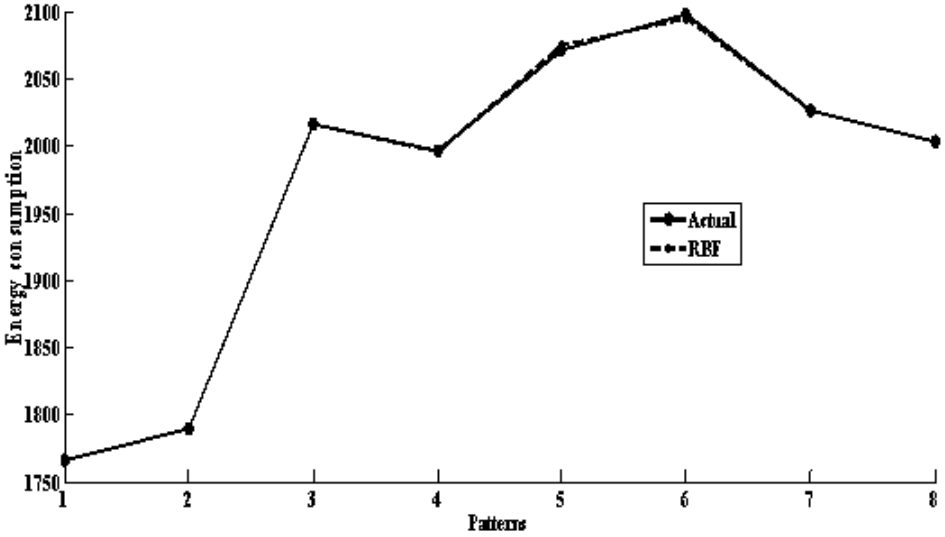

Figure 3: Comparison between the actual and RBF predictions

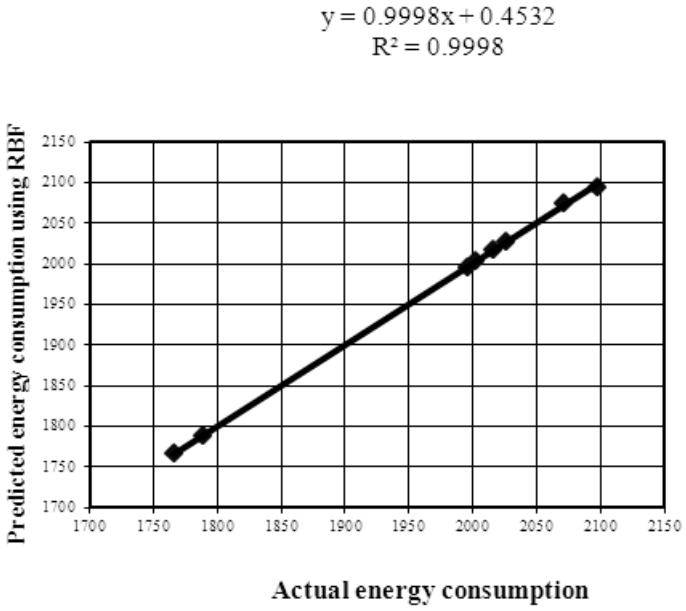

Figure 4: Regression analysis between the actual and RBF predictions

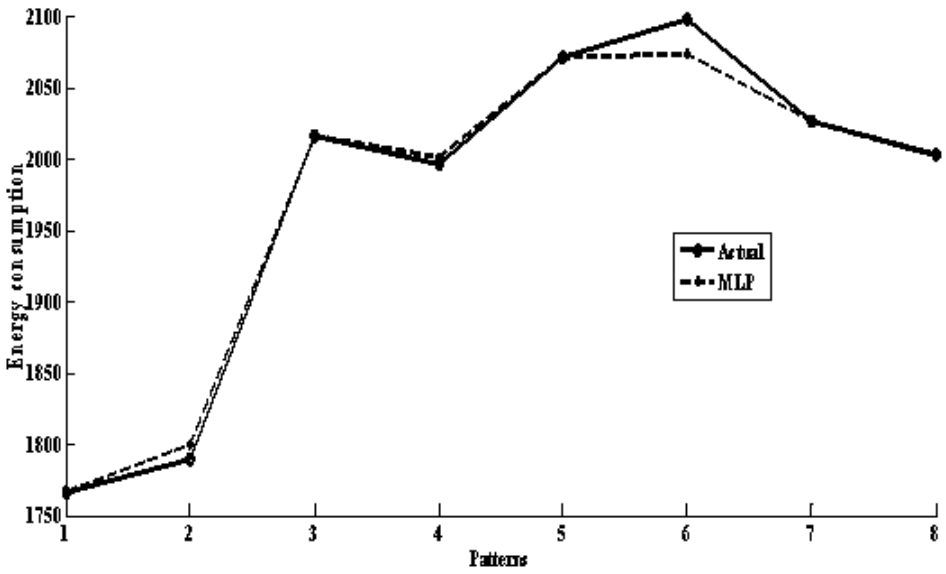

Figure 5: Comparison between the actual and MLP predictions

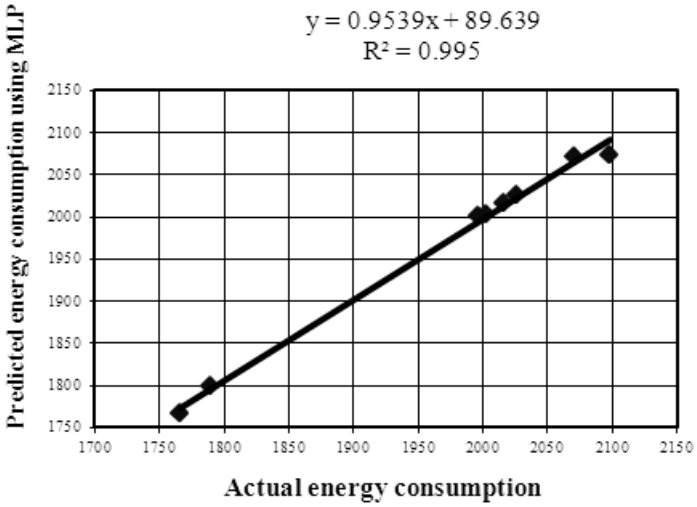

Figure 6: Regression analysis between the actual and MLP predictions

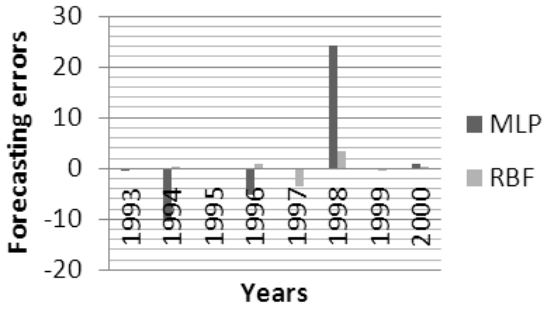

Figure 7: Deviation from actual data of the two models

6. Conclusion

Forecasting energy consumption is essential for the long-term development of South Africa, especially for the industrial sector which plays a pivoted role in the country's economic growth. In order to establish accurately the relationship between energy consumption and the economy of an industrial sector for estimating the energy consumption, ANN models were employed. In this paper, MLP and RBF models for estimating South Africa's industrial annual energy consumption were adapted. The measured annual energy consumption was compared with that estimated using MLP and RBF models. The predictive performance of each model was assessed using two statistical measures: R^2, MAPE and a study of the graphs were used. The results of the statistical measures suggest that RBF-model provides more accurate results than the MLP-model.

It has been demonstrated that the RBF-model gives more accurate results when compared with those obtained using the MLP network model. Both models deliver highly accurate predictions, since the MAPE values are below 5%. The developed model is suitable for South Africa's industrial sector. It is concluded that the predicted data generated by the RBF network is evidently suitable for estimating the

energy consumption of South Africa's industrial sector to formulate an accurate development plan and to implement a viable energy strategy.

References

Al-Alawi, S., Al-Badi, A., and Ellithy, K. (2003). An artificial neural network model for predicting gas pipeline induced voltage caused by power lines under fault conditions. *An artificial neural network model*, 69.

Amir Heydari, Shayesteh, K., and Kamalzadeh, L. (2006). Prediction of Hydrate formation temperature for natural gas using artificial neural network. *Oil and Gas Business*.

Anonymous. (2003). Integrated Energy Plan for the Republic of South Africa. South Africa.

Benghanem, M., and Mellit, A. (2010). Radial Basis Function Network-based prediction of global solar radiation data: Application for sizing of a stand-alone photovoltaic system at Al-Madinah, Saudi Arabia. *Energy*, 35, 3751-3762.

Bianco, V., Manca, O., and Nardni, S. (2009). Electricity consumption forecasting in Italy using linear regresion models. *Energy*, 34, 1413-1421.

Bishop, C. M. (1991). Improving the generalization properties of radial basis function neural networks. *Neural computation*, 3, 579-588.

Caiqing, Z., Ruonan, Q., and Zhiwen, Q. (2008). Comparing BP and RBF Neural Network for Forecasting the Resident Consumer Level by MATLAB. International Conference on Computer and Electrical Engineering.

Chatterjee, S., and Hadi, A. S., eds. (2006). *Regression Analysis by Example*, A John Wiley and Sons inc.

Chiou-Wei, S. Z., Chen, C.-F., and Zhu, Z. (2008). Economic growth and energy consumption revisited - Evidence from linear and non-linear Granger causality. *Energy Economics*, 30, 3063-3076.

Geem, Z. W., and Roper, W. E. (2009). Energy demand estimation of South Korea using artificial neural network. *Energy Policy*, 37, 4049-4054.

Hart, A. (1992). Using neural networks for classification tasks - some experiments on datasets and practical advice. *J.Opl. Res. Soc.*, 43, 215 - 226.

Hsu, C.-C., and Chen, C.-Y. (2003). Regional load forecasting in Taiwan-applications of artificial neural networks. *Energy conversion and Management*, 44, 1941-1949.

Huang, H., Hwang, R., and Hsieh, J. (2002). A new artificial intelligent peak power load forecaster based on non-fixed neural networks. *Electric Power Energy Syst*, 24, 245-250.

Kaukal, M., Akpinar, A., Komurcu, M. I., and Ozsahin, T. S. (2011). Modelling and Forecasting of Turkey's energy consumption using socio-economic and demographic variables. *Applied Energy*, 88, 1927-1939.

Lee, C.-C., and Chang, C.-P. (2007). The impact of energy consumption on economic growth: Evidence from linear and nonlinear models in Taiwan. *Energy*, 32, 2282-2294.

Lee, C. C., and Chang, C. P. (2005). Structural breaks, energy consumption, and economic growth revisited: evidence from Taiwan. *Energy Economics*, 27, 857-872.

Mabel, M. C., and Fernandez, E. (2008). Analysis of wind power generation and prediction using ANN: A case study. *Renewable Energy*, 33, 986-992.

Mata, J. (2011). Interpretation of concrete dam behaviour with artificial neural network and multiple linear regression models. *Engineering Structures*, 33, 903-910.

Mellit, A., and Kalogirou, S. (2008). Artificial intelligence techniques for photovoltaic applications: a review. *Prog Energy Comb Sci*, 34, 574-632.

Pao, H. T. (2006). Comparing linear and non-linear forecasts for Taiwan's electricity consumption. *Energy* (31), 2129-2141.

Tong, X., Wang, Z., and Yu, H. (2009). A research using hybrid RBF/Elman neural networks for intrusion detection system secure model. *Computer Physics Communication*, 180, 1795 - 1801.

Wang, L. (2009). Grey Incidence Analysis between Energy Consumption Structure and Chinese GDP Growth. *Proceedings of 2009 IEEE International Conference on Grey Systems and Intelligent Services, November 10-12, 2009*, Nanjing, China.

Wedding, D. K., and Cios, K. J. (1996). Time series forecasting by combining RBF networks, certainty factors, and the Box-Jenkins model. *Neurocomputing*, 10, 149 - 168.

World Bank. (1998). World Development Indicators. The International Bank for Reconstruction and Development/the World Bank Washington DC.

Zuptan, J., and Gasteiger, J., eds. (1999). *Neural Networks in Chemistry and Drug Design*, Wiley/VCH, New York.

Received 15 June 2011; revised 7 May 2012

Generation, characteristics and energy potential of solid municipal waste in Nigeria

Ityona Amber

Daniel M Kulla

Nicholas Gukop

Department of Mechanical Engineering, Ahmadu Bello University, Zaria, Nigeria

bstract

The generation, characteristics and energy potential of municipal solid waste for power generation in Nigeria is presented in this paper. Nigeria generates 0.44-0.66 kg/capita/day of MSW with a waste density of 200-400 kg/m^3 leading to large volumes of poorly managed waste. The direct burning of these wastes as a waste management option in the open air at elevated temperatures liberates heat energy, inert gases and ash which can be conveniently used for power generation and other applications. The net energy yield depends upon the density and composition of the waste; relative percentage of moisture and inert materials, size and shape of the constituents and design of the combustion system. MSW samples used in this study were obtained randomly from different dump sites in selected state capitals, at least one from each of the six geopolitical zones in Nigeria based on the spot sampling method of Corbit. An average calorific value of 17.23 MJ/kg with variable high water content of 20-49% was determined for MSW using a bomb calorimeter and on the basis of an incineration plant of capacity 1500 ton of MSW/day, 700kW/day of power can be generated.

Keywords: municipal solid waste, calorific value, waste to energy, proximate and ultimate analysis

1. Introduction

Municipal solid waste (MSW) comprises of combined domestic, commercial and industrial waste generated in a given municipality or locality (Fobil, 2005 Kothari, et al., 2010). The integrated solutions to problems of the waste management in the modern era provided by waste to energy or energy from waste, by the direct burning of mixed waste in open air at elevated temperatures in mass burning facilities liberates energy in the form of electricity or heat that can be conveniently used for power generation (Voelker, 1997). Traditionally this waste would have been disposed in a land fill site or incinerated in mass burning facilities without heat or energy recovery (IEA, 2003, Tsia, 2006, Kothari, et al., 2010). Waste to energy (WTE) technologies have the potential to reduce the volume of the original waste by 90%, depending on the composition, by recovering otherwise lost energy and metals in MSW, thus providing a means of alternate/renewable energy and a reduction of society's use of precarious energy resources can be realised (Voelker, 1997; Wang, 2009; Kathiravale, 2003; Kothari, et al., 2010). The heating value of mixed MSW is approximately about one-third of the calorific value of coal (8-12 MJ/kg as received for MSW and 25-30 MJ/kg for coal) (IEA, 2003). The net energy yield depends upon the density and composition of the waste; relative percentage of moisture and inert materials, which add to the heat loss; ignition temperature; size and shape of the constituents; design of the combustion system (fixed bed/ fluidised bed), etc (Fobil, 2005; Akkaya & Demir, 2009). Table 1 has heating values over that of coal such as plastic, polyethene and tyres.

Solid waste management has emerged as one of the greatest challenges facing state and local government environmental protection agencies in Nigeria. The volume of solid waste being generated continues to increase at a faster rate than the ability of the agencies to improve on the financial and technical resources needed to parallel this growth. Solid waste management in Nigeria is characterized by inefficient collection methods, insufficient coverage of the collection system and improper disposal

of solid waste. As such, most cities and towns are characterised by waste disposal dumpsites situated on any available free land roads streets, drainages etc. (www.punchng.com/news).

Nigeria, at present, peak power generation as supplied by the power holding company of Nigeria (PHCN) is below 4 MW to cater for a population of over 150 million, which has resulted in an acute and interrupted power supply (Nigeria power road map, 2010). This has led to the use of petrol and diesel generators and in 2009 it was reported that about 60 million Nigerians own generators for their electricity, while the same number of people spend a staggering N1.56 trillion ($13.35m) to fuel them annually.

At a current population growth rate of 2.03% and 7% economic growth, energy consumption and waste generation in Nigeria is expected to soar over the next few years. The exploitation of the non-conventional energy locked up in the urban solid municipal waste into grid energy through WTE will provide the dual advantage of minimising waste and recovering the 'hidden' energy. This makes it a very attractive waste management/power generation option for Nigeria.

The average waste density currently ranges between 280 to 370 kg/m^3 with waste generation rates ranging from 0.44 to 0.66 kg/capita/day (Ogwueleka, 2009). Table 2 shows the current populations and volumes of municipal solid waste generate in a few Nigerian cities for the years 1982, 1990, and projection for 2000 and 2010. It is evident that the amount of waste in these cities has more than doubled over the last two decades. The quantity and rate of MSW generation in each state is a function of the population, level of industrialization, social-economic status of the citizens and the kind of commercial activities predominant in the area. (Babayemi & Dauda, 2009; Nabegu, 2010.). The literature available presents some idea of what quantity of waste is generated, its composition and characteristics, but its suitability for power generation has not yet been fully addressed and needs to be if a certain waste is being considered for power generation.

The objective of this paper is to assess the quantity (generation), quality (physical and chemical) and energy of Nigerian MSW for power generation in Nigeria. The challenges and changes in quantity and quality of the Municipal Solid Waste in Nigeria has been reported in Ogwueleka, 2009, Onwughara,*et.al.,* 2010; and Babayemi & Dauda, 2009. Ogwueleka (2009) also in his paper reports that the Federal Government of Nigeria laws and regulations in Nigeria promulgated to protect the environment of which include the Federal Environmental Protection Agency Act of 1988 and the Federal Environmental Protection Agency (FEPA), created in 1999 under the FEPA Act decrees where each state and local government in the country set up its own environmental protection body for the protection and improvement of the environment within its jurisdiction, thus making municipal solid waste management as a major responsibility of state and local government environmental agencies. Assessments of MSW have been reported from China (Cheng *et al.,* 2007), South Korea (Ryu, 2010), Malaysia (Kathiravale *et.al.,* 2003) and Taiwan (Tsai and Kuo, 2010).

This paper presents the generation, characteristics and energy potential of municipal solid waste in Nigeria for power generation.

Table 1: Heating values for various fuels and MSW components

Source: Voelker, IEA (2003)

Fuel	Heating value (kJ/kg)
Anthracite coal	6454.274
Bituminous coal	6693.322
Peat	1721.14
Oil	8605.699
Natural gas	11474.27
Mixed MSW	2294.853
Mixed paper/ newsprint	3251.042/3800.85
Cardboard	3367.219
ploye thene	8934.15
polystyrene	7849.832
Mixed plastic	6741.131
Tyres	6597.703
leaves	2390.427

2. Methodology

The spot sampling method of Corbit, 1998 was adopted in the sampling and sorting protocol. The spot sampling method requires for the samples to be taken from dump sites from the same source where an amount of waste (about 30–50 kg) is to be taken and the total amount collected will form a sample size of about 200 kg, which is then sorted. Five samples of 10 kg each of the raw MSW is taken randomly from dump sites whose sources are generated by different activities from some selected state capitals which harbour the largest population and being the economic nerve of the respective states. The states were selected to reflect at least one city in each of the six geopolitical zones of Nigeria. The sampling was done between January and February, a period of dry season in most Nigerian cities. The sorting is carried out based on 5 different components as listed in Table 4. Segregated waste components were weighed. Subsamples, each weighing 5 kg were taken from the composite samples and oven-heated at 85°C to constant weight for determination of moisture content.

Table 2: Waste generation for 1982, 1990 and 2000
Source: Ogwueleka, (2009); Onwughara,et.al., (2010); Babayemi and Dauda, (2009)

City	*Population*	*Waste generated1982 (Tonnes)*	*Waste generated1990 (Tonnes)*	*Waste generation projected for 2000 (Tonnes*	*Waste generated 2010 (Tonnes)*	*Density (kg/m^3)*	*kg/ capita/ day*
Lagos	9 000 000	625 399	786 079	998 081	3 066 672	294	0.63
Kano	3 626 068	319 935	402 133	535 186	1 880 112	290	0.56
Ibadan	3 565 108	350 823	440 956	559 882	1 624 692	330	0.51
Kaduna	1 582 102	257 837	324 084	431 314	1 373 196	320	0.58
Port Harcourt	1 148 665	210 934	265 129	352 853	1 413 900	300	0.6
Makurdi	292 645	44 488	57 243	79 835	290 904	340	0.48
Onitsha	561 066	242 240	304 477	386 593	1 009 644	310	0.53
Nnsuka	111 017	144 000	370	0.44			
Abuja	99 871	135 272	197 660	177 420	280	0.66	
Abeokuta	NA	NA	NA	0.66			
Ado-Ekiti	NA	NA	NA	0.71			
Akure in	NA	NA	NA	0.54			
Ile-Ife	NA	NA	NA	0.46			
Ibadan	NA	55 200	NA	0.71			
Ilorin	NA	NA	NA	0.43			
Aba	NA	131 903	169 719	236 703	2 840 436	NA	NA
Uyo	NA	251 076	NA	NA			
Maiduguri	NA	1 020 000	NA	NA			
Warri	NA	67 447	91 396	133 531	800 652	NA	NA
Benin	NA	NA	NA				

Experimental determination of the physical and chemical characteristics, important parameters that determine energy recoverable from MSW was carried out by a proximate and ultimate analysis. The calorific value of MSW was determined in accordance to ASTM E 711-87.

The calculation of the potential of recovery of energy from MSW is obtained from equation 1 – 4, which requires the knowledge of its calorific value and organic fraction, as in thermo-chemical conversion of all of the organic matter, biodegradable as well as non biodegradable, which contributes to the energy output. Total waste quantity (W tonnes) is calculated from a rough estimated of waste in place using equation 1 (Akkaya, & Demir, 2009).

Total waste land filled (W tonnes) = Urban population x Waste generation rate (kg/person/year) x Fraction of waste in landfills or open dumps x Years of land filling x 0.001 (1)

Energy recovery potential (kWh) = NCV x W x 1000/860 = 1.16 x NCV x W (2)

Power generation potential (kW) = 1.16 x NCV x W/ 24 = 0.048 x NCV x W (3)

Conversion efficiency = η

Net power generation potential (kW) = η x 0.048 x NCV x W (4)

3. Results

The current waste generation rate for some Nigerian cites, the associated population of each city, and the tonnage per month is also given in Table 2.

4. Discussion

Waste characteristics influence the amount of energy within landfills. Different countries and regions have MSW with widely differing compositions.

The population and generation rates for selected cities sampled in this study are presented in Table 2. The waste composition and their percentages by weight are presented in Table 3. Further analysis of the sorted waste showed that constituents were quite similar except for the amount and proportion present in a waste dump site differed in proportion for each sample and this greatly influenced the type of activity dominant in the environment where the waste is generated and deposited.

The average percentage composition of various waste stream (Table 2) shows 43% organic component, 8% paper /cardboard/plastics and rubber, 26% glass, 3% metal and cans, 2% textile materials, and 2% residue.

Table 3: Percentage composition of waste stream characteristics

	Nnsuka	*Lagos*	*Makurdi*	*Kano*	*Onitsha*	*Ibadan*	*Maiduguri*	*Zaria*	*Average*
Food/organics	59.8	63	59.3	58	56.9	58.5	60.8	58.8	59.38
Paper/ Paper/ polythene/polythene	25.72	45	23.22	38.42	39.11	37.6	35.6	39.07	35.46
Textile	1.57	3.1	2.5	7	6.2	1.4	3.9	2.13	3.47
Glass &metal	2.5	3	3.6	2	9.2	0.6	4.3	5.15	3.79
Others (dust, ash, rubber, soil, bones, ceramics	9.4	19	14	22	15.4	8.9	31.3	4.33	15.545
Moisture content	20.79	28.36	20.27	18.88	21.17	23.52	17.95	18.33	21.15

Table 4: Energy content of MSW

Components	*Energy content (MJ/kg)*
Organic / food	11.59
Paper	10.14
Cardboard	11.033
Plastics	14.89
Polyethene	46.5
Metal glass and cans	
Textile	9.27
Net calorific value(MJ/kg) -	17.23
Moisture content	49.90%

The average calorific value for the raw waste analysed for drying or preheating is 11.38MJ/kg while for the oven dried MSW at 85oC gave a calorific value of 17.38 MJ/kg and a moisture content of 49.90%. The collected waste sample reveals organic wastes containing high concentration of bio-degradable matter which are suitable for energy recovery through anaerobic de-composition or dried and combusted and a high proportion of polythene waste from sachet drinking water popularly known as 'pure water', and shopping bags which has a calorific value of 14.89MJ/kg. The MSW samples collected from southern Nigeria cities had higher moisture content than the samples collected in the northern part which is attributed to the relative humidity of the location of interest.

The ultimate and proximate analysis (Table 4) shows the chemical analysis by mass of important elements of the MSW sample. These are important parameters for technical viability of energy recovery through different and selected treatment routes. The proximate analysis, ultimate/elemental analysis and the calorific values are required for the design of a suitable incineration plant.

On the basis of a 1500 ton of MSW/day incineration plant, MSW with average calorific values of 17.23MJ/kg, a conversion efficiency of 25% and 49% water content, the thermal treatment of MSW resulted in the generation capacity of 700 kWh of electricity per ton of MSW combusted. In practice, about 65 to 80 % of the energy content of the organic matter can be recovered as heat energy, which can be utilised either for direct thermal applications, or for producing power via steam turbine generators (with typical conversion efficiency of about 30%). Modern incinerators can reduce waste volume by 97% and convert metal and glass to ash which is currently being researched to be used in materials development.

Incineration is extensively used as an important method of waste disposal; it is associated with some polluting discharges which are of environmental concern, although in varying degrees of severity. These can fortunately be effectively controlled by installing suitable pollution control devices and by suitable furnace construction and control of the combustion process. The challenges using waste as fuel is poised in the heterogeneous composition of each dumpsite, strong variations in the composition which is both regional and seasonal dependent, variations in the calorific value, possibilities of and the presence or production of hazardous substances as well as the challenge of consistent collection and supply waste to operate a plate 24/7.

WTE adoption in Nigeria is at the moment not feasible due to a few of the factors as listed:

i) lack of advanced technology,

Table 5: Proximate and ultimate analysis

Proximate analysis (wet)	*Weight (%)*	*Elemental analysis (Dry)*	*Weight (%)*
Moisture content	49.90	Carbon content	51.33
Volatile matter content	38.28	Hydrogen content	6.77
Fixed carbon content	5.27	Nitrogen content	1.42
Ash content	5.25	Oxygen content	30.92
		Sulphur content	1.34

ii) lack of knowledge of the composition of specific landfills
iii) strength of solid waste management policy
iv) lack of proper enforcement and environmental education
v) low awareness and technical know how
vi) income status of individuals.

5. Conclusion

The generation, characteristics and the energy potential of MSW in Nigeria has been presented in this study. A calorific value of 17.23MJ/kg was obtained using a bomb calorimeter.

On the basis of a 1500 ton capacity incineration plant, 700 kWh of electricity per ton of MSW combusted can be generated.

Knowledge of the composition of specific landfills is very important. Lack of proper existing policies, legislation, waste handling and lack of awareness are obstacles for WTE Technology adoption in Nigeria.

References

ASTM E 711-87. Standard test method for gross calorific value of refuse-derived fuel by the bomb calorimeter.

Akkaya, E., & Demir,. A. (2009). Energy content estimation of municipal solid waste by multiple regression analysis. *In:* 5th International Advanced Technologies Symposium (IATS'09), 2009 Karabuk, Turkey. May 13-15.

Babayemi, J.O., & Dauda, K.T. (2009). Evaluation of Solid Waste Generation, Categories and Disposal Options in Developing Countries: A Case Study of Nigeria. *J. Appl. Sci. Environ. Management,* 13, 83 - 88.

Cheng,.H., Zhang, Y., Meng,.A., & Li,.Q. (2007). Municipal Solid Waste Fueled Power Generation in China: A Case Study of Waste-to-Energy in Changchun City. *Environ. Sci. Technol.* 41, 7509-7515.

Corbit, R.A. Standard test method for gross calorific value of refuse-derived fuel by the bomb calorimeter.

Fobil, J.N., & Carboo,.D. (2005). Evaluation of municipal solid wastes (MSW) for utilisation in energy production in developing countries. *Int. J. Environmental Technology and Management,* 5, 76-87.

IEA (2003). Municipal Solid Waste and its Role in Sustainability: A position paper. *In:* Bioenergy (ed.) www.ieabioenergy.com/media/40_IEAPositionPaper MSW.pdf.

Kathiravale, S., Abu., M.P., Yunus, M.M., & Abd-Kadir, K.Z.(2003). Predicting the Quality of the Refuse Derived Fuel from the Characteristics of the Municipal Solid Waste. *In:* 2nd Conference on Energy Technology Towards a Clean Environment, 12-14 February Phuket, Thailand.

Kathiravale, S., Abu., M.P., Yunus, M.M., & Abd-Kadir, K.Z.(2004). Energy potential from municipal solid waste in Malaysia. *Renewable Energy,* 29, 559-567.

Kothari, R., Tyagi, V.V. & Pathak,. A (2010). Waste-to-energy: A way from renewable energy sources to sustainable development. *Renewable and Sustainable Energy Reviews* 14 3164–3170.

Nabegu, A.B. (2010). An Analysis of Municipal Solid Waste in Kano Metropolis, Nigeria. *J Hum Ecology,* 31, 111-119.

Ogu, V.I. (2000). Private sector participation and municipal waste management in Benin City. *Environment & Urbanization,* 12, 103-117.

Ogwueleka, T.C. (2009). Municipal solid waste characteristics and management in Nigeria. *Iran. J. Environ. Health. Sci. Eng.,* 6, 173-180.

Onwughara,. I., Nkwachukwu,. N., Innocent, .C., & Kanno,.O.C. (2010). Issues of Roadside Disposal Habit of Municipal Solid Waste, Environmental Impacts and Implementation of Sound Management Practices in Developing Country 'Nigeria'. *International Journal of Environmental Science and Development,* Vol.1, No. 5,PP 409-418.

Othman, N., Basri,.N.E.A., Yunus,.M.N.M., & Sidek, L.M. (2008). Determination of Physical and Chemical Characteristics of Electronic Plastic Waste (Ep-Waste) Resin Using Proximate and Ultimate Analysis Method. *International conference on construction and building technology.*

Ryu,. C. (2010). Potential of Municipal Solid Waste for Renewable Energy Production and Reduction of Greenhouse Gas Emissions in South Korea. *Air & Waste Manage. Assoc.* 60:176 –183.

The Presidency Federal Republic of Nigeria (2010). Road map for power sector reform for customer driven sector wide plan to achieve stable power.

The Punch. Waste management: Big challenge here. www.punchng.com, Thursday, 27 May 2010.

Tsaia, W.T. & Chou, W.T. (2006). An overview of renewable energy utilization from municipal solid waste (MSW) incineration in Taiwan. *Renewable and Sustainable Energy Reviews,* 10, 491–502.

Tsai,.W. & Kuo, K. (2010). An analysis of power generation from municipal solid waste (MSW) incineration plants in *Taiwan Energy* 35 4824-4830.

Ugwuh, U. S. (2009). The state of solid waste management in Nigeria. *Waste Management,* 2009, 2787-2790.

Voelker, B.M. (1997). Waste-to-Energy: Solutions for Solid Waste Problems for the 21st Century. *www.p2pays.org/ref/09/08624.pdf*.

Wang,.L., Gang,.H., Gong,.X. & Bao,.L. (2009). Emission reductions potential for energy from municipal solid waste incineration in Chongqing.*Renewable Energy,* 34, 2074–2079.

Zaman, A.U. (2009). Life Cycle Environmental Assessment of Municipal Solid Waste to Energy Technologies. *Global Journal of Environmental Research,* 3, 155-163.

60m Nigerians now own power generators — MAN Vanguard Newspaper. www.vanguardngr.com/ DOI: 26th January 2009.

Received 5 May 2011; revised 1 June 2012

A specification of a flywheel battery for a rural South African village

Richard Okou
Department of Electrical Engineering, University of Cape Town

Adoniya Ben Sebitosi
Department of Mechanical and Mechatronics Engineering, University of Stellenbosch, South Africa

Pragasen Pillay
Department of Electrical and Computer Engineering, Concordia University, Canada

Abstract
The strong growth rates in the installed capacities of renewable energy technologies that have been posted in recent years demonstrate their capacity in the mitigation of green house gas emissions and climate change. The majority of these growths, however, have been realised in grid connected first world programs and do not require provision for energy storage. Most African rural areas are still far from the grid. Many upcoming developments such as cellular network repeater stations and health clinics must be operated from independent off grid PV installations. The intermittence of the resources dictates that reliable energy storage must be provided. The lead acid battery is currently the only available option but has well documented maintenance and disposal problems. The flywheel battery is an old technology that is re-emerging with a strong promise and could address the shortcomings of the lead acid battery. In this paper, a case study of a rural South African village load is depicted. Using a real utility database a possible specification for an electromechanical battery is derived. The authors further highlight the areas that will need future developments.

Keywords: energy storage, flywheel system, rural energy, South Africa

1. Introduction

Most rural electric loads are characterized by poor load factors with virtually no coincidence between generation and consumption. In the case of PV, for example, power generation is by daytime, while the lighting and infotainment dominated loads are almost entirely by night. Cynics have aptly likened operating such a system, without adequate storage, to milking a cow without a bucket. Energy storage remains by far the biggest challenge in rural electrification.

Electrical energy storage technology in sub-Saharan Africa is almost exclusively by chemical batteries, particularly the automotive lead acid type (Buchmann, 2001). The batteries have low initial prices but this is deceptive, as their short life spans imply routine replacement expenses. This increases the burden on the environment due to the frequent disposal of toxic materials. In addition, they have low depth of discharge capabilities and thus larger than necessary capacities are required, which further erodes their apparent cost advantage. There are certain battery types, which have labels like "solar batteries" with somewhat enhanced depths of discharge but this often comes with trade-offs.

Hunt (1998) refers to an inextricable link between power, energy and lifespan (in both age and charge-discharge cycles) that continues to baffle chemical battery researchers. Whenever any one of these three functions is enhanced, at least one of the remaining two deteriorates. For example, in order to deliver a required peak transient power, the design must offer high electrolyte to plate exposure but this in turn increases self-discharge rates and, hence, reduces the available energy. Ambient temperatures also affect charging characteristics and

general performance. Other issues range from simple ones like water loss (or drying up) to more abstract ones like electrolyte stratification. In renewable energy installations, batteries are often connected in series strings and charged while in use. Due to disparities in chemistry, different cells charge at different rates and the necessary equalization to allow the slow charging sections to top up cannot be carried out feasibly. Moreover due to the stochastic nature of resources, many generators are fitted with maximum power point trackers which often conflict with the set 'optimum' battery charging rates and results in dumping of excess power even when batteries are not fully charged. In addition, if battery cells should be kept at overcharge (say above 2.45volts in case of lead acid) for long periods, grid corrosion results. On the other hand, in cases of sustained low insolation and high load demand, the batteries will have to be exposed to long periods of deep discharge. This could lead to (the aforementioned) sulfation: a state that renders recharging difficult and at times impossible (Buchmann, 2001). Moreover, all chemical batteries suffer from high discharge shock, which compromises their life spans. Consequently, chemical batteries require expensive and highly skilled maintenance in order to yield maximum life. Skilled manpower and disposable income are rare commodities in African rural areas.

The flywheel (Hebner and Aanstoos, 2000; Post, 1996, Post *et al.,* 1993; Patel, 1999, Nasa, Bitterly 1998; Herbst *et al.,* 1998; Hayes *et al.,* 1999) is an age-old technology that has seen recent revival and could subsequently evolve to address the above concerns. The use of flywheels as reaction wheels (like porter's wheels) dates back to biblical times. The first electromechanical battery was however, only reported in the late 1940's in the urban Swiss vehicle called the gyro bus. Even then further research did not pick up until the 1970's, mainly for outer space programs but still kept a relatively low profile. The early 1990's saw a new revival as international political pressure increased demand for environmentally benign technologies. This was augmented by developments in strong lightweight materials, magnetic technology and solid-state electronics (Tsung *et al.,* 1993; Arnold *et al.,* 2001; Baaklini *et al.,* 2000; Tsai and Wu, 1971; Seireg *et al.,* 1970; Sung *et al.,* 1998; Halbach, 1980; Ofori and Lang, 1995). Subsequently, flywheel battery technology was shortlisted as one of the candidate technologies by the Partnership for a New Generation of Vehicles (PNGV) in the mid 1990's (Nap 1999, Sebitosi and Pillay 2003).

Potential attributes of the technology include long life spans, ability to charge or discharge at very high power rates through very deep cycles, no deterioration in performance with number of charge/recharge cycles and freedom from most of the chemical battery encumbrances. This technology has the potential to challenge the energy density of petroleum.

This paper will examine the possibility of using the environmentally benign electromechanical flywheel battery in rural sub-Saharan Africa. Conclusions will then be drawn as to the possibility of adopting the flywheel battery as electrical energy storage for rural requirements.

2. Kinetic energy storage

In principle, a flywheel stores energy in kinetic form, in a rotating wheel that is suspended on frictionless bearings in an aerodynamically drag-free vacuum enclosure.

The kinetic energy stored in a moving body is proportional to its mass and the square of its linear velocity.

$$KE = \tfrac{1}{2}mv^2 \tag{1}$$

When transformed into rotational motion one must consider the moment of inertia J. For the solid cylinder (Figure 1) rotating about its axis, the moment of inertia is defined as $J = \Sigma m_i r_i^2$, the sum of all elemental masses multiplied by the square of their distances from the rotational axis. As the sizes of these particles tend to zero they are virtually cubic with dimensions $\delta\varpi$, δr and h.

$$J = \int_{\theta=0}^{2\pi} \int_{r=0}^{R} \rho h \cdot d\omega \cdot dr \cdot r^2 \tag{2}$$

For a solid cylinder:

$$J = \tfrac{1}{2}mr^2 \tag{3}$$

And that for a hollow cylindrical system, as is typical of flywheels:

$$J = \tfrac{1}{2}m(r_o^2 + r_i^2) \tag{4}$$

Where r_i and r_o are the inner and outer radii respectively and the kinetic energy stored KE is given in equation (5).

$$KE = \tfrac{1}{2}J\varpi^2 = \tfrac{1}{4}m(r_o^2 + r_i^2)\varpi^2 \tag{5}$$

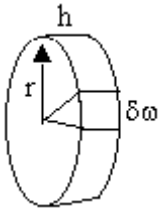

Figure 1: A solid cylinder with radius *r* and height *h*

The energy grows in proportion to the flywheel mass and the square of the angular velocity. So there is more emphasis on angular velocity rather than mass.

Consider a special case of a thin rotating ring. Its moment of inertia, J is given by equation (4). But as the thickness tends to zero $r_i = r_o = r$ and

$$J = \tfrac{1}{2}m(r_i^2 + r_o^2) = mr^2$$

But $v = r\varpi$
So kinetic energy:

$$KE = \tfrac{1}{2}mv^2 = \tfrac{1}{2}mr^2\varpi^2 = \tfrac{1}{2}J\varpi^2 \quad (6)$$

Where v is the linear velocity of a particle, r is the mean radius of the ring; m is its mass and ϖ its angular velocity.

The spinning subjects the rotor to stresses in proportion to the square of the angular velocity. These stresses can lead to failure. So, the maximum speed and therefore the maximum amount of energy storage attainable by the rotor is governed by its tensile strength.

$$KE = \frac{1}{2}m\frac{\sigma_h}{\rho} = \frac{1}{2}J\omega^2 \quad (7)$$

Where σ_h is the maximum allowable hoop stress for the ring, ρ is the density of the material.

The above expressions are only true for a thin ring. To get the total kinetic energy of a composite disk one would, in theory, have to sum up the energy in the nearly infinite thin rings. In practice the factors that determine rotor failure are much more complex. There is still lack of adequate experience and test data and much is still the subject of intense research. For example, while different composite flywheel designs may exhibit clearly different types of failure, similar designs may not necessarily fail in a similar manner.

3. The motor generator

In order to transfer energy to and from the spinning disk, a motor generator is used. The most popular choice is a permanent magnet synchronous machine, with an outer rotor design largely due to its high efficiency. The heart of this machine is an ironless magnetic array: an innovation by Klaus Halbach (Halbach, 1980) which reduces the stator losses to just the copper losses. The outer rotor is integrated into the flywheel, forming one unit instead of a machine with an attached flywheel.

An ideal Halbach cylinder is defined as an infinitely long structure where the magnitude of the magnetisation is constant and its orientation turns continuously. At an angular position ϕ in the cylinder, measured clockwise from the y-axis, the magnetisation has an orientation 2ϕ. The collective result is a uniform magnetic field, B^y in the y direction within the cylinder bore and a zero field outside the cylinder. The field is dependent only on the ratio between the inner r_i and outer r_o radii of the cylinder (or the difference between their natural logarithms) as given by equation (8).

$$B_y = J_r\, In\left(\frac{r_o}{r_i}\right) = J_r\left(In\, r_o - In\, r_i\right) \quad (8)$$

where J_r is the remnant field of the magnetic material of the cylinder.

In practice, however, approximations of this ideal design are constructed from a finite number, N, of short segments of high quality (rare-earth) magnets and systematically rotated to form an array as shown in Figure 2. It has the advantage of cutting down on cost of magnetic material as well as improving their stress performance. They can be arranged depending on the number of poles required. These magnets form the inner part of the motor rotor as illustrated in Figure 3. Unlike the ideal case, however, there's a finite stray field on the outside. There is also a possibility of some mild eddy current in the array magnets due to the current in the stator winding. In the illustrated practical dipole (Figure 2) the magnetic field B (in the bore) is dependent on the number of magnet elements used, as well. It is given by Halbach's theoretical treatment as equation (9).

$$B = J_r\, In\left(\frac{r_o}{r_i}\right)\eta \quad (9)$$

Where

$$\eta = \left[\frac{\sin(2\pi/N)}{(2\pi/N)}\right]$$

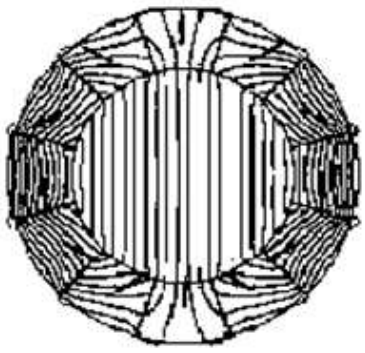

Figure 2: Magnetic field distribution of a dipole Halbach array

As illustrated in Figure 3, the winding is on the inner core which forms the stator, while the magnet array is moulded with the composite rotor with which it spins. The losses to be expected from the configuration in Figure 3 are copper losses in the

stator windings, rotor bearing losses and no air drag losses in the vacuum chamber. Therefore, the deceleration torque on no load (which is the self-discharge factor for the battery) is constant and not dependent on rotor speed. Bearing losses are minimized by the use of magnetic rather than mechanical bearings. The copper winding for the armature is sometimes made from tubing to enable the circulation of cooling oil.

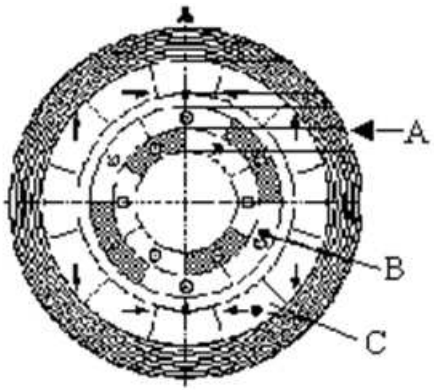

Figure 3: A cross-section of an ironless motor generator (complete) with the composite rotor (A is the composite ring, B is the electrical winding 3-phase 4 pole, C is the magnet array)

The performance of the machine can then be summarized as follows. Since the field strength, B and the depth of the magnetic ring, l are constant, the torque developed during charging will depend on charging (armature) current.

So for the dipole above, with I_{eff} as the effective current and l, as the magnetic depth, the torque T is given by

$$T = B\frac{\sqrt{2}}{3}qlI_{eff}\ Sin\left(\frac{\pi}{q}\right) \qquad (10)$$

Where, q is the number of phases for the machine.

The choice of a dipole version of the Halbach's magnet arrangement has been further supported in Post (1993) on the grounds that it makes the inductive coupling between the magnets and the windings relatively insensitive to the radial gap between them. This eases the mechanical clearance between them.

Ofori-Tenkorang *et al*. (1995) showed that the torque developed by a permanent magnet synchronous motor using the Halbach array (with an ironless core) is much higher than for a conventional array using the same weight and type of magnets.

4. Power electronics

The function of this sub-system is to condition the power to and from the generator (Amc, Bowler). This is necessitated by the fact that the flywheel motor generator has a continually variable voltage and frequency. Likewise, the levels of power from an external source like a wind turbine or a PV generator often vary with time. Currently the most p opular drive components are insulated gate bipolar transistors (IGBT). These are driven by appropriate control electronics. Figure 4 illustrates a typical 3-phase flywheel battery /power conditioner scenario.

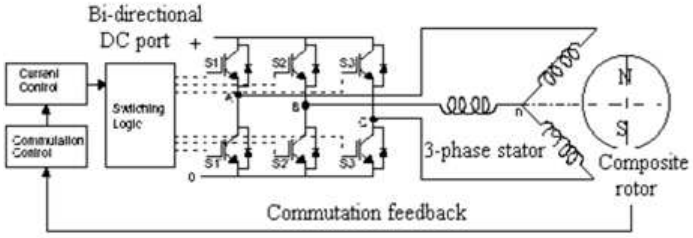

Figure 4: Flywheel motor/generator connected to a DC bus via a power-conditioning configuration using a 6-digit pulse topology

The DC port is bi-directional depending on whether the battery is in generating or charging mode and could be connected directly to a DC generator and DC load or via an inverter to an AC load. In Figure 4 the IGBTs are designated as S1, S2, etc. They are operated by micro-controllers in a 6-pulse bridge topology. Commutation is enabled by rotor position feedback obtained from Hall Effect sensors built into the stator to detect the position of the rotor magnetic field.

The mounting is such that they each generate a square wave with 120° phase difference over one electrical cycle of the motor (Figure 5). The amplifier drives two of the three motor phases with DC current during each specific Hall sensor state. The technique is reputed to result in a very cost-effective amplifier (Amc).

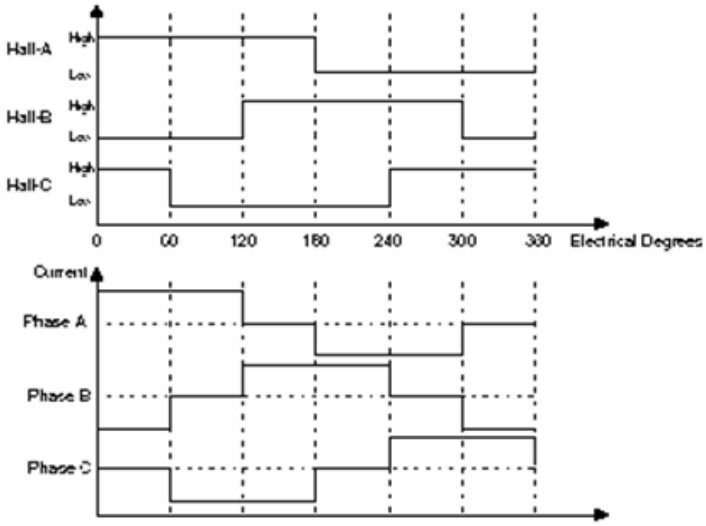

Figure 5: Hall sensor based commutation

5. Possible flywheel battery specification for rural application

From what has been mentioned, the energy stored in a flywheel battery is proportional to the system

moment of inertia, J and the square of the rotor system angular speed (for convenience, details of the power conditioning equipment will assume to be ideal). If the rated angular speed of the flywheel rotor is ϖ_R, then maximum energy that can be stored is E_F such that

$$EF = \tfrac{1}{2}J\varpi_R^2 \quad (11)$$

If the maximum permissible depth of discharge for the battery is 90%, then there would be a balance of 10% of the energy at which point the rotor speed would be ϖ_o, such that

$$\omega_o = \sqrt{\frac{\omega_R^2}{10}} = 0.316\omega_R \quad (12)$$

The terminal voltage of the flywheel generator is linearly proportional to the rotor speed. Therefore, the terminal voltage at 90% depth of discharge (DOD) would be 31.6% of the full speed voltage, V_R, which is the rated voltage. Considering the internal impedance to be negligible, the open circuit voltage should be approximately equal to the output bus voltage even at full load. Let the flywheel battery be designed to deliver its continuous rated power P_R over the entire operating speed range. Then by Ohm's law, the current drawn at the minimum operating speed would be the highest permissible or rated current.

Figure 6 is a 24-hour electric load profile of a rural household from a database of the South African National Rationalised Specifications (NRS) Load Research Project for Garagapola village. It will be assumed that this represents a typical daily load profile. The daily peak load is 7.85A, with an average of 0.66A and hence, a load factor of 8.4%. The total energy consumed by the household at a supply voltage of 230V was (24 x 0.66 x 230) = 3643.2 Wh.

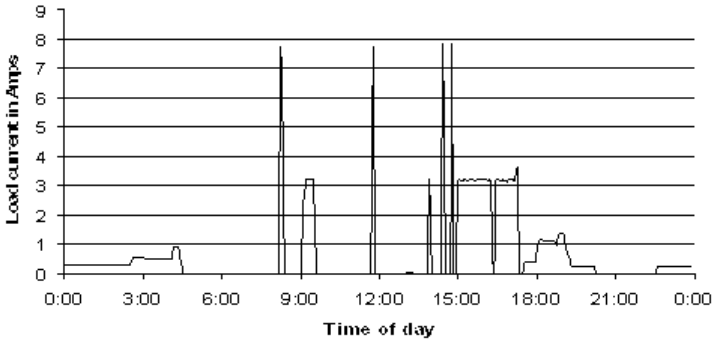

Figure 6: A 24-hour load profile recorded by NRS for a household in Garagapola village

Consider the above to be an off-grid rural household operating from a stochastically distributed renewable energy source, which would require a storage battery. It is regular practice for off-grid storage facilities to be specified for several autonomous days each being equivalent to the average daily requirement. So if this household were to have a storage capacity to last for 2 autonomous days (plus one normal day) then the available battery capacity would be (3643.2 x 3) =10929.6 Wh. Since the maximum allowable depth of discharge for the flywheel battery is 90%, then the flywheel battery capacity must be (10929.6 Wh ÷ 90%) = 12144 Wh. This capacity, however, does not take losses into account. If a battery charge-discharge efficiency of 80% is assumed (Post, 1996) then final value is (12144 Wh. ÷ 0.8= 15180 Wh).

Let the flywheel be designed for a rated speed ϖ_R of 60 000 revolutions per minute, which is 2 000π radians per second.

From the above, 15180 Wh = 3600 x 15.18 kilo joules = $\tfrac{1}{2}J(2000\pi)^2$ (where, J is the flywheel rotor system inertia).

Therefore,

$$J = 2.77 \times 10^{-3} kg - m^2$$

Household peak power demand = (7.85 x 230) = 1.81 kW. Allowing for a margin of error, the battery could be rated for continuous power of 2 kW. As stated, the validity of this specification is required for the entire operating speed range and must therefore be applicable at the minimum state of charge. In this case, when there is only 10% of storage capacity and at a rotor speed (and hence at a bus voltage) of 31.6% of the rated.

Let the full rated voltage be 100V, then at 10% state of charge (SOC) the voltage will be 31.6V.

Then the rated current, I_R must equal to the rated power divided by the minimum operating voltage

$$I_R = 2000/31.6 = 63.30\ Amp$$

The load torque exerted on the flywheel is proportional to the generator current (which is the load current) and therefore the maximum load torque will be at the rated load current. This should be true for both charging and discharging modes. But power, P is the product of torque, T and angular speed, w.

Therefore,

$$P = T\varpi = K_F q I_{eff}\varpi \quad (13)$$

Where,

$$K_F = B\frac{\sqrt{2}}{3} l\ Sin\left(\frac{\pi}{q}\right)$$

is the torque constant and qI_{eff} = total load current.

From equation (12) the minimum flywheel speed is given by ϖ_o such that

$$\omega_o = 0.316\omega_R = 0.316\left(\frac{2\pi.60000}{60}\right) = 632\pi$$

Radians per second.

Then from equation (13) the machine torque constant, K_F can be calculated using rated power at minimum speed.

$$K_F = \frac{P}{632\pi \cdot qI_{eff}} = \frac{2000}{632\pi \cdot 63.3} = 0.02 \qquad (14)$$

Let the design be a three-phase ($q=3$) machine

$$K_F = B\frac{\sqrt{2}}{3}(3 \cdot l \cdot \sin\frac{\pi}{3}) = B\sqrt{\frac{2}{3}} \cdot l = 0.02 \qquad (15)$$

From equation (9)

$$B = J_r \ln\left(\frac{r_o}{r_i}\right)\left(\frac{\sin\left(\frac{2\pi}{N}\right)}{\left(\frac{2\pi}{N}\right)}\right)$$

Using the dipole in Figures 2 and 3, the number of magnets used is 12. Let N = 12. The remanent field of grade 32 rare earth, Nd-Fe-B (Neodymium Iron Boron) is typically $J_r=1.15$ tesla.

$$B = 1.15 \ln\frac{r_o}{r_i}\left(\frac{\sin\frac{\pi}{6}}{\frac{\pi}{6}}\right) = \frac{3}{\pi}\ln\frac{r_o}{r_i}$$

In Post (1996) the value for r_o/r_i is assumed to be 1.5. Using this figure the value of the dipole strength, B is

$$B = \frac{3}{\pi} \times \ln 1.5 = 0.39 \quad tesla$$

From equation (13), the expression for the axial length l, can be found

$$l = \frac{0.02}{B\sqrt{\frac{2}{3}}} = 0.05 \quad meters$$

Since the rated power of 2000W must be available at minimum angular speed of 632π then the maximum torque T is given by:

$$T = \frac{2000}{632\pi} = 1.01Nm$$

Let the battery be required to maintain a maximum self-discharge rate of 90% per month on no-load. Then the total amount of energy lost this way must be ≤90% of full storage capacity $\leq 90\% \times 15180Wh = 13662.9Wh$. Therefore, the average self-discharge rate = 13662.9 Wh in (24 x 30) hours or 18.98 W.

Assuming a total absence of air drag in the containment chamber, these losses are due to bearing friction and proportional to the rotor mass. The resulting deceleration torque T_d is therefore constant and is equal to the product of the average speed over the deceleration range and the average rate of loss of power. Speed range is 2000π to 632π radians per sec. So the average speed is 1316π rad/sec. $T_d \cdot 1316\pi = 18.98W$, therefore the permissible bearing frictional torque should not exceed $T_d = \frac{18.98}{1316\pi} = 4.6 \times 10^{-3}$ Nm

From equation (4),

$$J = \frac{1}{2}m\left(r_o^2 + r_i^2\right)$$

Let the inner radius r_i = 25mm. From Post (1993) it is assumed that:

$$r_o/r_i = 1.5$$

Using the same assumption the outer radius

$$r_o = 1.5 \times 25 = 37.5mm$$

Therefore, the rotor mass =

$$m = \frac{2J}{(r_o^2 + r_i^2)} = 2.73kg$$

6. Flywheel structure and magnetic bearings

A configuration structure of total flywheel system and rotor mass is proposed as shown in Figure 7. The total system and the hollow shaft are fixed in between two plates to ensure the stability of the flywheel system. The Halbach machine is embedded in the flywheel and the entire system levitated. The stator winding are fixed on the shaft.

There are numerous types and configurations of magnetic bearings. The choice of this combination was to suite the flywheel design, support the total weight of the rotor and accommodate a Halbach array PM machine. The magnet ring pairs at the bottom of system, as shown in Figure 7, are applied to levitate total weight of flywheel mass and other peripheral components. The stator of radial active magnetic bearing is appended by 6 suspension steel

rods to ensure the stability of the stator. The axial magnetic bearings are used to keep the system axially stable. The rotor of axial magnetic bearing is connected with the rotor of radial magnetic bearing by the axial bearing radial bearing coupling. All these three parts are levitated and rotate with the flywheel.

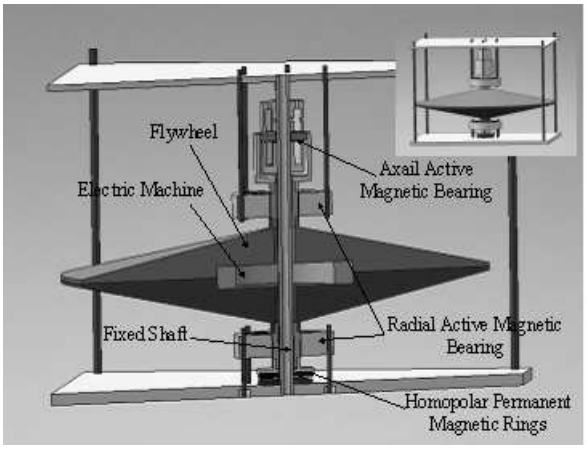

Figure 7: Flywheel structure

6.1 Repulsive magnetic force analysis of Homopolar PM magnets ring pairs

The repulsive force between two homopolar permanent magnetic ring pairs, as shown in Figure 8, are applied to suspend the weight of the flywheel and this reduces the losses in the coil and iron losses in the active magnetic bearing. In order to reduce the dimension and increase stiffness of magnetic bearing, this type of magnetic ring is designed from high remnant flux density and high coercive force material NdFeB.

Figure 8: Homopolar permanent magnetic suspension ring pair

The force between the two magnetic rings can be calculated by the magnetic charge method, equivalent current method, Maxwell equation method and virtual work method. In this design process, the equivalent current method is applied as shown in Figure 9.

A virtual magnet plate is assumed inside the ring to form a large magnet plate. Then, the repulsive magnetic force between the two large plates, between one virtual magnet plate and one large plate and between two virtual magnet plates can be calculated by the equivalent current method.

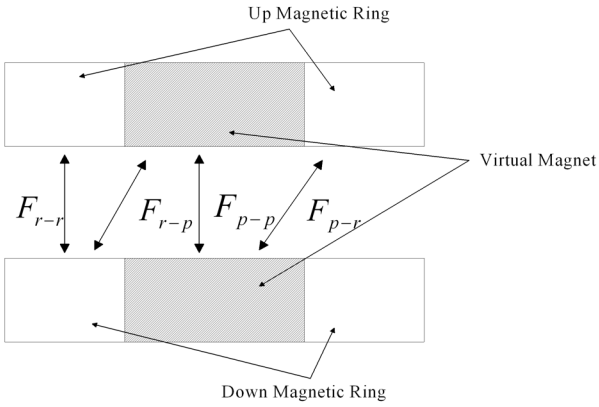

Figure 9: Virtual method to calculate magnetic force

A model with various lengths of the airgap was simulated in Finite Element (FE) software Flux 2D/3D and compared with the equivalent current method. The results are shown in Figure 10. From Figure 10, the repulsive magnetic force between the two magnet ring pairs calculated by the equivalent current method matches the FE method closely. Therefore, by applying the equivalent current method, the relationship between the weight of the flywheel and the length of airgap can be optimized.

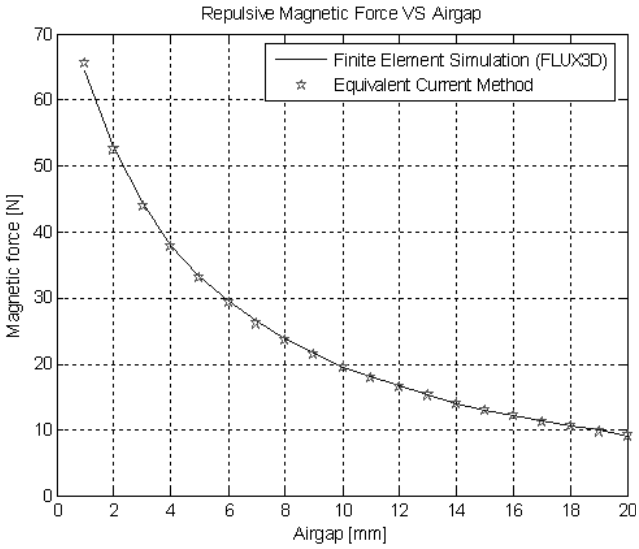

Figure 10: Repulsive magnetic force VS airgap

6.2 Attractive magnetic force analysis of axial active magnetic bearings

This section illustrates the design and performance of the axial active magnetic bearings. As shown in Figure 11, when a current is applied in the coil, the flux passes through the shell of the York and the plate to induce the magnetic attractive force as shown in Figure 12.

The equivalent magnetic circuit is shown in Figure 13. In order to simplify the model, only the

slot leakage and edge effect are taken into account. The magnetic saturation is neglected.

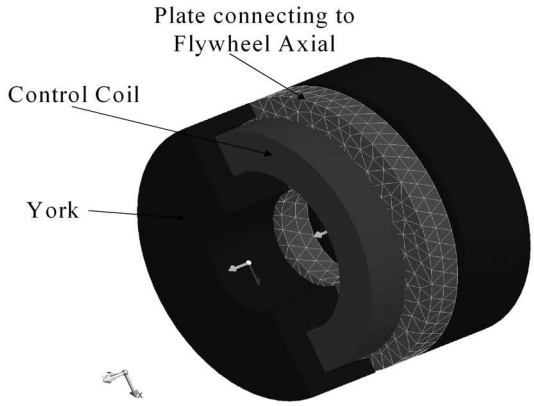

Figure 11: Active axial magnetic bearing

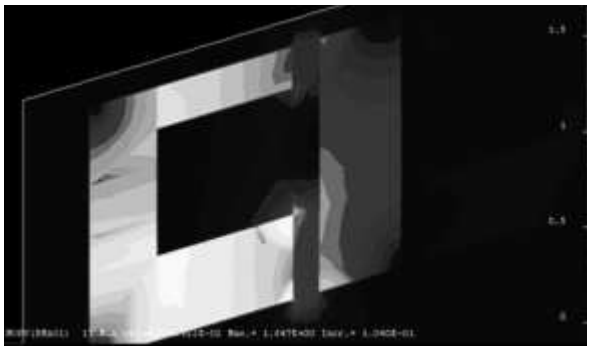

Figure 12: Flux in the magnetic bearing

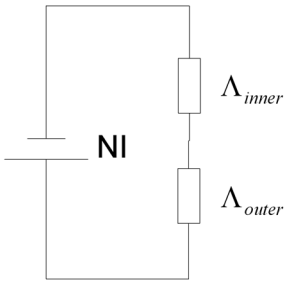

Figure 13: Equivalent magnetic equation of active axial magnetic bearing

The structure is analyzed and simulated in Flux2D/3D by FE method. The result is shown in Figure 14.

The results from the two methods are closely correlated. For a large excitation current, the simulation result is smaller than the analysis result, which is anticipated because of magnetic saturation in the magnetic material. Furthermore, this current Vs force curve can be applied in transient analysis of flywheel.

6.3 Attractive magnetic force analysis of radial active magnetic bearing

The structure and performance of the eight pole radial active magnetic bearing is simulated in

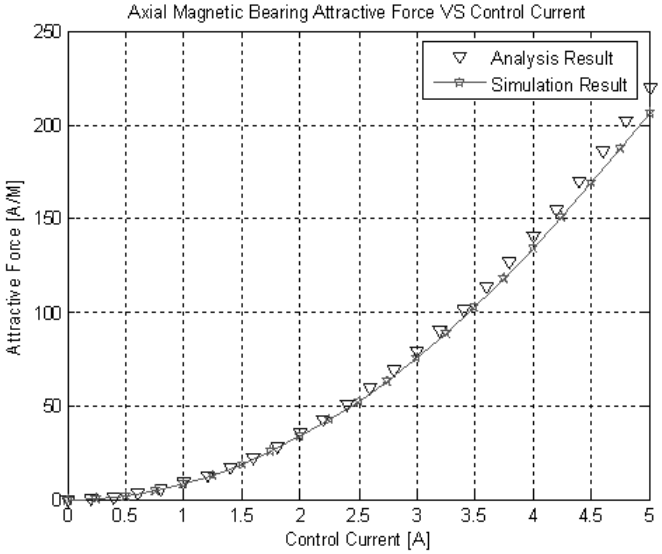

Figure 14: The attractive force of active axial magnetic bearing vs control current

Flux2D/3D. This is charged with control of the radial stability of the system. The structure of radial active magnetic bearing is shown in Figure 15. The inner part is the rotor and is coupled to the flywheel and shaft. The outer part is the stator of bearing and the middle is the coil.

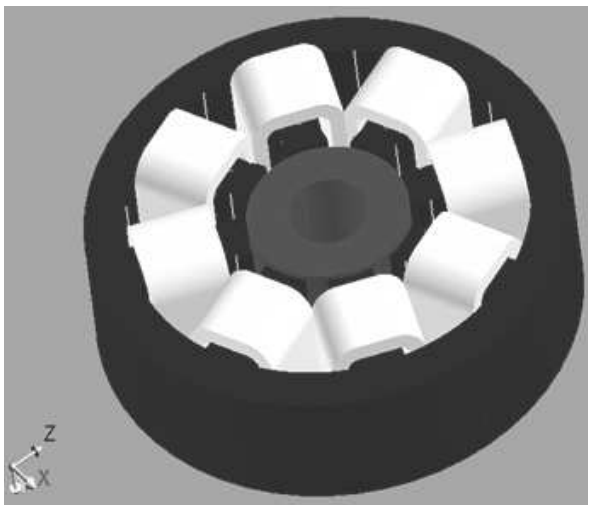

Figure 15: Eight pole radial active magnetic bearing

The 8 poles are separated into four sections to induce four direction attractive forces: Positive X, Negative X, Positive Y, and Negative Y. The coil in the two pole pairs are wound in contrary directions. This is done such that the flux passes from one pole into another one, rather than pass into other poles as shown in Figure 16.

In order to avoid the saturation in the steel, the flux density in the air gap is kept at 0.9T and this happens when the control current is 3.6A. The corresponding induced magnetic force is 200N as shown in Figure 17.

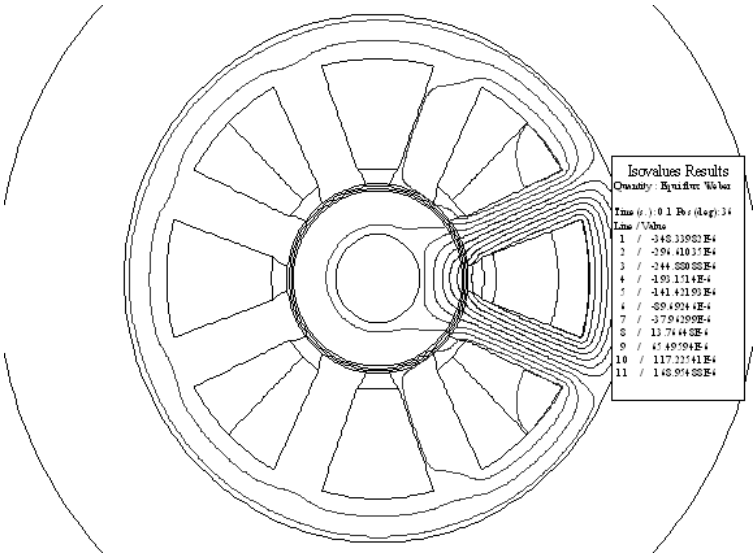

Figure 16: Flux in the radial magnetic bearing

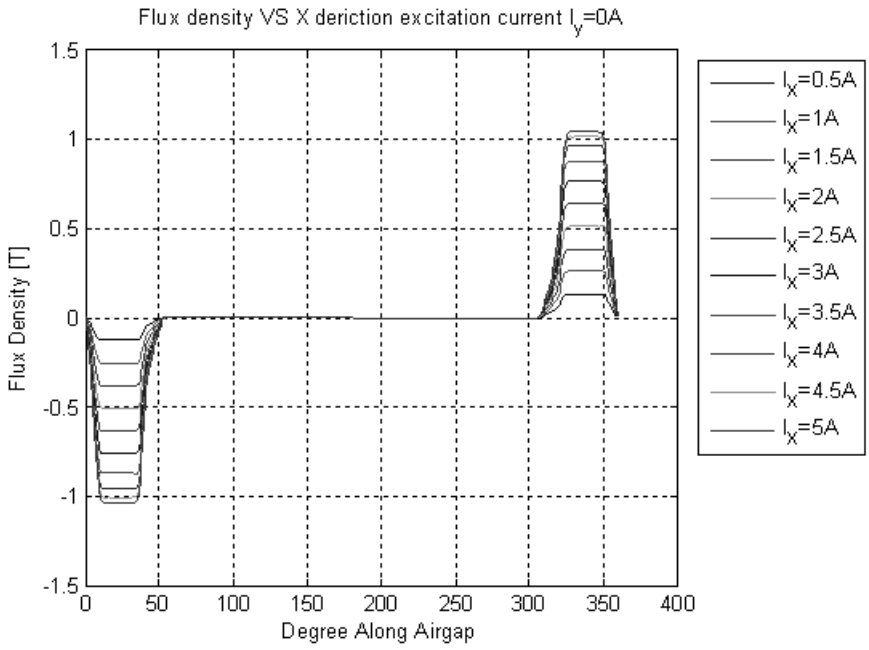

Figure 17: Flux density along the airgap versus X direction current

From Figures 16 and 17, almost all the flux passes through positive X direction pole pairs. In order to avoid the wrong flux circuit, the right pole of Positive Y direction poles pairs should be the same polarity as the upper pole of positive X direction pole pairs. The positive X, Y direction coil are excited by various control current. The various flux densities in the air gap are shown in Figure 17 and 18.

The analysis model of radial magnetic bearing was developed. The attractive force of X and Y direction is calculated and compared with Finite Element method with various control current as shown in Figures 19 and 20.

At the designed maximum current, the magnetic attractive force calculated by analysis method matches the result of FE method perfectly as shown in Figure 19. When the control current is more than 3.6A the magnetic attractive force is more than 200N and the difference between two methods increases. This is reasonable, because in the analysis method, the magnetic intensity drop in the steel is neglected. At large working flux density, the steel saturates.

In Figure 20, the positive Y direction control current varies and the results of the analysis match the FE Methods with close correlation. This happens when the control current is less than 3A and force is less than 150N. When the Control current is increased beyond 3A, the attractive force on positive X direction is reduced as shown in Figure 19.

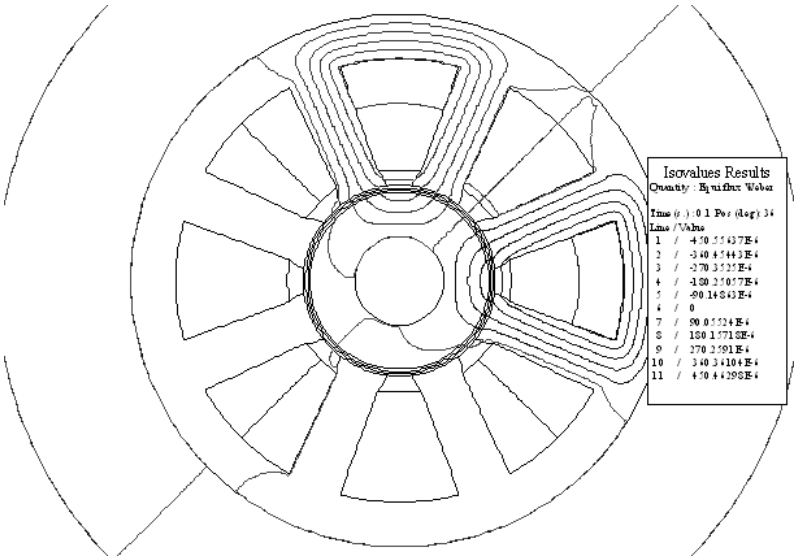

Figure 18: Flux in the radial magnetic bearing

This property is anticipated and contributes to the saturation of magnetic material on rotor; however, this is not important. The control current on the positive X direction is sinusoidal and on Y is co-sinusoidal for the Y direction in order to induce a rotating attractive force to offset the centrifugal force of flywheel. That means, when control current on the positive Y direction is more than 3A, the control current on the positive Y direction will be very small.

7. The present and future of the flywheel battery

The foregoing example has mainly focused on the electromagnetic analysis of the battery. The assumptions made with respect to the Halbach array would hold reasonably true. However, there are issues, for example, the requirement that battery self-discharge be less than 90% per month that may currently be viewed as an extreme demand. Consequently, a number of values obtained, like the rotor mass could be grossly at variance with reality. Moreover, the machine was assumed to behave ideally with respect to important issues, like rotor stresses, material properties and thermal dissipation.

The example, however, has importance, in that the off-grid household load depicted is unlike the most common terrestrial applications for flywheel batteries (like seamless power transfer during grid instability or short outages) whose purpose is mainly high power delivery for time bridging. Thus, the example provides a load magnitude and duration that are significantly different and helps to highlight issues that may not arise during the aforementioned common applications.

In general, current technical concerns for the flywheel battery technologists include structural

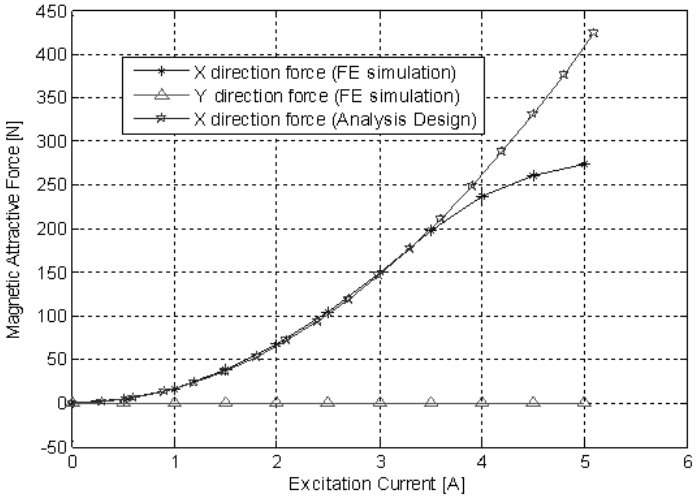

Figure 19: Attractive force versus positive X direction control current

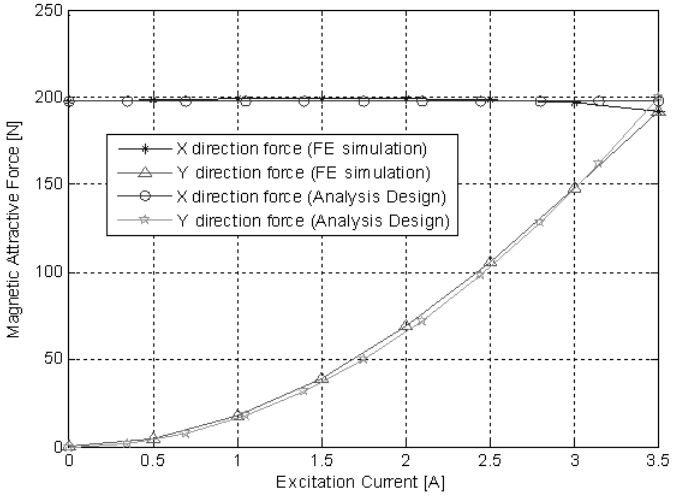

Figure 20: Attractive force versus positive Y direction control current

integrity of the rotor, the speed capability of the suspension bearings and the speed and power handling capability of the motor/generator and control electronics. Suspension bearings and motor/generator and drive technologies have applications in many other fields and have consequently seen relative advancement. Rotor structural integrity however, poses by far the biggest challenge in the development of the flywheel as a viable battery system. The issue is of such gravity and importance that the area of research transcends normal competition and groups of researchers have been developed to pool resources and assemble combined expertise (Pichot *et al.*, 1997).

Over the years, a variety of flywheel shapes from a range of materials have been designed with the aim to maximize the stored energy. The important parameters influencing failure of a rotor disk are fabrication imperfections (misfit), mean radius, thickness, material property, load gradation and speed. These are the sub-system indices of merit, all of which must be optimized simultaneously to achieve the best and most reliable design.

Numerous fibre materials exist including glass, graphite and carbon fibres. These have varying material strengths and are further differentiated by the reinforcements used during the construction process. The reinforcement (for example, epoxy) combines with the fibre to form a composite material. The epoxy or any other reinforcement with which it must be mixed has a substantially lower strength value, often of the order of 50%. The fibre constitutes only about 60% (by volume), resulting in a strength reduction of two. This then forms the design basis. Then one has to include allowances for fatigue. Fatigue is the systematic weakening of a material as a result of sustained stress over a period. This will vary depending on environmental factors like temperature and chemical corrosion due to water vapour.

The above considerations being for hoop strength alone, the designer will have to consider radial and axial strengths, which are also limited by the strength of the polymer matrix. For these forces, the fibre represents a discontinuity in the matrix and the design allowable should not exceed 15% of the matrix tensile strength. Structural stress issues do impact on the electrical design as well, for example, due to the fragility of the magnets forming the Halbach array, they must be assembled close to the hub. This compromises the power density of the generator. Along with rotor failures comes the problem of designing safe containment. As a consequence of these safety concerns, the PNGV later opted to defer development of the flywheel battery (as progress was deemed too slow to meet set deadlines of 2004 for concept model vehicles) but would continue to monitor progress in other programs mentioned later. In the case of a rural application, however, underground containment has been found to satisfactorily address the safety concerns.

There is also great optimism as the carbon fibres strengths are projected to improve from the current strengths of 1 000 000 psi to 3 000 000 psi within this decade, implying a possible increase of 200% in stored kinetic energy. At this strength, the achievable material tip speeds will exceed 2 kilometres per second. Composite carbon fibre disks have an added safety advantage at failure. Unlike metallic disks, which disintegrate into dangerous solid shrapnel, in the case of a burst (which is the worst case scenario in rotor failure), fibre absorbs much of the energy by converting to cotton-like shred.

Another important factor is the cost. According to (Joseph *et al.*, 2002) the current cost of lead-acid batteries ranges between $50–$100 per kWh compared to $400–$800 per kWh for flywheel systems. This disparity currently gives the chemical batteries an edge. As for efficiency, flywheels (at 80 - 85%) are currently equal or better than state-of-the-art chemical batteries. Operational results of 93% have been reportedly achieved (Bitterly, 1998) by NASA and 90-95% (Chen *et al.,* 2009, Ribeiro *et al.,* 2001).

Lifespan is another major advantage of the flywheel battery, with estimates of at least 20 years as compared to between 3 and 5 years for chemical batteries. This is, however, compromised by their (currently) much higher self-discharge rates as compared to chemical batteries.

The biggest advantage held by flywheels, however, is that being an emerging technology, their potential has barely been tapped as compared to the centuries-old chemical systems which in all probability are unlikely to make major advances (Khartechenko, 1998). This is without considering environmental issues. At the forefront of rotor integrity and safety research is the Defense Advanced Research projects Agency (DARPA). In rotor dynamics, hub rim interface, strength optimisation and fatigue life are collaborations between independent groups with funding mainly from NASA. These include, Glen Research Centre (NASA GRC), Engineering Model Flywheel Energy Storage Systems, Small Business Research Contracts, Auburn Centre for Space Power and University of Texas/NASA Safe Life Criteria. Existing NASA and Boeing databases, like the Gas Turbine Engine Program are reinforcing efforts by University of Texas A&M, GRC and University of Virginia on high rpm developments, among others, that constitute the National Aerospace Flywheel Program.

8. Concluding remarks

The potential of the electromechanical battery has been highlighted as well as the shortcomings of continued use of chemical batteries. This paper has

examined the basics of kinetic energy storage as well as the machine design equations of an ironless permanent magnet synchronous motor-generator. Using these design equations a special battery supply for a rural African application has been specified. Pending research issues have been highlighted as well as the optimistic projections of the near future. With improved technologies it should therefore be possible, using machine design equations and given load requirements and availability of energy resources, to design an appropriate flywheel storage battery, that can be manufactured in Africa.

Moreover, the life cost cycle of the flywheel battery, which includes the potential for a long lifespan with virtually no maintenance as well as the positive environmental attributes are major advantages.

References

Arnold S. M., Saleeb A. F. and Al-Zoubi N. R. (2001). Deformation and Life analysis of composite flywheel disc and multi-disk systems. *NASA/TM-210578*.

Baaklini G. Y., Konno K. E. *et al.,* (2001). NDE methodologies for composite flywheel certification. *SAE (01)3655*.

Bitterly J. G. (1998). Flywheel Technology: Past, Present and 21st Century projections. *IEEE AES Systems Magazine*.

Brushless Amplifiers, Servo Drives and Amplifiers, Advanced Motion Controls, 3805, Calle, Tecate, Camarillo, CA 93012, USA. http://www.a-m-c.com/download/engnotes.pdf.

Buchmann I. (2001). Can the Lead Acid battery compete in modern times? *Cardex Electronics Inc.* http://www.batteriesdigest.com/ask_isidor.htm

Chen H., Cong Y., Yang W., Tan C., Li Y. and Ding Y. (2009). Progress in electrical energy storage System: a critical review, Prog. *Nat. Sci. 19 (3): pp. 291–312*.

Halbach K. (1980). Design of permanent multi-pole magnets with oriented rare earth cobalt material. *Nuclear Instruments and Methods 169: p1-10*.

Hayes R. J., Kajs J. P. *et al.* (1999). Design and testing of a flywheel battery for a transit bus. SAE (01)1159.

Hebner R., and Aanstoos T. (2000). Energy Storage for sustainable systems: A white paper on the benefits and challenges of kinetic energy storage," Centre for Electromechanics, University of Texas at Austin. http://www.ece.gatech.edu/research/UCEP/2000-nsf/Presentations/Hebner.pdf

Herbst J. D., Manifold S. M. *et al.* Design fabrication and testing of a 10MJ composite flywheel energy storage rotors. *SAE 981282*.

http://space-power.grc.nasa.gov/ppo/projects/flywheel/

Hunt G. L. (1998). The great battery search. *IEEE Spectrum, November 1998*.

Joseph B., Hebner R., and Walls A. (2002). Flywheel Batteries Come Around Again. *IEEE Spectrum, pages 46-51*.

Khartchenko, N. (1998). Advanced Energy Systems. Taylor and Francis.

Bowler M.E. Flywheel energy systems: current status and future prospects. *Trinity flywheel power, San Francisco California*.

Mukund R. Patel. (1999). Flywheel Energy storage for spacecraft Power Systems. *SAE (01) 2589*.

Ofori-Tenkorang J., and Lang J. H. (1995). A comparative analysis of torque production in Halbach and conventional surface-mounted permanent-magnet synchronous motors. *IAS '95: Conference record of the IEEE Industry Applications conference*.

Pichot M. A., et al. (1997). Flywheel Battery Containment Problem. *Society of Automotive Engineers-970242*.

Post R. F. (1996). A new look at an old idea, the electromechanical battery. *Science and Technology Review* 1996.

Post R. F., Fowler T. K., and Post S. F. (1993). A High Efficiency Electromechanical Battery. *Proceedings of the IEEE, (3) 81*.

Review of the research program of the Partnership for a New Generation of Vehicles: Fifth Report (1999).(http://www.nap.edu/open-book/0909064430/html/38.html)

Ribeiro P. Johnson B., Crow M., Arsoy A and Liu Y. (2001). Energy storage systems for advanced power applications, Proc. *IEEE 89 (12): pp. 1744–1756* .

Sebitosi A. B. and Pillay P. (2003). Applications of Advances in Automotive Electronics to Rural Electrification: The 42V Power-net for Rural Electrification. *Proceedings of the IEEE PES General Meeting 13*.

Seireg A. and Surana K. S. (1970). Optimum design rotating disk. *J. Engr. For industry, Trans. of the ASME, 92: pp1-10*.

Sung K. Ha, Dong-Gun Lee and-Jin Kim. Optimization of hybrid composite rotor in flywheel battery. *SAE 981899*.

Tsai S. W. and Wu E. M. (1971). A general theory of strength for anisotropic materials, *Journal of Composite Materials*.

Tsung-Ying Lee, Nanming Chen. (1993). Optimal capacity of the battery energy storage system in a power system. *IEEE Transactions on Energy conversion, 8*.

Received 11 October 2011; revised 4 June 2012

Details of authors

Bukola O Bolaji *B Eng (Mech Eng) M Eng (Thermofluids) PhD (Build Serv Eng)*
Senior Lecturer and Head of Department, Department of Mechanical Engineering
College of Engineering, University of Agriculture, Abeokuta, Nigeria
Tel: +234 803 578 5662
E-mail: bobbolaji2007@yahoo.com
Bukola Bolaji is a mechanical engineer with a master's degree in thermofluids and a PhD in Building Services Engineering. He is a member of the Nigerian Society of Engineers, Environment Behaviour Association of Nigeria, and Nigerian Institution of Engineering Management. He has consulted in a variety of industries in Nigeria on refrigeration, air-conditioning and solar power systems for over fifteen years.

Currently he is the Head of Department of Mechanical Engineering, College of Engineering, University of Agriculture, Abeokuta, Nigeria. His research interests are in the areas of refrigeration and air-conditioning, solar thermal systems, solar power systems, and environmental engineering. He is a member of Agricultural Mechanization and Energy Research Group of the Institute of Food Security, Environmental Resources and Agricultural Research, Abeokuta, Nigeria.

Delson Chikobvu *(PhD Mathematical Statistics)*
Lecturer: Mathematical Statistics and Actuarial Science, Department of Mathematical Statistics and Actuarial Science, University of the Free State, South Africa
Tel: +27 51 401 2779
E-mail: Chikobvu@ufs.ac.za
Dr Delson Chikobvu is a lecturer in Mathematical and Actuarial Science, Department of Mathematical Statistics and Actuarial Science, University of the Free State.

Brett Cohen *BSc (Chem Eng) PhD (UCT)*
Senior Researcher, Energy Research Centre, University of Cape Town, Rondebosch
Tel: +27 72 434 2208
E-mail: brett.cohen@uct.ac.za
Brett Cohen has a PhD in Chemical Engineering from UCT, focussing on the management of solid hazardous wastes. Since completing his PhD, Brett has worked in both academia and consulting on a wide range of sustainability-related projects in South Africa, Australia and the United Kingdom. He is currently a senior researcher at the Energy Research Centre at UCT as an expert in energy modelling, as well as a principal consultant at The Green House, a consultancy based in Cape Town.
Brett's interest areas span those related to energy modelling and management, climate risks and opportunities, scenario and futures planning, technology assessment, industrial ecology, decision support, facilitation and strategy development. His work draws on experience from chemical process engineering, multi criteria decision analysis techniques, network theories, natural systems and economics to develop robust and defensible system models.

Stephen Davis *BSc (Hons) (Wits) MSc (Operations Research) (UCT)*
Independent researcher and facilitator; Associate at Project 90 by 2030
Tel: +27 82 508 9750
E-mail: sjdavismail@gmail.com
Stephen Davis is a behaviour change researcher and leadership programme facilitator with a master's degree from the University of Cape Town in Operations Research (awarded cum laude). He has an honours degree in Statistics and Actuarial science, which he completed at the University of the Witwatersrand in 1997. Most recently he worked for four and a half years with the Energy Systems Analysis and Planning Group at UCT's Energy Research Centre, where he managed research in the area of residential energy efficiency, lectured and convened the Energy Modelling and Analysis masters module, and supervised several M Sc and BSc (Honours) students. His focus as an energy researcher is on modelling behavioural aspects of energy consumption, and the implications for policy and planning, and he also facilitates leadership programmes with a sustainability focus.

Oliver Dzobo
Department of Electrical Engineering, University of Cape Town
E-mail: Oliver.Dzobo@uct.ac.za
Oliver Dzobo received his B Sc (Eng.) degree in electrical engineering from the University of Zimbabwe, Harare, Zimbabwe, in 2004. He received his M Sc degree in electrical engineering in 2010 and is currently working toward a PhD degree from the University of Cape Town. His research area is in the application of outage costs to power system reliability.

Trevor Gaunt
Department of Electrical Engineering, University of Cape Town
E-mail: CT.Gaunt@uct.ac.za
Trevor Gaunt is a Professor in the Department of Electrical Engineering at the University of Cape Town. He has 40 years of experience with an equipment manufacturer, electricity utility, consulting firm and now at university, where he is responsible for undergraduate and postgraduate teaching, and the financial and technical management of research projects in power delivery system planning and design.

Rupert Gouws *B Eng (Elect) M Eng (Elect) PhD (Elect Eng) Pr Eng CMVP*
Senior Lecturer, School of Electrical, Electronic and Computer Engineering, North-West University, Potchefstroom, South Africa
Tel: +27 18 299 1902
Fax: +27 18 299 1977
E-mail: rupert.gouws@nwu.ac.za
Rupert Gouws holds a Ph.D. degree in Electrical and Electronic Engineering from the North-West University (Potchefstroom campus). He has consulted to a variety of industry and public sectors in South Africa and other countries in the fields of energy engineering and engineering management. Currently he is appointed as a senior lecturer specialising in energy engineering, electrical machines and control at the North-West University. The Engineering Council of South Africa (ECSA) registered him as a Professional Engineer and the Association of Energy Engineers (AEE) certified him as a Certified Measurement and Verification Professional (CMVP).

Nicholas Gukop
Nicholas Gukop is a graduate of the Department of Mechanical Engineering, Ahmadu Bello University, Zaria, Nigeria. His research work and interest is in Waste- to energy.

Ronald Herman
Department of Electrical Engineering, University of Cape Town
E-mail: Ronald.Herman@uct.ac.za
Dr Ron Herman obtained a BSc (Eng.) degree from the University of Cape Town in 1962. After working with Eskom, he joined the staff of the University of Stellenbosch, completing M Sc and PhD degrees in Electrical Engineering. He is currently a part-time Senior Research Officer at the University of Cape Town.

Amber Ityona *B Eng (Mech) M Sc (Mech) M Sc (Energy)*
Lecturer, Thermofluids and Energy, Department of Mechanical Engineering, Ahmadu Bello University, Nigeria
Tel: +234 80328 74720
E-mail: amberity@yahoo.com
Amber Ityona is a mechanical engineer with a master's degree in mechanical engineering and energy. He research is in energy systems and solar energy. His current research spans on waste to energy options for integration into the Nigerian energy mix and solar thermal energy utilisation.

Adisa A Jimoh *Pr. Eng. (South Africa) B.Eng. (Elec. Eng.) M Eng. (Elec. Eng.)(ABU) PhD (Elec. Eng.)(McMaster) SMIEEE SMSAIEE MNSE*
Research Niche Area Leader: Energy and Industrial Power Systems, Head of Department: Electrical Engineering, Tshwane University of Technology, Pretoria
Tel: +27 12 382 4964
Fax: +27 12 382 4964
Cell: +27 82 787 0251
E-mail: jimohaa@tut.ac.za
Adisa Jimoh (Senior Member, IEEE) is an electrical engineer with bachelor's, master's and PhD degrees. He has been a faculty member in several universities for 32 years.

Pule A Kholopane *B Sc (Production) (Fort Hare), B Sc M Sc (Operations Management) (Hertfordshire), PhD (Engineering Management) (Johannesburg)*
Senior Lecturer, Quality and Operations Management, University of Johannesburg, South Africa
Cell: +2771 433 5364
E-mail: pulek@uj.ac.za
Pule Kholopane is a Senior Lecturer, Quality and Operations Management, University of Johannesburg, South Africa.

Estie le Roux *B Eng (Elect)*
Research Assistant, School of Electrical, Electronic and Computer Engineering, North-West University, Potchefstroom, South Africa
Tel: +27 18 299 1902
Fax: +27 18 299 1977
E-mail: estie.leRoux@nwu.ac.za
Estie le Roux holds a B Eng degree in Electrical and Electronic Engineering from the North-West University (Potchefstroom campus). Her research interests include energy engineering, electrical systems and water heating systems.

Kulla Dangana Mallam *B Eng (Mech) M Sc (Energy), PhD (Renewable energy)*
Lecturer, Thermofluids and Energy, Department of Mechanical Engineering, Ahmadu Bello University, Nigeria
Tel: +234 803604 3394
E-mail: dmkulla2@yahoo.com
Kulla Dangana Mallam is a mechanical engineer with a master's degree in mechanical engineering and a PhD in renewable energy. He has conducted numerous researches in renewable energy at the Department of mechanical engineering Ahmadu Bello University, Zaria, Nigeria. Currently, he is involved in research of emissions from improved wood stoves in Nigeria.

Oludolapo A Olanrewaju *B Sc (Elec. Eng.) M Sc (Industrial Eng.) (Ibadan)*
PhD student, Industrial Engineering Department, Tshwane University of Technology, South Africa
Cell: +27 79 089 4923
E-mail: dlp4all@yahoo.co.uk
Oludolapo A Olanrewaju is a PhD student in the Industrial Engineering Department, Tshwane University of Technology.

Simisha Pather-Elias *B Sc (Hons) (Rhodes) MSc (Rhodes) MSc (Engineering) (Cape Town)*
Executive Assistant; Botanical Society of South Africa
Tel: +27 83 457 3597
E-mail: simishap@gmail.com
Simisha Pather-Elias obtained a master's degree in Biotechnology from Rhodes University in 2005 and thereafter worked as a Scientific Officer at UCT in the Bioprocess Engineering Research Unit working on several projects relating to environmental sustainability. In 2011, she was awarded a master's degree in Energy and

Development at the Energy Research Centre at UCT.

She has since worked for Conservation International's Climate Action Partnership division where she engaged with government, business and civil society on climate change mitigation and adaptation technologies and ecosystem based demonstration projects.

Simisha is currently employed at the Botanical Society of South Africa, a non-profit organisation. As the Executive Assistant, she assists the Director with managing operations, maintaining and building on the sustainability profile of the organisation and extending the portfolio of projects through forming partnerships with international and national organisations.

Richard Okou *B Sc (Elec Eng) (MAK) M Sc (Sustainable Energy Engineering) (KTH)*
PhD Student, Department of Electrical Engineering, University of Cape Town
Tel: 27 (0) 21 650 4821
E-mail: Okxric001@uct.ac.za

Richard Okou holds a Bachelor of Science in electrical engineering from Makerere University (2004), Uganda and an M Sc in Sustainable Energy Engineering from the Royal Institute of Technology in Stockholm, Sweden. He is currently pursuing his PhD in Electrical Engineering at the University of Cape Town. He worked as a United Nations Volunteer IT specialist for 2 years as a team leader for the Cisco networking program in Uganda. Mr. Okou has consulted in renewable energy technologies, energy management, planning and designing of energy systems, rural electrification and feasibility studies for hydro power generation. He is a student member of IEEE.

Pragasen Pillay *PhD FIEEE*
Professor and NSERC/Hydro-Québec Senior Chair, Department of Electrical & Computer Engineering
Concordia University,1515 Saint Catherine Street West, S-EV005.159 Montreal, Quebec - H3G 2W,1 Canada
Tel: 1 514 848 2424 ext. 3108
Fax: 1 514 848 2802
E-mail: pillay@encs.concordia.ca

Pragasen Pillay (F'05) received the Bachelor's degree from the University of Kwa-Zulu Natal, Durban, South Africa, in 1981, his Master's degree from the same University in 1983, and his PhD degree from Virginia Polytechnic Institute and State University, Blacksburg, in 1987.

Currently, he is a Professor in the Department of Electrical and Computer Engineering, Concordia University, Montreal, Canada, where he holds the NSERC/Hydro Quebec Industrial Research Chair. From 1988 to 1990, he was with the University of Newcastle-upon-Tyne, Newcastle-upon-Tyne, U.K. From 1990 to 1995, he was with the University of New Orleans. From 1995 to 2007 he was with Clarkson University, Potsdam, NY, where he held the Jean Newell Distinguished Professorship in Engineering. He is also an Adjunct Professor at the University of Cape Town, Cape Town, South Africa. His research and teaching interests are in modelling, design, and control of electric motors and drives for industrial and alternate energy applications.

Dr Pillay is a member of the IEEE Power Engineering, IEEE Industry Applications (IAS), IEEE Industrial Electronics, and IEEE Power Electronics Societies. He is a member of the Electric Machines Committee and Past Chairman of the IEEE Industrial Drives Committee of the IAS, Past Chairman of the Induction Machinery Subcommittee of the IEEE Power Engineering Society, Past Chairman of the Awards Committee of the IAS Industrial Power Conversion Department. He has organized and taught short courses in electric drives at IAS Annual Meetings. He is a Fellow of the Institution of Electrical Engineers and Technologists, U.K., and a Chartered Electrical Engineer in the U.K. He is also a Member of the Academy of Science of South Africa. He was a recipient of a Fulbright Scholarship for his PhD and received the Order of Mapungubwe from the President of South Africa in 2008 for contributions to South Africa in the area of energy conservation.

Adoniya Ben Sebitosi *B Sc (Eng)(Hons) (Nairobi) PhD (Cape Town) CEng MIET MIEEE MIDiagE MIEK*
Professor, Centre for Renewable and Sustainable Energy Studies, Department of Mechanical and Mechatronic Engineering, University of Stellenbosch, Matieland 7600

Prof. Adoniya Ben Sebitosi obtained his B Sc (Eng) with honours in electrical engineering from the University of Nairobi in 1977. He then joined industry and obtained extensive technical and managerial experience. His responsibilities included industrial quality assurance and training of service engineers in various countries in sub-Saharan Africa. He consequently attained various professional qualifications including Registered Engineer of Kenya and Chartered Engineer of the United Kingdom.

In 2001 he joined the Department of Electrical Engineering at the University of Cape Town and subsequently obtained his M Sc (Eng) and PhD degrees with distinction. He was nominee for the Joseph Arenow best PhD award in 2005. He was a Senior Research Officer/Lecturer in the Department of Electrical Engineering, UCT with responsibilities in lecturing, research and student supervision at undergraduate and postgraduate levels until end of 2008.

He joined Stellenbosch University in 2009 as Senior lecturer and subsequently became full professor at the beginning of 2012. He is rated as established researcher by the NRF. He has published 25 papers in international journals including Elsevier's Energy Policy and IEEE Transactions on Energy Conversion as well as 27 conference proceedings. He is also a reviewer for several international journals and the National Research Fund (NRF) of South Africa as well as member of journal editorial boards.

His research and professional interests include rational use of energy, renewable energy, water-energy nexus, energy policy, rural energisation, industrial quality assurance and power quality. His hobbies include writing African indigenous poetry and African cultural dance. He is extensively travelled particularly across sub-Saharan Africa.

Caston Sigauke *M Sc (Operations Research)*
Lecturer: Operations Research and Statistics, School of Mathematical and Computer Sciences, Department of Statistics and Operations Research, University of Limpopo, South Africa

Tel: +27 (0) 15 268 2188
Fax: +27 (0) 15 268 3487
Cell: +27 835 255 684
E-mails: csigauke@gmail.com and
caston.sigauke@ul.ac.za
Caston Sigauke is a lecturer in Operations Research and Statistics in the School of Mathematical and Computer Sciences, University of Limpopo. He is a PhD student in Statistics at the University of the Free State.

Forthcoming energy and energy-related conferences and courses: 2012–2013

SEPTEMBER 2012

10 – 12

FUNDAMENTALS FOR ENERGY MANAGEMENT TRAINING
Emperors Palace, Gauteng, South Africa
Contact: Izelle Bosman
E-mail: izelle@entf.co.za

29

PV SOLAR GRID CONNECTION & EPS CONTRACTS COURSE

Solar Con Training Centre, Modderfontein, Johannesburg, South Africa
Contact: Johanna
Tel: 011 440 4633
E-mail: info@solarcon.co.za
Website: www.solarcon.co.za

30 – 4 October

THE GREEN POWER MINI-MBA
Dubai, United Arab Emirates
Contact: Daniel VonBurg, Green Power Training Manager
Tel: +44 (0) 207099 0600
E-mail: daniel.vonburg@greenpowerconferences.com
Website: www.greenpowerconferences.com

OCTOBER 2012

15 - 19

MANAGING REFORM AND REGULATIONS IN THE ELCTRICITY AND WATER SECTORS
Graduate School of Business, University of Cape Town, Cape Town, South Africa
Contact: Prof. Anton Eberhard, Graduate School of Business, University of Cape Town
Tel: +27 21 406 1361
Website; www.gsb.uct.ac.za/mir

16 – 17

VIRIDIS AFRICA CLEAN TECH INVESTMENT SUMMIT
Killarney Country Club, Johannesburg, South Africa
Contact: Suza Adam, Spindle Communications
Tel: 011 880 0364
Fax: 011 788 3697
Cell: 082 789 9777
E-mail: suza.adam@spindlecommunications.com
Website: www.spindlecommunications.com

19 – 21

LOW CARBON EARTH SUMMIT 2012
Guangzhou, China
Website: www.bitcongress.com/nef2012/

27

PV SOLAR & WIND ENERGY COURSE
Solar Con Training Centre, Modderfontein, Johannesburg, South Africa
Contact: Johanna
Tel: 011 440 4633
E-mail: info@solarcon.co.za
Website: www.solarcon.co.za

NOVEMBER 2012

24

PV SOLAR GRID CONNECTION AND EPS CONTRACTS COURSE
Solar Con Training Centre, Modderfontein, Johannesburg, South Africa
Contact: Johanna
Tel: 011 440 4633
E-mail: info@solarcon.co.za
Website: www.solarcon.co.za

APRIL 2013

8 – 10

POWER & ELECTRICITY WORLD AFRICA 2013
Sandton Convention Centre, Johannesburg, South Africa
Contact: Sean Testa, Terrapin
Tel: 011 516 4048
E-mail: sean.testa@terrapin.com

15 - 18

POWER & ELECTRICITY WORLD ASIA 2013

Marina Bay Sands Convention Centre, Singapore
Contact: Philip Parba, General Manager, Terrapin Asia
Tel: +65 6322 2791
E-mail; philip.parba@terrapin.com
Website: www.saeec2012.org.za

Visit www.erc.uct.ac.za for further events and details